The grapevine defences

Walking towards the "hidden" role of dirigent proteins in *Vitis vinifera* secondary metabolism

Alexandre Filipe Guerreiro Borges

Dissertation presented to obtain the Ph.D degree in Biochemistry

Instituto de Tecnologia Química e Biológica António Xavier | Universidade Nova de Lisboa

Oeiras, December, 2014

The work presented in this thesis was developed at:

Disease and Stress Biology Laboratory
Instituto Superior de Agronomia
Tapada da Ajuda
1349-017 Lisboa – Portugal

REQUIMTE, Departamento de Química
Faculdade de Ciências e Tecnologia
2829-516 Caparica, Portugal

Supervised by:
Doctor Ricardo Boavida Ferreira
Doctor Ana Maria Lourenço
Doctor Sara Monteiro

Financial support:
Ph.D grant – SFRH / BD / 61903 / 2009

Table of Contents

Acknowledgements

I would like to acknowledge:

- my supervisors Dr. Ricardo Boavida Ferreira, Dr. Ana Maria Lourenço and Dr. Sara Monteiro for accepting me as their student and for the great support over these years.

- all those who directly or indirectly contributed to this work, colleagues, friends and family.

- FCT for funding.

Abbreviation List

ACT	Actin
AR	Anthocyanidin reductase
BLAST	Basic Local Alignment Search Tool
BMGY	Buffered complex glycerol medium
BMMY	Buffered complex methanol medium
CAD	Coniferyl-alcohol dehydrogenase
CaOMT	Caffeic acid *O*-methyltransferase
CBS	Centraal bureau, Schimmelcultures
CCR	Cinnamoyl-CoA reductase
CEV	*Consumo Em Verde*, S.A.
ConGlu	Coniferin beta-glucosidase
Ct	Cycle threshold
CTAB	Hexadecyltrimethyl ammonium bromide
CYP	Cyclophilin
DDCA	Dehydrodiconiferylalcohol
DFR	Dihydroflavonolreductase
DIR	Dirigent proteins
DMSO	Dimethyl sulfoxide
E	PCR amplification efficiency
EDTA	Ethylenediaminetetraacetic acid
EF1	Elongation factor 1 α
F5H	Ferulate-5-hydroxylase
GGCE	Guaiacylglycerol 8-*O*-4'-coniferyl ether
HPLC	High performance liquid chromatography
IMAC	Immobilized metal affinity chromatography
KEGG	Kyoto Encyclopedia of Genes and Genomes
L2	Ribosomal protein L2
MAPK	Mitogen activated protein kinase
MHA	Mueller-Hinton Agar
MIC	Minimum inhibitory concentration
NCBI	National Center for Biotechnology Information
NF	Normalization factors
ORF	Open reading frame
PAGE	Polyacrylamide gel electrophoresis
PAL	Phenylalanine ammonia lyase
PAMPs	Pathogen-associated molecular patterns
PDA	Potato Dextrose Agar
PEP	Phosphoenolpyruvate carboxylase
PMSF	Phenylmethylsulfonylfluoride
PRR	Pinoresinol reductase
PTI	PAMP-triggered immunity

qRT-PCR	Quantitative reverse transcription polymerase chain reaction
SAR	Systemic acquired resistance
SDS	Sodium dodecyl sulfate
SSH	Suppressive subtraction hybridization
STS	Stilbene synthase
SV	Stability value
TFA	Trifluoroacetic acid
YPD	Yeast extract peptone dextrose
UBC	Ubiquitin conjugating enzyme
UDP-GT	Coniferyl-alcohol glucosyltransferase
UFGT	UDP-glucose:flavonoid 3-*O*-glucosyltransferase
VAG	vacuolar ATPase subunit G
VBA	Visual Basic Application
WoL	Window-of-linearity

Abstract

Abstract

Grapevine is one of the most cultivated fruit crop worldwide with *Vitis vinifera* being the species with the highest economical importance due to the high quality standards of its berries. Nonetheless, it is also the most susceptible *Vitis* species to fungal pathogens. Among others, relevant fungal diseases currently threatening grapevine cultures are powdery mildew, caused by *Erysiphe necator*, and esca, a disease complex comprised of several fungi in which *Phaeomoniella chlamydospora* and *Phaeoacremonium aleophilum* participate. The increased tolerance of *E. necator* to fungicides together with the rapid expansion of esca in the vineyards, pose them as serious problems to worldwide viticulture. Regardless of what the future solution for these problems will be, an increased understanding on the molecular aspects underlying pathogenesis and the defence mechanisms of the host is required.

In this study, we explored several aspects of *V. vinifera* secondary metabolism in the plant-pathogen interaction context, attempting to provide new information to our current knowledge on the grapevine defences.

Common approaches to study plant-pathogen interactions often involve, at least at one point, transcriptomic analysis and gene transcript quantification. Nevertheless, accurate gene transcript quantification strongly relies on appropriate reference gene selection for sample normalization. As a tool for this work and forthcoming gene expression studies on grapevine, we determined the most suitable reference genes, among a set of selected candidates, to be used in grapevine samples during biotic and abiotic stresses considered relevant for the species. Although the expression stability of the candidate genes was slightly affected by different stimuli on the same tissue, bigger changes are observed when comparing two different tissues. Therefore, a careful

selection of the reference genes must be performed prior to any gene expression study.

In a second task, an attempt was made to characterize, at a transcriptomic level, the compatible interaction between *V. vinifera* and *E. necator* following a long term interaction. We identified several genes of the host, mainly related to secondary metabolism and/or signalling pathways. The nature of those genes, as well as their up or downregulation in infected leaves, evidences both the plant attempt to fight the pathogen and potential host manipulation by the fungus. Among those genes, a gene encoding a dirigent (DIR) protein (*VvDIR1*) was highly upregulated in infected leaves. Hypothesizing an important role of *Vv*DIR1 in pathogenesis, following tasks addressed directly or indirectly the physiological role of *Vv*DIR1 and other DIR/DIR-like genes encoded in *V. vinifera* genome. Analysis of *Vv*DIR1 putative metabolic neighbourhood transcripts did not correlate with the high overtranscription observed for *Vv*DIR1, suggesting physiological functions other than the predicted. Although we confirmed its expected function, the previous hypothesis was not ruled out.

Following work was focused on the remaining *Vv*DIR family, involving evaluation of tissue specific transcription, response to stress and possible participation on the stilbenoid biosynthetic pathway, namely in the regioselective control of *trans*-resveratrol dimerization. *V. vinifera* genome analysis revealed that grapevine encodes the second largest DIR family described to date. Most of the analyzed *Vv*DIR genes were expressed ubiquitously in plant organs but evidence of tissue specific expression was also observed. No fungal induced transcription was detected for the other analyzed *Vv*DIR genes. *Vv*DIR candidates, selected for recombinant expression, were also not active towards resveratrol. In a final attempt to detect guiding activity in resveratrol dimerization, protein extracts from leaves and canes were analyzed. While leaves showed no influence in the

reaction, the canes displayed regioselective activity during resveratrol dimerization. The unexpected formation of a new symmetric trans-resveratrol dimer has occurred.

Finally, as a complementary task, we evaluated grapevine methanolic extracts as well as isolated phenolic compounds (hydroxycinnamic and stilbene derivatives) for their antimicrobial activity against fungal pathogens affecting grapevine and human pathogenic bacteria. Interesting results were obtained for some stilbene derivatives which displayed a high toxicity against gram-positive bacteria.

Resumo

A videira é uma das principais culturas a nível mundial, sendo a *Vitis vinifera* a espécie com maior importância económica devido à qualidade elevada das suas uvas. No entanto, é também a espécie de *Vitis* mais susceptível ao ataque de fungos patogénicos. Entre as várias doenças fúngicas que ameaçam actualmente esta cultura, o oídio, causado pelo fungo *Erysiphe necator*, e a esca, uma doença provocada por um complexo de vários fungos onde se incluem, com um papel importante, os fungos *Phaeomoniella chlamydospora* e *Phaeoacremonium aleophilum*, encontram-se entre as mais relevantes.

A evolução de mecanismos de resistência aos fungicidas actualmente apresentados por *E. necator,* associada a uma rápida expansão da esca acarretam sérios problemas para o futuro da viticultura mundial. Independentemente da solução que se possa encontrar para o controlo destas doenças, é imperativo conseguir uma melhor compreensão dos aspectos moleculares subjacentes aos mecanismos de patogenicidade e de defesa do hospedeiro.

No trabalho associado a esta dissertação de doutoramento, foram analisados vários aspectos do metabolismo secundário de *V. vinifera* no contexto da interacção planta-agente patogénico, numa tentativa de aumentar o conhecimento actual sobre os mecanismos envolvidos na defesa da videira a estes agentes.

As abordagens comuns para estudar interacções hospedeiro-agente patogénico envolvem, muitas vezes, a análise do transcritoma e a quantificação da expressão génica. No entanto, ambos os estudos dependem fortemente de uma selecção cuidadosa dos genes de referência mais adequados para proceder à normalização dos resultados obtidos. Como base para os estudos de expressão génica deste trabalho, identificaram-se os genes de referência mais estáveis, dentro de um conjunto de possíveis candidatos, seleccionados em amostras de videira

sujeitas a stresses bióticos e abióticos. Embora se tenha verificado que a estabilidade destes genes era ligeiramente afectada por estímulos diferentes sobre o mesmo tecido, foram observadas maiores alterações quando se compararam dois tecidos diferentes do que quando se estudaram estímulos distintos. Como tal, a selecção correcta dos genes de referência pode ser a chave do sucesso de qualquer estudo de expressão de genes.

Numa segunda etapa deste trabalho, foi efectuada uma tentativa de caracterizar, a nível do transcritoma, a interacção compatível *V. vinifera* - *E. necator* após uma exposição prolongada do hospedeiro ao fungo. Foram identificados vários genes do hospedeiro, especialmente alguns relacionados com o metabolismo secundário e / ou com vias de sinalização. A natureza destes genes, bem como a sua regulação positiva ou negativa em folhas infectadas, evidencia tanto a tentativa das plantas para combater o agente patogénico como a manipulação das células do hospedeiro pelo fungo. Entre esses genes, o gene que codifica uma proteína dirigente (DIR; *VvDIR1*) foi identificado, tendo-se posteriormente verificado ser fortemente regulado em folhas infectadas, levantando a hipótese se deverá desempenhar um papel importante no mecanismo de patogenicidade.

O trabalho prosseguiu com a realização de diferentes estudos para que, directa ou indirectamente, fosse possível determinar o papel fisiológico do gene *VvDIR1* e de outros genes que codificam para proteínas dirigentes anotadas no genoma de *V. vinifera*. A análise de transcritos de genes na hipotética vizinhança metabólica de *Vv*DIR1 não demonstrou existir uma correlação com a sua sobre-expressão elevada, sugerindo funções fisiológicas diferentes das que inicialmente se tinham considerado.

A sequência dos estudos seguintes focou-se em vários dos restantes membros da família *Vv*DIR de videira, envolvendo a avaliação da sua expressão específica nos diferentes tecidos da planta, na resposta ao

stresse e na sua possível participação na via biossintética dos estilbenóides, ou seja, no controle regio-selectivo da dimerização do *trans*-resveratrol. A análise do genoma de *V. vinifera* revelou que esta espécie codifica a segunda maior família de proteínas dirigentes descritas até hoje. No entanto, a maioria dos genes *VvDIR* analisados é expresso ubiquamente nos diferentes órgãos das plantas, embora tenham sido encontradas evidências para uma expressão específica e dependente do tecido em estudo. Não foi possível detectar uma indução da expressão dos genes analisados em resposta ao ataque dos fungos em estudo. Da mesma forma, não foi possível co-relacionar a expressão de nenhum destes genes seleccionados para produção heteróloga com a dimerização do resveratrol. Numa última tentativa para detectar actividade na dimerização direccionada do resveratrol, foram analisados extractos proteicos de folhas e ramos de videira. Enquanto os extractos das folhas não tiveram qualquer influência na reacção que se processou *in vitro*, os extractos dos ramos apresentaram uma actividade regio-selectiva bastante significativa no processo de dimerização do resveratrol, ocorrendo a formação inesperada de um novo dímero simétrico de trans-resveratrol, não descrito na literatura.

Finalmente e como uma tarefa complementar, foi avaliada a actividade antimicrobiana de extractos metanólicos de videira e de compostos fenólicos isolados (derivados hidroxicinâmicos e estilbenos) contra fungos patogénicos que afectam a videira e bactérias patogénicas humanas, tendo-se obtido resultados muito interessantes para alguns derivados dos estilbenos que exibem uma elevada toxicidade contra as bactérias gram-positivas.

Chapter I: Introduction

Introduction

Grapevine (*Vitis* species) may have been used by mankind since the early existence of modern man [1]. Apparently, fruits of wild *Vitis* were already used by pre-historic civilizations long before its domestication [2]. Exactly when and where domestication took place is unknown but it appears to have occurred between the seventh and fourth millennia BC in a geographical area between the Black Sea and Iran [3]. *V. vinifera* is originated from its ancestor *V. silvestris and* is the single *Vitis* species that acquired significant economic interest over time [3,4]. The domestication process has had impact on several agronomic traits of the species including size of the berries, sugar content and production yields [5]. However, it could not account for resistance to pathogens which did not coexist with the host.

The most dramatic examples of *V. vinifera* pest and disease susceptibility concern the sequential arrival in Europe of three major problems in the nineteenth century: powdery mildew, phylloxera and downy mildew [6]. All were native from North America and had devastating consequences by the time they were introduced in Europe [6-8]. Phylloxera (*Daktulosphaira vitifoliae*), an aphid parasite feeding on *Vitis* species, colonizes the roots of the plant forming root galls which act as nutrient reservoirs for the colony. While in susceptible natural hosts (American species) those galls or nodosities are superficial, in *V. vinifera* they develop on metabolically active parts of the plant, destroying the whole root system upon infestation with the insect [9].

Some American *Vitis* species, such as *V. riparia* and *V. rupestris* are resistant to phylloxera [10]. They were part of the only viable, now well implemented, solution against phylloxera: grafting *V. vinifera* aerial parts on resistant rootstocks, and thus preserving desirable agronomic traits [11].

American *Vitis* are also regarded as resistant to *Erysiphe necator* and *Plasmopara viticola*, the causal agents of powdery mildew and downy mildew, respectively [12]. However, these pathogens infect the aerial, photosynthetic tissues of the plant [6,13]. In the same way phylloxera epidemics “could not” be addressed by replacing *V. vinifera* with American *Vitis* species, in the case of powdery mildew and downy mildew, microbial control was, and still is, achieved by massive application of fungicides [13,14].

Although phylogenetically distinct (*E. necator* – Ascomycota; *P. viticola* – Oomycota), both pathogens can be similar in several aspects. They are specific (or compatible) to the same host, infect the same tissues of the plant (green tissues including leaves, berries and young shoots) and share the same nutritional lifestyle (obligate biotrophs) [6,13]. They constitute a well known example of convergent evolution. Chemical control has been achieved differently for each pathogen, using sulfur-based compounds for powdery mildew [15] and copper formulations for downy mildew [14]. However, there are also examples of fungicides effective against both pathogens [16]. Being obligate biotrophs, these pathogens fully rely on living plant tissues for their survival [17]. Therefore, they must be able to invade the plant with minimal damage to the host´s cells while extracting the necessary nutrients for their growth and propagation [18].

Infection is usually limited to the epidermis of the host and the actual invasion is accomplished by the use of a high precision chemical drilling mechanism [18]. In fact, the penetration of only a single host cell can be sufficient for abundant mycelium formation leading to the successful sporulation of the colony [19]. Nutrient depletion from host is achieved by the use of highly specialized infection structures called haustoria, which develop inside the plant cell [20]. The role of these fungal organs goes far beyond the simple nutrient depletion of the host. Apparently, these sophisticated structures are the “control room” of the infection, being able

to redirect the host's metabolism to fulfil the nutritional needs of the pathogen at the same time they manipulate the plant defences and/or recognition mechanisms [17]. An impressive demonstration of gene expression control over the host is the so-called green island effect [21]: a detached barley leaf was inoculated with *Blumeria graminis* (responsible for barley powdery mildew) on one side and then placed in darkness to accelerate senescence of the leaf. Only those cells underneath the fungal colony on the uninoculated side remained green, indicating that the fungus was capable of actively suppressing senescence of the host tissue.

The remarkable complexity of biotrophic host-pathogen interactions, their particular consequences in grapevine cultures and their recent increased fungicide resistance, make *E. necator* and *P. viticola* priority research areas in worldwide viticulture.

Apart from the biotrophic mildews, affecting the aerial parts of the plant, other problematic grapevine diseases concern the fungal colonization of the woody parts of the plant. Esca disease is a complex grapevine wood disease which is achieving an unprecedented and increasing worldwide importance. Consequences of the disease, caused by colonization and blocking of the vascular part of the plant, include poor growth, decline and dieback of the vineyards [22,23].

All species of *Vitis* and cultivars of *V. vinifera* are believed to be susceptible to esca, including American vines. First thought as affecting only mature grapevines, concern arises as the disease can now be frequently found in much younger plants [24-26]. Moreover, infected plants can remain externally asymptomatic for several years while the disease slowly progresses [23,24]. Present understanding on esca disease has shown that it comprises a number of distinct diseases caused by at least three fungi, *Phaeomoniella chlamydospora*, *Phaeoacremonium aleophilum* [23,27,28] and *Fomitiporia mediterranea* [29-31], acting alone, in combination or in succession [23,24]. The first two ascomycetes are

responsible for vascular necroses, while the other is responsible for wood decay [24,32]. The fact this disease can be asymptomatic for long periods of time, allowing dissemination, together with the fact that no efficient cure exists [33], poses Esca as a serious threat to the viticulture in future years.

Increasing public concern over the widespread use of toxic, chemical fungicides, the decreasing number of commercially available efficient fungicides, and the advent of grapevine wood diseases raises serious doubts about the future of worldwide viticulture. The specific and intricate molecular interactions which underly each host – fungal pathogen interaction for the establishment of pathogenesis, including attempts to modulate each other´s gene expression, calls for a change from chemical to biological control.

In the last years, our understanding of molecular aspects of grapevine-fungal interactions has increased largely. However, a fair deal of work remains to be done, to precisely decipher and characterize the mechanisms of pathogen detection and the subsequent activation of host's defences.

Unraveling the nature of biomolecules essential for pathogen virulence or plant defence and the chemical synthesis of bioactive homologues, together with molecular engineering methodologies capable of speeding up the achievements of natural evolution, will probably constitute one of our translational tools to shape the future of food production.

In this Thesis, an attempt was made to improve our current knowledge on *V. vinifera* secondary metabolism in a plant-pathogen context. With several studies relying on a transcriptomic approach, we initially determined suitable reference genes for accurate qRT-PCR gene expression quantification in grapevine samples under relevant biotic and abiotic stimuli. Next, we characterized the long term interaction between *V. vinifera* and *E. necator*, determining host genes that were differentially expressed upon infection. Following work focused mainly on assessing

the potential role of *Vv*DIR in grapevine defence mechanisms and secondary metabolism. First, we investigated the function of *Vv*DIR1, a highly induced gene upon powdery mildew infection. Secondly, we explored the remaining members of *Vv*DIR family for possible connections with the stilbenoid biosynthetic pathway. In a third approach, we analyzed grapevine protein extracts for the presence of DIR/DIR-like activity towards the stilbenoid resveratrol. Finally, we evaluated the antimicrobial potential of the grapevine phenolic content, including isolated phenolic compounds, against several microorganisms comprising grapevine and human pathogens.

Given specificity of some of the issues addressed in this Thesis, a detailed introduction on each topic can be found on the corresponding Chapter.

References

1. McGovern P (2003) Ancient wine: The search for the origins of viniculture: Princeton University Press.
2. Zohary D, Spiegel-Roy P (1975) Beginnings of fruit growing in the old world. Science 187: 319-327.
3. Terral J-F, Tabard E, Bouby L, Ivorra S, Pastor T, et al. (2010) Evolution and history of grapevine (*Vitis vinifera*) under domestication: new morphometric perspectives to understand seed domestication syndrome and reveal origins of ancient european cultivars. Annals of Botany 105: 443-455.
4. Bouby L, Figueiral I, Bouchette A, Rovira N, Ivorra S, et al. (2013) Bioarchaeological insights into the process of domestication of grapevine (*Vitis vinifera* L.) during roman times in southern France. PLoS ONE 8: e63195.
5. Nicole S, Barcaccia G, Erickson D, Kress J, Lucchin M (2013) The coding region of the *UFGT* gene is a source of diagnostic SNP markers that allow single-locus DNA genotyping for the assessment of cultivar identity and ancestry in grapevine (*Vitis vinifera* L.). BMC Research Notes 6: 502.

6. Gessler C, Pertot I, Perazzolli M (2011) *Plasmopara viticola* : a review of knowledge on downy mildew of grapevine and effective disease management. Phytopathologia Mediterranea 50: 3-44.
7. Hawthorne DJ, Via S (1994) Variation in performance on two grape cultivars within and among populations of grape phylloxera from wild and cultivated grapes. Entomologia Experimentalis et Applicata 70: 63-76.
8. Frenkel O, Brewer MT, Milgroom MG (2010) Variation in pathogenicity and aggressiveness of *Erysiphe necator* from different *Vitis* spp. and geographic origins in the eastern united states. Phytopathology 100: 1185-1193.
9. Kellow AV, Sedgley M, Van Heeswijck R (2004) Interaction between *Vitis vinifera* and grape phylloxera: changes in root tissue during nodosity formation. Annals of Botany 93: 581-590.
10. Granett J, Walker MA, Kocsis L, Omer AD (2001) Biology and management of grape phylloxera. Annual Review of Entomology 46: 387-412.
11. Gale G (2002) Saving the vine from phylloxera: a never-ending battle. In: Sandler M, Pinder R, editors. Wine, a scientific exploration: CRC Press. pp. 70-91.
12. Ferreira RB, Monteiro S, Freitas R, Santos CN, Chen Z, et al. (2006) Fungal pathogens: The battle for plant infection. Critical Reviews in Plant Sciences 25: 505-524.
13. Gadoury DM, Cadle-Davidson L, Wilcox WF, Dry IB, Seem RC, et al. (2012) Grapevine powdery mildew (*Erysiphe necator*): a fascinating system for the study of the biology, ecology and epidemiology of an obligate biotroph. Molecular Plant Pathology 13: 1-16.
14. Gisi U, Sierotzki H (2008) Fungicide modes of action and resistance in downy mildews. European Journal of Plant Pathology 122: 157-167.
15. Gadoury DM, Pearson RC, Riegel DG, Seem RC, Becker CM, et al. (1994) Reduction of powdery mildew and other diseases by over-the-trellis applications of lime sulfur to dormant grapevines. Plant Disease 78: 83-87.
16. Reuveni M (2001) Activity of trifloxystrobin against powdery and downy mildew diseases of grapevines. Canadian Journal of Plant Pathology 23: 52-59.

17. Panstruga R (2003) Establishing compatibility between plants and obligate biotrophic pathogens. Current Opinion in Plant Biology 6: 320-326.
18. Keller M (2010) Chapter 7 - Environmental constraints and stress physiology. In: Keller M, editor. The science of grapevines. San Diego: Academic Press. pp. 227-310.
19. Shirasu K, Nielsen K, Piffanelli P, Oliver R, Schulze-Lefert P (1999) Cell-autonomous complementation ofmloresistance using a biolistic transient expression system. The Plant Journal 17: 293-299.
20. Perfect SE, Green JR (2001) Infection structures of biotrophic and hemibiotrophic fungal plant pathogens. Molecular Plant Pathology 2: 101-108.
21. Schulze-Lefert P, Vogel J (2000) Closing the ranks to attack by powdery mildew. Trends in Plant Science 5: 343-348.
22. Rumbou A, Rumbos I (2001) Fungi associated with esca and young grapevine decline in Greece. Phytopathologia Mediterranea 40.
23. Mugnai L, Graniti A, Surico G (1999) Esca (black measles) and brown wood-streaking: Two old and elusive diseases of grapevines. Plant Disease 83: 404-418.
24. Surico G, Mugnai L, Marchi G (2006) Older and more recent observations on esca: a critical overview. Phytopathologia Mediterranea 45: S68-S86.
25. Surico G, Mugnai L, Marchi G (2008) The esca disease complex integrated management of diseases caused by fungi, phytoplasma and bacteria. In: Ciancio A, Mukerji KG, editors: Springer Netherlands. pp. 119-136.
26. Romanazzi G, Murolo S, Pizzichini L, Nardi S (2009) Esca in young and mature vineyards, and molecular diagnosis of the associated fungi. European Journal of Plant Pathology 125: 277-290.
27. Crous PW, Gams W (2000) *Phaeomoniella chlamydospora* gen. et comb. nov., a causal organism of petri grapevine decline and esca. Phytopathologia Mediterranea 39: 112-118.
28. Crous PW, Gams W, Wingfield MJ, vanWyk PS (1996) *Phaeoacremonium* gen nov associated with wilt and decline diseases of woody hosts and human infections. Mycologia 88: 786-796.

29. Cortesi P, Fischer M, Milgroom MG (2000) Identification and spread of *Fomitiporia punctata* associated with wood decay of grapevine showing symptoms of esca. Phytopathology 90: 967-972.
30. Fischer M (2002) A new wood-decaying basidiomycete species associated with esca of grapevine: *Fomitiporia mediterranea* (Hymenochaetales). Mycological Progress 1: 315-324.
31. Fischer M (2006) Biodiversity and geographic distribution of basidiomycetes causing esca-associates white rot in grapevine : A worldwide perspective. Phytopathologia Mediterranea 45: S30-S42.
32. Luque J, Martos S, Aroca A, Raposo R, Garcia-Figueres F (2009) Symptoms and fungi associated with declining mature grapevine plants in northeast Spain. Journal of Plant Pathology 91: 381-390.
33. Andolfi A, Mugnai L, Luque J, Surico G, Cimmino A, et al. (2011) Phytotoxins produced by fungi associated with grapevine trunk diseases. Toxins 3: 1569-1605.

Chapter II: Reference Gene Validation for Quantitative RT-PCR during Biotic and Abiotic Stresses in *Vitis vinifera*

This chapter was adapted from the following manuscript:

Borges AF, Fonseca C, Ferreira RB, Lourenço AM, Monteiro S (2014) Reference gene validation for quantitative RT-PCR during biotic and abiotic stresses in *Vitis vinifera*. PLoS ONE 9: e111399.

Author contribution:

AFB performed the majority of the experimental work and wrote the manuscript.

Abstract

Quantitative reverse transcription polymerase chain reaction (qRT-PCR) is currently amongst the most powerful techniques to perform gene expression studies. Nevertheless, accurate gene expression quantification strongly relies on appropriate reference gene selection for sample normalization. Concerning *Vitis vinifera*, limited information still exists as for which genes are the most suitable to be used as reference under particular experimental conditions. In this chapter, seven candidate genes were investigated for their stability in grapevine samples referring to four distinct stresses (*Erysiphe necator*, wounding and UV-C irradiation in leaves and *Phaeomoniella chlamydospora* colonization in wood). The expression stability was evaluated using geNorm, NormFinder and BestKeeper. In all cases, full agreement was not observed for the three methods. To provide comprehensive rankings integrating the three different programs, for each treatment, a consensus ranking was created using a non-weighted unsupervised rank aggregation method. According to the last, the three most suitable reference genes to be used in grapevine leaves, regardless of the stress, are *UBC*, *VAG* and *PEP*. For the *P. chlamydospora* treatment, *EF1*, *CYP* and *UBC* were the best scoring genes. Acquaintance of the most suitable reference genes to be used in grapevine samples can contribute for accurate gene expression quantification in forthcoming studies.

Introduction

Among the several existing techniques to analyze mRNA levels, quantitative reverse transcription polymerase chain reaction (qRT-PCR) is currently the most widely used due to its high sensitivity and reproducibility [1]. However, accurate gene expression quantification strongly relies on appropriate reference gene selection for sample normalization [2-4]. Though this requirement has always been an important criterion for gene expression quantification studies, during the early stages of qPCR expansion and data analysis development, reference gene selection was rather based on assumptions more than evidence on expression stability. As consequence, several studies might have been conducted using unsuitable or unvalidated reference genes [5,6]. Recent awareness regarding this matter has lead to an increasing number of studies whose main objective is to evaluate the expression stability of candidate genes for normalization in qPCR analysis [7-10]. Under the most diverse experimental conditions, including a variety of organisms or tissues and a multitude of biotic and abiotic stimulus, such analysis can provide a valuable tool for accurate gene expression quantification in forthcoming studies. To assess the gene expression stability of potential reference genes, several programs and statistical algorithms have been developed, facilitating the analysis and selection of suitable reference genes for the desired experimental condition. geNorm, NormFinder and BestKeeper are among the most widely used algorithms [2,11,12]. With respect to *Vitis vinifera*, a non-model organism, some studies have already been conducted in order to evaluate and validate qRT-PCR reference genes to be used during different developmental stages in berries or abiotic stresses in leaves such as drought and temperature [13-15]. Concerning biotic stresses, reference genes suitable either for the early or later stages of infection with *Plasmopara viticola* (downy mildew) have also been evaluated [6,16,17].

For the most part, studies on stress conditions affecting plants often include extreme temperatures, drought, pathogen attack, UV-C irradiation and wounding [18]. Nevertheless, for *V. vinifera* species, still no information exists referring to reference gene expression stability during potentially relevant stresses such as *Phaeomoniella chlamydospora* infection, wounding and UV-C irradiation.

Grapevine diseases caused by fungal pathogens, can have a major agricultural impact. Both *E. necator* and *P. chlamydospora* are among the most concerning species. While the former, the causal agent of powdery mildew, infects all the green tissues of the plant, the second is a wood colonizing fungus, known to participate in the esca disease complex. Taken together, these diseases account for huge economical losses and, therefore, represent priority research areas [19-21].

Due to their sessile nature, plants are permanently exposed to a wide range of structurally damaging agents which include environmental stresses such as wind, rain or hail, and herbivore attack. Wound occurrence is inevitable and, besides compromising the physical structure of the plant, it constitutes a potential infection site for pathogens [18,22]. To cope with this dual threat, plants might have evolved to integrate both wounding and pathogen response. In fact, some studies have already demonstrated that both stresses can share common signaling pathways and, moreover, regulate the same stress responsive genes. For this reason, wound response stands as an important area of interest in plant studies [23,24].

As for the UV-C stimulus, though such short wavelength radiation is not likely to reach the ground, it has been shown, in several species, that UV-C irradiation can enhance host resistance to pathogens [25]. In addition, and in the particular case of *V.vinifera*, apart from increasing disease resistance, UV-C was shown to induce the accumulation of several phenolic defense-related compounds, including resveratrol and other

stilbene derivatives. Thus, UV-C irradiation constitutes a practical experimental model to study plant defense responses [26,27].

Given the relevance of gene expression studies and the still scarce information regarding suitable reference genes for qPCR analysis in grapevine samples, we aimed to determine the most stable reference genes, among seven candidates, during four distinct stresses: *E. necator* infection, *P. chlamydospora* inoculation, wounding and UV-C irradiation.

Materials and Methods

Plant material and growth conditions

Grapevine (*Vitis vinifera* L., cultivar Touriga Nacional) cuttings used in the experiment were collected from Centro Experimental de Pegões, Portugal and subjected to heartwood disease screening through microbiology assays. Sample collection was gently and duly authorized by Dr. Antero Martins, Associação Portuguesa para a Diversidade da Videira (PORVID), Portugal. The microbiologic screening was performed using the bottom of the cuttings. Thin wood slices were removed from each cutting, surface-sterilized (ethanol, flame and sodium hypochlorite) and then placed in 0.03% (w/v) chloramphenicol-containing potato dextrose agar (PDA) medium (five slices per cutting). The plates were incubated at room temperature for a maximum period of one month, during which morphological identification of the microorganisms present in the wood was performed. Diseased cuttings were discarded.

Healthy *V. vinifera* cuttings, with three buds each, were rooted in water and then transferred to soil (1 L pot per plant). Plants were maintained in a growth chamber at 25 ºC with a photoperiod of 16 h (480 $\mu mol.m^{-2}.s^{-1}$). After one month of acclimatization period, whole plants or detached leaves were subjected to the different treatments

Plant treatments

For the powdery mildew (PM) treatment, all plants within the same growth chamber were simultaneously inoculated with *E. necator* by direct contact with naturally infected grapevine leaves. The primary inoculum was collected from a vineyard in Instituto Superior de Agronomia, Lisbon, Portugal and passed to a set of grapevines in greenhouse which provided the experimental inoculum source. Plants were allowed to grow with generalized powdery mildew infection for 30 days prior to sample collection. Fully expanded leaves (fourth and fifth positions from the tip of each shoot) with and without *E. necator* infection symptoms (visible mycelia on the upper leaf surface) were harvested.

For the wounding treatment, fully expanded leaves were cut using a sterile razor blade. Each leaf was subjected to six 1 cm-long cuts and collected 24h after the treatment. Control samples were left untreated and maintained under the same conditions.

For the UV irradiation treatment, leaves were detached and their undersides were exposed to UV-C radiation (Philips TUV 30 W, 92 μW cm-2 at 253 and 7 nm) at a distance of 15 cm from the source during 10 min. Following irradiation, treated and control samples were incubated in a dark wet chamber at room temperature for 48h.

For the *Phaeomoniella chlamydospora* treatment, a pure fungal isolate was obtained from CBS (CBS 239.74) and propagated in PDA medium at 23ºC in the dark. Inoculation was performed at the base of the primary shoot by removing a small section of the bark with a scalpel and placing a 5 mm inoculation plug (sliced from the actively growing margin of the fungal colony) into the wound (mycelium side down). Each wound was then covered with moist cotton wool and sealed with parafilm. The same procedure was followed for negative control plants using non inoculated PDA plugs. Plants were maintained under the above described conditions for one week prior to sample collection.

Following the mentioned incubation periods for individual treatments, all samples were harvested and immediately frozen in liquid nitrogen. Biological replicates for all treatments and corresponding controls were created by pooling either four leaves or two 5 cm-long stem sections per sample.

RNA extraction and cDNA synthesis

Total RNA extraction was performed using the Rapid CTAB (hexadecyltrimethyl ammonium bromide) method, especially suited for high phenolic content material, adapted as follows [28]. Biological samples were ground in liquid nitrogen, homogenized at approximately 150 mg per mL in extraction buffer (2% (w/v) CTAB, 2.5% (w/v) polyvinylpoly-pyrrolidone (PVPP), 2 M NaCl, 100 mM Tris-HCl pH 8.0, 25 mM ethylenediaminetetraacetic acid (EDTA), 2% (v/v) β-mercaptoethanol) and incubated at 65 ºC for 10 min. Samples were extracted twice with one volume of chloroform:isoamylic alcohol (24:1, v/v) and centrifuged at 12,000 *g* during 10 min at 4 ºC. The recovered aqueous phase was supplemented with ¼ volume of 10 M LiCl and incubated during 30 min at 4 ºC. RNA was collected by centrifugation at 21,000 *g*, 4 ºC during 20 min, and resupended in 500 μL of pre-warmed (65 ºC) SSTE buffer (0.5% w/v sodium dodecyl sulfate (SDS), 1 M NaCl, 10 mM Tris-HCl pH 8.0, 1 mM EDTA). Samples were again extracted with one volume of chloroform:isoamylic alcohol (24:1, v/v) followed by centrifugation at 12,000 *g* during 10 min. The recovered supernatant was supplemented with 0.7 volumes of cold isopropanol and immediately centrifuged at 21,000 *g*, 4 ºC during 15 min. RNA *pellet* was washed with 70% (v/v) ethanol and resuspended in water. Prior to reverse transcription, samples were treated with RQ1 RNase-Free Dnase (Promega) according to the manufacturer's protocol.

All samples were reverse transcribed using ThermoScript RT-PCR System (Invitrogen) as described by the manufacturer. cDNA was synthesized from 1.5 μg of total RNA and oligo(dT)$_{20}$ primers. RT reactions were carried at 55 ºC for 60 min.

Primer design and qPCR

PCR primers were designed with Beacon Designer software (Premier Biosoft International) to target amplicons between 80 and 300 bps. Amplification specificity was first assessed though Primer-BLAST (http://www.ncbi.nlm.nih.gov/tools/primer-blast/) using *V.vinifera* database as template. qPCR was performed with iQ SYBR Green supermix (Bio-Rad) using iCycler equipment (Bio-Rad). Prior to use, cDNA samples were diluted to 50 ng/μL. Reaction mixtures (20 μL) were prepared according to the following: 5 μL of the diluted template, 1 μL primer mix (10 μM each), 10 μL iQ SYBR Green supermix (Bio-Rad), 4 μL H_2O. Thermal cycling was composed of an initial denaturation step for 3 min at 95 ºC, 40 cycles at 95 ºC for 10 s, 55 ºC for 30 s and 72 ºC for 30 s. All reactions were performed in triplicate and amplification specificity was confirmed through melting curve analysis.

Data analysis

Raw data (i.e. not baseline-corrected) belonging to each individual amplification curve were imported from iQ5 into LinRegPCR software (version 11.0) for baseline and PCR efficiency estimation. Log-linear phases were automatically determined containing four to six points with the highest correlation coefficient. According to the obtained linear regressions, individual PCR amplification efficiencies were calculated. Student's *t*-test was used to compare amplification efficiencies of each amplicon between treated samples and corresponding controls of the same treatment ($P < 0.05$). Since no differences were observed, mean efficiencies for each amplicon within each treatment were used for

subsequent analysis. *Ct* values were retrieved using a fluorescence threshold defined within a common window-of-linearity (WoL) for each dataset.

To evaluate the expression stability of the selected candidate genes for the different stimuli, three different Visual Basic Application (VBA) applets for Microsoft Excel were used: geNorm v.3.5 [2], NormFinder v. 0953 [11] and BestKeeper [12]. Input file creation and subsequent data analysis was performed according to the corresponding manuals. For both GeNorm and NormFinder software, *Ct* values were transformed into relative quantities (amplification efficiency corrected) using the lowest *Ct* sample as calibrator. For BestKeeper analysis, raw *Ct* values as well as PCR amplification efficiencies were directly inserted into the software.

Consensus ranks, integrating the results of the different algorithms, were generated using a non-weighted unsupervised rank aggregation method. Data analysis was carried out using the RankAggreg v. 0.4-3 package [29] for R. RankAggreg input was a matrix of rank-ordered genes according to the different algorithms used. Comprehensive ranks were obtained from the calculated Spearman footrule distances and the Cross-Entropy Monte Carlo algorithm.

Results and Discussion

Expression profile of candidate reference genes

As mentioned above, reference gene validation for qRT-PCR expression studies has become a fundamental requisite for reliable quantification results. To provide information regarding potential reference genes for future use in qRT-PCR studies involving *V. vinifera*, we decided to evaluate the expression stability of a set of commonly used housekeeping genes during four distinct stimuli comprising biotic and abiotic stresses [30-32]. These include powdery mildew infection, mechanical wounding

and UV-C irradiation in leaves and xylem colonization with *P. chlamydospora* in woody tissues. Treatment selection was based on its potential application for future gene expression studies in grapevine. To avoid co-regulation events, candidate genes were chosen taking into consideration their participation in distinct metabolic pathways. Accordingly, the selected candidates for this study were genes encoding cyclophilin (*CYP*), elongation factor 1 α (*EF1*), ribosomal protein L2 (*L2*), phosphoenolpyruvate carboxylase (*PEP*), ubiquitin conjugating enzyme (*UBC*), vacuolar ATPase subunit G (*VAG*) and actin (*ACT*). Following PCR amplification of the selected genes in all biological samples, a general overview of the expression profile and relative abundance of each candidate gene was obtained by plotting the *Ct* values obtained for all samples (control and treatment) under the different conditions studied (Figure 1). *ACT* expression stability upon *E. necator* infection (Figure 1a) was not assessed as it was not initially considered as a candidate for this particular stimulus. The main reasons underlying this choice were related to the nature of this host-pathogen interaction. Likewise, other commonly used reference genes, such as tubulin or glyceraldehyde-3-phosphate dehydrogenase, were not evaluated. Biotrophic pathogens, like *E. necator*, are known for their essential and highly specialized infection structures, the haustoria [33]. Among other functions, haustoria are responsible for the nutrient supply of the pathogen, uptaking amino acids and monosaccharides from the host cells [34].

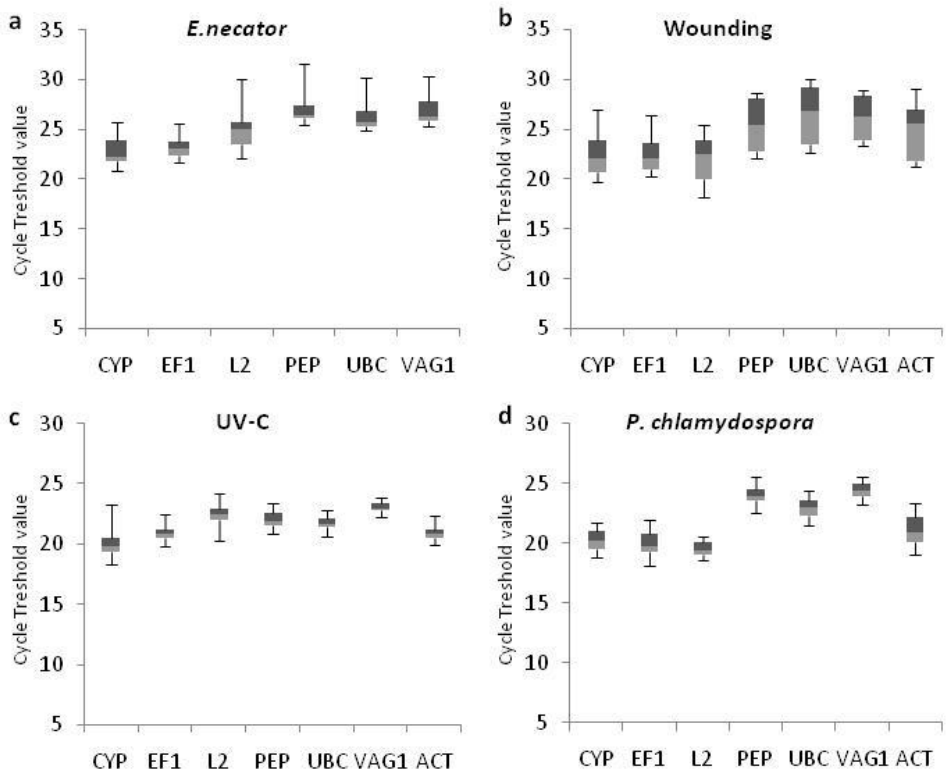

Figure 1. Expression profile of candidate normalization genes in grapevine samples during (a) leaf infection with *E. necator*, (b) leaf wounding, (c) leaf irradiation with UV-C and (d) wood infection with *P. chlamydospora*. Absolute *Ct* values for each treatment and the corresponding controls were combined. Each sample group comprises 5 to 7 biological replicates. The boxes indicate the 25th and 75th percentiles. Lines within the boxes represent the median. Maximum and minimum values are represented by wiskers

Hence, the pathogen is expected to directly and greatly affect carbohydrate pools in the host, making genes encoding glycolytic enzymes such as glyceraldehyde-3-phosphate dehydrogenase highly likely targets for gene transcriptional modulation and therefore unsuitable to be used as reference genes in qRT-PCR. For similar reasons, actin and tubulin were not within the group selected for candidate reference genes. Plant cytoskeleton is well known to play an important role in defense against pathogens, with several studies reporting actin and tubulin rearrangements in the host upon pathogen attack [35].

Regarding *ACT* gene, the the same exclusion arguments could be used for some of the other treatments, namely wounding and *P. chamydospora* infection. Nevertheless, and though contradictory, its expression stability was evaluated for the remaining experiments. The mentioned inconsistency was resultant from a reasonable time lapse occurring between the *E. necator* experiments and the remaining. At the point of the last experiments, it was considered that the expression evaluation of a supposedly "not ideal" reference gene would be useful for comparison purposes.

Concerning the expression profile of the candidate genes, all displayed moderate expression levels with mean *Ct* values ranging from 19.7 to 27.2 for *L2* and *PEP* during *P.chlamydospora* and *E. necator* interactions, respectively. Minimum *Ct* values, meaning higher abundance, were observed for *EF1* (18.1) during *P. chlamydospora* interaction, whilst *PEP* displayed the highest *Ct* (31.6) for *E. necator* treatment. Overall, gene expression variation across samples within each treatment ranged from 1.9 to 7.9 *Ct*s with the highest expression fluctuations being observed for the wounding experiment. Though preliminary information can be obtained through absolute *Ct* analysis, to correctly assess the expression stability of candidate genes, raw amplification data must be first linearized. This was carried out by converting the *Ct* values into relative quantities which were normalized to the sample with the lowest *Ct*.

Primer pair amplification efficiencies

To perform data linearization, PCR amplification efficiencies (*E*) must be taken into consideration, preventing significant bias from being introduced in the generated results [36,37]. *E* values were estimated using the absolute fluorescence increase method (Table 1) [37,38]. LinRegPCR software (version 11.0), developed by Ruijter *et al*., 2009, was used to individually analyze each sample and determine amplification efficiencies

based on a proper baseline correction. Considering that *E* value for one primer pair might differ among stimuli and, moreover, between control and treated samples in the same stimulus, we separately analyzed each sample group.

Table 1. Candidate genes and primer pairs for qRT-PCR normalization in grapevine samples

					PCR amplification Efficiency (*E* %)			
Gene	Accession number	Primer	Sequence 5'-> 3'	Amplicon lenght (bp)	PM[a]	Wound	UV-C	Pch[c]
CYP	ES880796	Fw	ACAGCCAAGACCTCGTG	138	78,8	91,2	91,1	78,3
		Rv	GCCTTCACTGACCACAAC					
EF1	GU585871.1	Fw	GAACTGGGTGCTTGATAGGC	164	86,7	93,1	91,4	77,8
		Rv	AACCAAAATATCCGGAGTAAAAGA					
L2	AJ441290.2	Fw	TCTACTTCAACCGATATGC	199	92,3	93,7	96,3	83,3
		Rv	CCACCTGTCCGACTG					
PEP	AF236126.1	Fw	CCTCCTCCTCCAGATTGC	198	89,6	94,0	97,8	82,9
		Rv	GGCTTGCTTGATTCCATTATC					
UBC	EE253706	Fw	CATAAGGGCTATCAGGAGGAC	161	87,2	92,7	94,8	83,4
		Rv	TGGCGGTCGGAGTTAGG					
VAG	XM_002281110.1	Fw	TTGCCTGTGTCTCTTGTTC	174	91,8	92,3	99,1	84,0
		Rv	TCAATGCTGCCAGAAGTG					
ACT	XM_002282480	Fw	GACTACCTACAACTCCATCAT	113	[b]	94,2	92,6	82,5
		Rv	TCATTCTGTCAGCAATACCA					
PAL[d]	XM_002268220	Fw	TTCCGAACCGAATCAAGG	193	[b]	90,2	91,5	[b]
		Rv	GGAGCACCGTTCCAAGC					

[a] Powdery mildew (*Erysiphe necator*)
[b] Not determined
[c] *Phaeomoniella chlamydospora*
[d] Responsive gene used for differential expression quantification

Though amplification efficiencies for each gene may vary depending on the treatment, no differences ($p < 0.05$) were observed between control and treated samples of the same stimulus. Thus, mean *E* values (Table 1) were used for subsequent analysis.

Reference gene expression stability

Following baseline estimation and amplification curve analysis for all qPCR reactions, the statistical analysis to evaluate the expression stability of the candidate genes was performed using three different programs: geNorm [2], NormFinder [11] and BestKeeper [12]. Though all aim to determine which candidate genes are the most stable under certain conditions, they run under different algorithms and mathematical models. Therefore, the stability ranking of the putative reference genes might differ

depending on the program used [39]. GeNorm analysis relies on the intuitive principle that the expression ratio of two ideal reference genes should always remain constant across all samples. Accordingly, it calculates a gene expression stability measure (M) based on the average pairwise expression ratio between each gene and each of the remaining candidates. It performs a stepwise exclusion of the least stable gene and recalculates M values until only the two best ranked candidates are left. Lower M values are indicative of higher stability. The main drawback of geNorm, and consequently one of the most important criteria to be aware of, is that candidate genes must not be co-regulated. This would introduce significant bias as identically regulated genes tend to be top ranked in geNorm even if their expression levels fluctuate considerably among samples [2]. On the other hand, NormFinder analysis, a model-based variance estimation method, displays less sensitivity to co-regulation events. Expression stability of candidate genes is evaluated according to their overall expression variation among the sample set. For each of the analyzed genes, NormFinder calculates a stability value (SV) according to which a ranking is generated. Similarly to geNorm, a lower SV value is indicative of higher stability [11]. The third and last tool adopted to assess the gene expression stability was BestKeeper software. Unlike the previous methods, input data for this software consists of raw *Ct* values instead of relative quantities. Nevertheless, amplification efficiencies are also considered. The expression variability is assessed through coefficient of variance and standard deviation analysis. The software calculates a "BestKeeper index" referring to each sample and compares the candidate genes based on their pairwise correlation with this index value. Candidates displaying a higher Pearson's correlation coefficient (*r*) correspond to the most stably expressed [12].

Following our gene expression variation analysis over the four particular experimental conditions, the candidate genes were rank ordered

according to the stability parameters calculated by each program (Table 2).

As expected, regardless of the experimental condition and similarly to other reference gene evaluation studies, the studied genes performed differently depending on the analysis program used. Therefore, in the absence of an ideal or preferred method, it is not possible to determine the precise candidate genes most stable under each condition. However, in certain cases, a simple overview of the three ranks can reveal particular tendencies. For instance, for the *E. necator* treatment, *VAG1* was consistently ranked among the two most stable genes. Yet, *UBC*, whose M value was the same as *VAG1*, was ranked fourth according to NormFinder and BestKeeper. Full agreement was observed regarding *L2*, which was the worst ranked gene in all three methods. As for the wounding stimulus, a higher discrepancy is observed among the three methods. While *PEP* displayed the best stability performance when evaluated by geNorm and NormFinder, it was classified as one of the worst genes by BestKeeper. A similar situation occurs for *UBC*. Despite the significant discrepancies occurring among the ranks generated by the three softwares, one must also be aware that, in some of those cases, the ranks were generated based upon small differences in the stability parameters indicating that the genes involved might possess expression variations very close to each other.

Table 2. Grapevine candidate reference gene stability rankings during different treatments according to geNorm, NormFinder and BestKeeper

Rank	Program					
	geNorm		NormFinder		BestKeeper	
	Gene	M	Gene	SV	Gene	CC
E. necator						
1	*UBC*	0.238	*VAG1*	0.219	*PEP*	0.953
2	*VAG1*	0.238	*CYP*	0.231	*VAG1*	0.911
3	*PEP*	0.290	*EF1*	0.237	*CYP*	0.885
4	*CYP*	0.331	*UBC*	0.251	*UBC*	0.878
5	*EF1*	0.402	*PEP*	0.265	*EF1*	0.856
6	*L2*	0.757	*L2*	0.875	*L2*	0.382
Wounding						
1	*PEP*	0.287	*PEP*	0.786	*UBC*	0.997
2	*UBC*	0.287	*L2*	0.939	*VAG1*	0.996
3	*ACT*	0.366	*CYP*	0.952	*ACT*	0.995
4	*VAG1*	0.471	*VAG1*	0.961	*CYP*	0.985
5	*L2*	0.531	*EF1*	1.060	*L2*	0.978
6	*CYP*	0.692	*UBC*	1.170	*PEP*	0.977
7	*EF1*	0.776	*ACT*	4.918	*EF1*	0.945
UV-C						
1	*UBC*	0.152	*VAG1*	0.111	*L2*	0.897
2	*VAG1*	0.152	*UBC*	0.151	*UBC*	0.821
3	*PEP*	0.267	*PEP*	0.184	*PEP*	0.800
4	*L2*	0.400	*ACT*	0.352	*VAG1*	0.747
5	*ACT*	0.505	*EF1*	0.640	*ACT*	0.519
6	*CYP*	0.661	*CYP*	0.684	*CYP*	0.133
7	*EF1*	0.746	*L2*	0.948	*EF1*	0.050
P. chlamydospora						
1	*EF1*	0.282	*EF1*	0.062	*ACT*	0.986
2	*CYP*	0.282	*CYP*	0.068	*EF1*	0.965
3	*VAG1*	0.335	*PEP*	0.081	*PEP*	0.955
4	*UBC*	0.362	*UBC*	0.082	*CYP*	0.955
5	*ACT*	0.396	*VAG1*	0.090	*UBC*	0.942
6	*PEP*	0.410	*L2*	0.091	*VAG1*	0.933
7	*L2*	0.421	*ACT*	0.096	*L2*	0.922

SV, stability value; CC, Pearson coefficient of correlation

As for the UV-C irradiation treatment, a reasonable consistency is observed, where for all methods, both *UBC* and *PEP* are among the three best ranked genes. *CYP* on the other hand, was classified as the second worst gene regardless of the analysis type. For the last treatment addressed in this work, *P. chlamydospora* infection in woody tissues, a clear difference is observed when the stability rankings are compared with

the previous treatments. Both *EF1* and *CYP*, which were constantly amongst the worst scoring genes, are, in this case, two of the most stable candidates. Though the biotic stress itself can cause significant gene expression variations, also a considerable effect is expected due to tissue/organ specific metabolism.

Consensus stability rankings

Considering that each of the previous methods has its own limitations and no agreement exists for which software is the most suitable for expression stability analysis, a common approach to perform these studies often involves the use, comparison and integration of all three methods. Several strategies exist to create a comprehensive stability ranking integrating the results of the three applets. In general, each gene is assigned a certain weight corresponding to the rank obtained for each program (*e.g.* 1-most stable to 7- least stable). Subsequent rank aggregation methodologies are then employed, which can, for instance, rely on straightforward arithmetic and geometric mean of the ranks [40-42]. However, in this work a different methodology, suggested by Mallona (2010) and followed by Goulão (2012), was used. The outputs of the different applets were merged by means of a non-weighted unsupervised rank aggregation method using the Cross-Entropy Monte Carlo algorithm. According to the previous method, an optimal stability ranking list for each experimental condition was created (Figure 2).

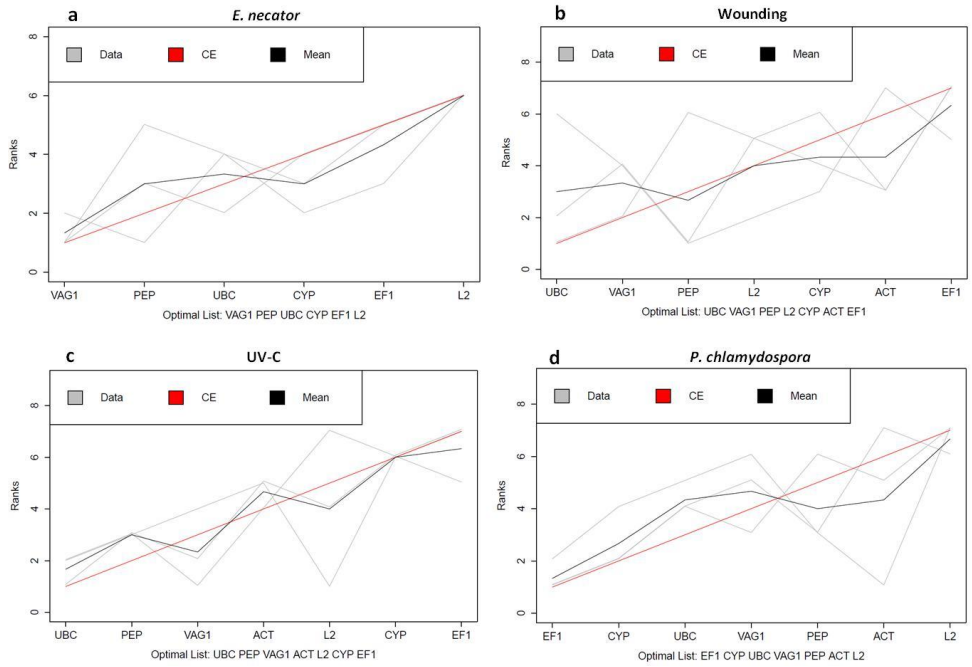

Figure 2. Consensus stability rankings generated by Monte Carlo algorithm for (a) leaf infection with *E. necator*, (b) leaf wounding, (c) leaf irradiation with UV-C, and (d) wood infection with *P. chlamydospora*. RankAggreg (v. 0.4-3) package for R was used to compute Monte Carlo algorithm with the Spearman footrule distances on the rank lists generated by each applet. Individual stability measurements (geNorm, NormFinder or BestKeeper) are shown in grey, average rank positions in black and the computed Monte Carlo model in red

Overall, the rank aggregation method supports some of our initial observations. When comparing the different optimal lists obtained for each treatment, we can also observe that, for all the three stresses involving grapevine leaves, despite the scoring differences, *UBC*, *VAG1* and *PEP* are consistently ranked within the most stable genes. Concerning *P. chlamydospora* treatment, *EF1*, *CYP* and *UBC* are, among all candidates, the most stable reference genes.

For the particular case of *E. necator* infection, an inevitable attempt was made to correlate our results with similar available studies reporting the most appropriate grapevine normalization genes upon pathogen interaction, namely *Plasmopara viticola*, the causal agent of downy mildew [6,16,17]. Though distinct, both pathogens have similar infection

mechanisms, lifestyles and colonize the same tissues. In fact, even though different sets of genes were used in each study, a certain degree of accordance can be observed, at least in one of the cases, when some of the same genes are evaluated. In the work conducted by Selim [17], in which four of the present genes were also evaluated, *UBC* was ranked as the most stably expressed in *P. viticola* infected leaves. In addition, *EF1*, as well as *CYP*, were the two worst ranked candidates. Conversely, in the work developed by Monteiro [16], also addressing *P. viticola* leaf infection, *EF1* was, at all times, one of top ranked genes.

In order to further validate the suitability of the top ranked genes identified in this study, we decided to perform the differential expression quantification of a potentially responsive gene, phenylalanine ammonia lyase (*PAL*), for two of the tested conditions (wounding and UV-C irradiation). Given its extensive characterization as the central precursor for phenolic compounds and the general acceptance as a defense related gene whose expression can be induced by a variety of stresses, *PAL* expression changes caused by the selected stimuli would be predictable to occur [43,44]. In an attempt to evaluate the potential bias arising due to improper reference gene selection, we calculated the fold change expression of *PAL* using both the best and the worst ranked genes for normalization (Figure 3).

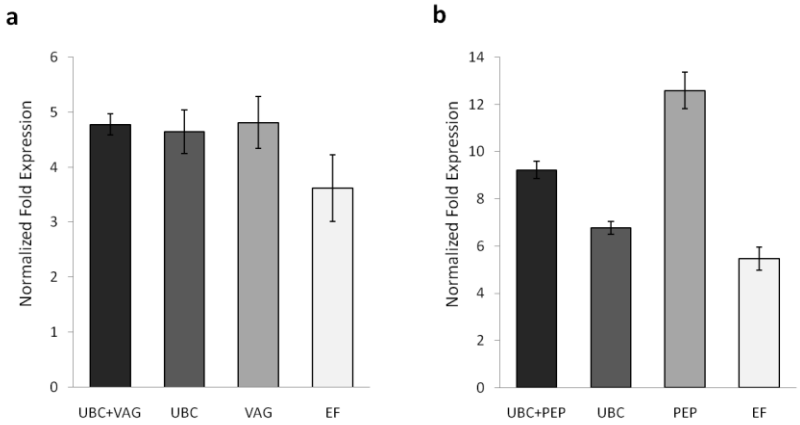

Figure 3. Differential gene expression of *PAL* in grapevine leaves induced by (a) wounding and (b) UV-C irradiation. Relative gene expression quantification was performed for each condition using four different normalization factors derived from: the combination of the two top ranked genes, the best ranked gene, the second most stable gene and the worst ranked gene.

For each of the treatments, fold change expression values were determined using different normalization factors (NF) derived from: the combination of the two most stable reference genes, the best ranked gene, the second best gene and the worst ranked gene. As expected, regardless of the treatment, an upregulation of *PAL* was observed in all cases. For the wounding experiment (Figure 3a), the calculated expression values using the combined and isolated best genes as NFs (*UBC* and *VAG*) were comparable among themselves, with fold change values of 4.78 (*UBC*+*VAG*), 4.65 (*UBC*) and 4.81 (*VAG*). When using the NF corresponding to the most unstable gene (*EF*), a fold change of 3.62 was obtained. Despite the noticeable difference between the normalization with the worst and best genes, a certain degree of consistency exists within all four quantifications. This suggests that the expression of these candidate genes (*UBC*, *VAG* and *EF*), and possibly of all the remaining, was not significantly affected by the experimental wounding stress. On the other hand, for the UV-C treatment (Figure. 3b), larger discrepancies can be observed among the evaluated candidates. *PAL* gene expression

normalized to the combination of the two best ranked genes (*UBC* and *PEP*) indicated a 9.22 fold change. However, when normalized for each of the candidates individually, the calculated upregulation was 6.77 (*UBC*), 12.59 (*PEP*) and 5.47 (*EF*). Such accentuated differences highlight not only the importance of selecting the most appropriate reference genes for each experimental conditions, but also the necessity to use multiple genes for sample normalization.

Taken together, besides supporting the already accepted idea that no universal reference genes exist, our results provide information regarding the suitability of potential qRT-PCR reference genes to be used in grapevine samples for distinct biotic and abiotic stresses. Such knowledge might prove useful in transcriptomic studies contributing for accurate gene expression quantification.

References

1. Bustin S (2000) Absolute quantification of mRNA using real-time reverse transcription polymerase chain reaction assays. Journal of Molecular Endocrinology 25: 169-193.
2. Vandesompele J, De Preter K, Pattyn F, Poppe B, Van Roy N, et al. (2002) Accurate normalization of real-time quantitative RT-PCR data by geometric averaging of multiple internal control genes. Genome Biolology 3: 0034.
3. Artico S, Nardeli S, Brilhante O, Grossi-de-Sa M, Alves-Ferreira M (2010) Identification and evaluation of new reference genes in *Gossypium hirsutum* for accurate normalization of real-time quantitative RT-PCR data. BMC Plant Biology 10: 49.
4. Derveaux S, Vandesompele J, Hellemans J (2010) How to do successful gene expression analysis using real-time PCR. Methods 50: 227-230.
5. Chao WS, Doğramaci M, Foley ME, Horvath DP, Anderson JV (2012) Selection and validation of endogenous reference genes for qRT-PCR analysis in leafy spurge (*Euphorbia esula*). PLoS ONE 7: e42839.

6. Gamm M, Héloir M-C, Kelloniemi J, Poinssot B, Wendehenne D, et al. (2011) Identification of reference genes suitable for qRT-PCR in grapevine and application for the study of the expression of genes involved in pterostilbene synthesis. Molecular Genetics and Genomics 285: 273-285.
7. Gantasala N, Papolu P, Thakur P, Kamaraju D, Sreevathsa R, et al. (2013) Selection and validation of reference genes for quantitative gene expression studies by real-time PCR in eggplant (*Solanum melongena* L). BMC Research Notes 6: 312.
8. Goulao L, Fortunato A, C. Ramalho J (2012) Selection of reference genes for normalizing quantitative real-time PCR gene expression data with multiple variables in *Coffea* spp. Plant Molecular Biology Reporter 30: 741-759.
9. Reddy DS, Bhatnagar-Mathur P, Cindhuri KS, Sharma KK (2013) Evaluation and validation of reference genes for normalization of quantitative real-time PCR based gene expression studies in peanut. PLoS ONE 8: e78555.
10. Zhu J, Zhang L, Li W, Han S, Yang W, et al. (2013) Reference gene selection for quantitative real-time PCR normalization in *Caragana intermedia* under different abiotic stress conditions. PLoS ONE 8: e53196.
11. Andersen CL, Jensen JL, Ørntoft TF (2004) Normalization of real-time quantitative reverse transcription-PCR data: A model-based variance estimation approach to identify genes suited for normalization, applied to bladder and colon cancer data sets. Cancer Research 64: 5245-5250.
12. Pfaffl M, Tichopad A, Prgomet C, Neuvians T (2004) Determination of stable housekeeping genes, differentially regulated target genes and sample integrity: BestKeeper – Excel-based tool using pair-wise correlations. Biotechnology Letters 26: 509-515.
13. Reid K, Olsson N, Schlosser J, Peng F, Lund S (2006) An optimized grapevine RNA isolation procedure and statistical determination of reference genes for real-time RT-PCR during berry development. BMC Plant Biology 6: 1-11.
14. Coito J, Rocheta M, Carvalho L, Amâncio S (2012) Microarray-based uncovering reference genes for quantitative real time PCR in grapevine under abiotic stress. BMC Research Notes 5: 1-12.
15. Gonzalez-Aguero M, Garcia-Rojas M, Di Genova A, Correa J, Maass A, et al. (2013) Identification of two putative reference genes from

grapevine suitable for gene expression analysis in berry and related tissues derived from RNA-Seq data. BMC Genomics 14: 878.

16. Monteiro F, Sebastiana M, Pais MS, Figueiredo A (2013) Reference gene selection and validation for the early responses to downy mildew infection in susceptible and resistant *Vitis vinifera* cultivars. PLoS ONE 8: e72998.
17. Selim M, Legay S, Berkelmann-Löhnertz B, Langen G, Kogel KH, et al. (2012) Identification of suitable reference genes for real-time RT-PCR normalization in the grapevine-downy mildew pathosystem. Plant Cell Reports 31: 205-216.
18. Logemann E, Hahlbrock K (2002) Crosstalk among stress responses in plants: Pathogen defense overrides UV protection through an inversely regulated ACE/ACE type of light-responsive gene promoter unit. Proceedings of the National Academy of Sciences of the United States of America 99: 2428-2432.
19. Fischer M, Kassemeyer HH (2003) Fungi associated with esca disease of grapevine in Germany. Vitis 42: 109-116.
20. Gaforio L, Garcia-Munoz S, Cabello F, Munoz-Organero G (2011) Evaluation of susceptibility to powdery mildew (*Erysiphe necator*) in *Vitis vinifera* varieties. Vitis 50: 123-126.
21. Bertsch C, Ramírez-Suero M, Magnin-Robert M, Larignon P, Chong J, et al. (2013) Grapevine trunk diseases: complex and still poorly understood. Plant Pathology 62: 243-265.
22. Reymond P, Weber H, Damond M, Farmer EE (2000) Differential gene expression in response to mechanical wounding and insect feeding in *Arabidopsis*. The Plant Cell Online 12: 707-719.
23. Cheong YH, Chang H-S, Gupta R, Wang X, Zhu T, et al. (2002) Transcriptional profiling reveals novel interactions between wounding, pathogen, abiotic stress, and hormonal responses in *Arabidopsis*. Plant Physiology 129: 661-677.
24. Leon J, Rojo E, Sanchez-Serrano JJ (2001) Wound signalling in plants. Journal of Experimental Botany 52: 1-9.
25. Kunz BA, Cahill DM, Mohr PG, Osmond MJ, Vonarx EJ (2006) Plant responses to UV radiation and links to pathogen resistance. In: Kwang WJ, editor. International Review of Cytology: Academic Press. pp. 1-40.
26. Pezet R, Perret C, Jean-Denis JB, Tabacchi R, Gindro K, et al. (2003) δ-Viniferin, a resveratrol dehydrodimer: One of the major stilbenes

synthesized by stressed grapevine leaves. Journal of Agricultural and Food Chemistry 51: 5488-5492.
27. Bonomelli A, Mercier L, Franchel J, Baillieul F, Benizri E, et al. (2004) Response of grapevine defenses to UV—C exposure. American Journal of Enology and Viticulture 55: 51-59.
28. Gambino G, Perrone I, Gribaudo I (2008) A Rapid and effective method for RNA extraction from different tissues of grapevine and other woody plants. Phytochemical Analysis 19: 520-525.
29. Pihur V, Datta S, Datta S (2009) RankAggreg, an R package for weighted rank aggregation. BMC Bioinformatics 10: 62.
30. Mallona I, Lischewski S, Weiss J, Hause B, Egea-Cortines M (2010) Validation of reference genes for quantitative real-time PCR during leaf and flower development in *Petunia hybrida*. BMC Plant Biology 10: 4.
31. Nicot N, Hausman J-F, Hoffmann L, Evers D (2005) Housekeeping gene selection for real-time RT-PCR normalization in potato during biotic and abiotic stress. Journal of Experimental Botany 56: 2907-2914.
32. Jain M, Nijhawan A, Tyagi AK, Khurana JP (2006) Validation of housekeeping genes as internal control for studying gene expression in rice by quantitative real-time PCR. Biochemical and Biophysical Research Communications 345: 646-651.
33. Panstruga R (2003) Establishing compatibility between plants and obligate biotrophic pathogens. Current Opinion in Plant Biology 6: 320-326.
34. Hückelhoven R (2005) Powdery mildew susceptibility and biotrophic infection strategies. FEMS Microbiology Letters 245: 9-17.
35. Schmidt SM, Panstruga R (2008) Cytoskeleton functions in plant-microbe interactions. Physiological and Molecular Plant Pathology 71: 135-148.
36. Peccoud J, Jacob C (1998) Statistical estimations of PCR amplification rates. In: Ferré F, editor. Gene quantification: Birkhäuser Boston. pp. 111-128.
37. Ramakers C, Ruijter JM, Deprez RHL, Moorman AFM (2003) Assumption-free analysis of quantitative real-time polymerase chain reaction (PCR) data. Neuroscience Letters 339: 62-66.
38. Ruijter JM, Ramakers C, Hoogaars WM, Karlen Y, Bakker O, et al. (2009) Amplification efficiency: linking baseline and bias in the

analysis of quantitative PCR data. Nucleic Acids Research 37: e45.

39. Castro-Quezada P, Aarrouf J, Claverie M, Favery B, Mugniéry D, et al. (2013) Identification of reference genes for normalizing RNA expression in potato roots infected with cyst nematodes. Plant Molecular Biology Reporter 31: 936-945.
40. Exposito-Rodriguez M, Borges A, Borges-Perez A, Perez J (2008) Selection of internal control genes for quantitative real-time RT-PCR studies during tomato development process. BMC Plant Biology 8: 131.
41. Figueiredo A, Loureiro A, Batista D, Monteiro F, Varzea V, et al. (2013) Validation of reference genes for normalization of qPCR gene expression data from *Coffea* spp. hypocotyls inoculated with *Colletotrichum kahawae*. BMC Research Notes 6: 388.
42. Xie F, Xiao P, Chen D, Xu L, Zhang B (2012) miRDeepFinder: a miRNA analysis tool for deep sequencing of plant small RNAs. Plant Molecular Biology 80: 75-84.
43. MacDonald MJ, D'Cunha GB (2007) A modern view of phenylalanine ammonia lyase. Biochemistry and Cell Biology 85: 273-282.
44. Mellway RD, Tran LT, Prouse MB, Campbell MM, Constabel CP (2009) The wound-, pathogen-, and ultraviolet B-responsive MYB134 gene encodes an R2R3 MYB transcription factor that regulates proanthocyanidin synthesis in poplar. Plant Physiology 150: 924-941.

Chapter III: Transcriptomic Changes Following the Compatible Interaction *Vitis vinifera* - *Erysiphe necator*

This chapter was adapted from the following manuscript:

Borges AF, Ferreira RB, Monteiro S (2013) Transcriptomic changes following the compatible interaction *Vitis vinifera-Erysiphe necator*. Paving the way towards an enantioselective role in plant defence modulation. Plant Physiology and Biochemistry 68: 71-80.

Author contribution:

AFB executed all the experimental work and wrote the manuscript.

Abstract

The compatible interaction between *Erysiphe necator* and *Vitis vinifera* induces significant alterations in the host transcriptome, affecting essentially those genes involved in signalling and secondary metabolite biosynthetic pathways. The precise transcriptomic changes vary from the early events to later stages of infection. In the present work, suppressive subtraction hybridization (SSH) was used to identify several differentially expressed transcripts in symptomatic and asymptomatic leaves from powdery mildew infected grapevines following a long term interaction. The detected transcripts show little or no correlation with similar expression studies concerning the early stages of infection which suggests distinct host responses occur before and after the infection is established. The transcription level of thirteen genes was assessed through *q*RT-PCR using appropriately selected and validated normalization genes. With one exception, all these genes underwent moderate levels of differential transcription, with $\log_2$-fold change values ranging from -2.65 to 4.36. The exception, a dirigent-like (*DIR*) protein, was upregulated over 180 fold in symptomatic leaves, suggesting an important role for stereochemical selectivity in the compatible interaction *E. necator-V. vinifera*. *DIR* copy number was determined in the genome of three grapevine cultivars exhibiting high (Carignan), moderate (Fernão Pires) and low (Touriga Nacional) sensitivity to *E.necator*. It was found to be a two-copy gene in all cultivars analyzed. Further analysis involving DIR metabolic neighbourhood transcripts was performed. The possible physiological significance of the detected *DIR* upregulation is discussed.

Introduction

Erysiphe necator, the causal agent of powdery mildew (PM) in *Vitis vinifera*, represents, from an economic point of view, one of the most devastating diseases affecting grapevine worldwide [1]. Although its propagation can be minimized by chemically-synthesized antifungal compounds, the inevitable increase in fungicides used to prevent and contain this disease comprises a potential environmental threat [2]. It is, therefore, of utmost importance to improve our knowledge on the molecular and biochemical mechanisms underlying *Vitis vinifera–Erysiphe necator* interaction. Numerous studies regarding this and other host-pathogen systems have shown that complex transcriptomic and subsequent metabolic changes occur within the host in response to the pathogen [3]. As soon as the plant detects the presence of a pathogen, the induced defence response is triggered. Cell surface-located receptors are responsible for initial pathogen recognition, detecting pathogen-associated molecular patterns (PAMPs) and activating a kinase cascade-mediated signal transduction [4]. The resulting modifications range from upregulation of constitutive defense-related genes to transcriptionally induced or post-transcriptionally regulated disease-associated proteins, which may lead to PAMP-triggered immunity (PTI) [5]. Even though PTI can, occasionally, protect the plant from microbial invasion and/or proliferation during compatible interactions, it constitutes a nonhost-resistance mechanism against nonadapted pathogens [6].

When dealing with compatible plant-pathogen interactions, PTI is often, at least partially disabled through the use of effector proteins [5,7]. This is particularly relevant in pathosystems where the pathogen is an obligate biotrophic fungus, as in *V. vinifera-E. necator* interaction. Unlike facultative biotrophic or hemibiotrophic fungi which can survive outside the host or switch to necrotrophy, *E. necator* and other obligate biotrophic pathogens are entirely dependent on living plant tissue for their growth and

propagation [8]. Therefore, they develop a highly sophisticated interaction with their hosts. Apparently, these pathogens have the ability to suppress or durably avoid preformed and induced host defenses including hypersensitive response. In addition, they seem to be able to redirect the host metabolism according to their nutritional needs [9,10].

Among all *Vitis* species, *V. vinifera* cultivars display the highest susceptibility to powdery mildew. Other species such as *V. labrusca*, *V. rupestris* and *V. aestivalis* exhibit several degrees of powdery mildew resistance which can be somehow related to their co-evolution with *E. necator* during a long course of time [11]. A comparative transcriptomic study between *V. vinifera* and *V. aestivalis* suggests that the differential disease susceptibility among *Vitis* species goes beyond genome variation and is more likely to be determined by transcriptional regulation [12]. Recent evidence supporting this hypothesis shows a significant transcriptomic difference between compatible and incompatible interactions involving grapevine and *E. necator*. The differential gene expression induced by *E. necator* was observed to be limited to three transcripts in *V. aestivalis* against 625 PM-responsive genes found in *V. vinifera* up to 48 h postinoculation (hpi). The reason why such a weak PM-induced response occurs in *V. aestivalis* may be connected to its constitutive transcriptomic profile which is already defence-oriented when compared to *V. vinifera* [13]. The observed transcriptome changes in *V. vinifera* during the course of infection is consistent with the theory that these sophisticated pathogens are, somehow, able to circumvent host defense/recognition mechanisms [9]. Many differentially expressed defense-related proteins reached their maximum levels at 12 hpi and then declined as the fungal infection became established [13]. Similar results were reported for barley (*Hordeum vulgare*) powdery mildew, where compatible and incompatible interactions with the pathogen *Blumeria graminis* caused analogous plant expression patterns during the first 16 h

of infection. After this period, the expression of some of these defense-related genes declined to lower levels in susceptible plants, at 24 and 32 hpi [14]. Many of these genes are involved in plant secondary metabolism which, in *V. vinifera-E. necator* interaction, apparently shift the metabolism towards phenylpropanoid synthesis via the pentose phosphate and shikimate pathways. As a result, lignin, stilbene and dihydroflavonol metabolic branches are also upregulated.

Among all the differentially expressed reported genes, dirigent proteins (DIR) represent a particularly interesting defence-related multigene family [13]. DIR proteins (from Latin: *dirigere* = to guide or align) are proteins devoid of catalytic activity which dictate the stereochemistry of reactions catalyzed by other proteins. They were first reported as auxiliary proteins in lignan biosynthesis where they were shown to regio-stereochemically control the monolignol radical coupling catalyzed by peroxidases, namely dimerization of coniferyl alcohol to afford (+)-pinoresinol [15]. DIR discovery and their subsequent detection in all land plants examined to date explain the usually observed lignan optical activity in biological samples [16]. Lignans are characterized for their recognized antifungal activity, but also for their chemical structure, with several chiral centers, allowing regio-stereochemical diversity along their biosynthetic route [17]. The observation that, under pathological conditions, this diversity is restricted to favor the formation of a single enantiomer highlights the potential importance of DIR enantioselective character in plant defence. Previous studies on lignan properties have already shown differential antimicrobial activity between enantiomers, one being up to four times more toxic than the other [18].

In this study, we report the detection of several *V. vinifera* defense-related genes whose expression was found to be affected following the long term interaction with *E. necator.* The differential gene expression between symptomatic and asymptomatic leaves of powdery mildew infected

grapevines was confirmed and quantified by qRT-PCR using previously validated normalization genes. Among the detected transcripts, a *DIR*-like gene, whose expression was significantly affected, highlights its potential importance in this plant-pathogen interaction. We further investigated whether *V. vinifera DIR* gene dosage could be related to *E. necator* susceptibility, determining genomic *DIR* copy number for grapevine cultivars with different PM susceptibility degrees. Moreover, an attempt was made to correlate the observed *DIR* upregulation with the relative transcript levels of several genes participating in the metabolic surroundings of coniferyl alcohol, the putative DIR "substrate".

Materials and Methods

Plant material and growth conditions

Grapevine (*Vitis vinifera* L., cultivar Touriga Nacional) cuttings used in the experiment were collected from Centro Experimental de Pegões, Portugal, and subjected to heartwood disease screening through microbiology assays. The microbiologic screening was performed using the bottom of the cuttings. Thin wood slices were removed from each cutting, surface-sterilized (ethanol, flame and sodium hypochlorite) and then placed in 0.03% (w/v) chloramphenicol-containing PDA medium (five slices per cutting). The plates were incubated at room temperature for a maximum period of one month, during which morphological identification of the microorganisms present in the wood was performed. Diseased cuttings were discarded.

Healthy *V. vinifera* cuttings, with three buds each, were rooted in water and then transferred to soil (1 L pot per plant). Plants were maintained in a growth chamber at 25 ºC with a photoperiod of 16 h (480 $\mu mol.m^{-2}.s^{-1}$). After acclimatization, all plants were simultaneously inoculated with *E. necator* by direct contact with naturally infected grapevine leaves. The

primary inoculum was collected from a vineyard at Instituto Superior de Agronomia, Lisbon, Portugal and passed to a set of grapevines in a greenhouse which provided the experimental inoculum source. Leaves from the greenhouse plants were used to inoculate all the plants in the growth chamber. Plants were allowed to grow with generalized powdery mildew infection for 30 days prior to sample collection. After the infection stage, fully expanded leaves (fourth and fifth positions from the tip of each shoot) with and without *E. necator* infection symptoms (visible mycelia on the upper leaf surface) were randomly harvested and frozen in liquid nitrogen. Biological replicates for symptomatic (S) and asymptomatic (A) conditions were created by pooling four leaves of each condition per sample. All leaves of each pool were collected from different plants from the same experimental setup.

RNA extraction

Total RNA extraction was performed using the CTAB (hexadecyltrimethyl ammonium bromide) method (Chang *et al*., 1993), especially suited for high phenolic content material [19]. Leaves were ground in liquid nitrogen, homogenized at 1 g per 20 mL in extraction buffer (2% (w/v) CTAB, 2% (w/v) polyvinylpoly-pyrrolidone, 2 M NaCl, 100 mM Tris-HCl pH 8.0, 25 mM EDTA, 2% (v/v) β-mercaptoethanol) and incubated at 65 ºC for 10 min. Samples were extracted twice with one volume of chloroform:isoamylic alcohol (24:1, v/v) and centrifuged at 12,000 *g* during 30 min. The recovered aqueous phase was supplemented with ¼ volume of 10 M LiCl and incubated overnight at 4 ºC. RNA was collected by centrifugation at 12,000 *g*, 4 ºC during 20 min, and resupended in 1.5 mL of pre-warmed (37 ºC) SSTE buffer (0.5% w/v SDS, 1 M NaCl, 10 mM Tris-HCl pH 8.0, 1 mM EDTA). Each sample was divided in two and again extracted with one volume of chloroform:isoamylic alcohol (24:1, v/v) followed by centrifugation at 15,000 *g* during 10 min. The recovered

supernatant was supplemented with 2.5 volumes of ethanol and incubated for 2 h at -20 ºC. RNA was precipitated by centrifugation at 4 ºC, 15,000 *g* during 30 min. The *pellet* was washed with 70% (v/v) ethanol and resuspended in water. Prior to RT-PCR, samples were treated with RQ1 RNase-Free Dnase (Promega) according to the manufacturer's protocol.

Supression subtractive hybridization libraries

Each sample, S and A cDNAs, used to perform SSH was synthesized from 4 μg of total RNA, using the BD SMART™ PCR cDNA Synthesis Kit (Clontech). Following PCR cycle optimization for each sample, both cDNA templates were amplified by LD-PCR through 23 temperature cycles according to the manufacturer's protocol. SSH was performed using the PCR-Select cDNA Subtraction Kit (Clontech) following the manufacturer's instructions. Both S and A samples were used as tester and driver for forward and reverse subtractions, respectively. SSH cDNA pools were cloned and transformed using pCR2.1 vector and TOP10 chemically competent *Escherichia coli* from TA Cloning Kit (Invitrogen). Transformed cells were plated on LB agar plates containing kanamycin (50 μg.mL-1) overlaid with X-Gal (40 μL of 40 mg.mL-1).

Dot-blot library screening

White colonies from both subtractions were randomly picked from the libraries, transferred to liquid LB (50 μg.mL^{-1} kanamycin) in 96-well plates and incubated overnight at 37 ºC with agitation. cDNA inserts from each colony were amplified directly from 1 μL of the corresponding liquid culture in a 20 μL PCR reaction using the Advantage cDNA PCR Kit & Polymerase Mix (Clontech). Reaction mixtures were prepared with the primers Nested Primer 1 (5' TCGAGCGGCCGCCCGGGCAGGT 3') and Nested Primer 2R (5' AGCGTGGTCGCGGCCGAGGT 3'), complementary to the adaptors used in the subtraction process. Thermal cycling was performed using the following parameters: initial denaturation step at 94

ºC for 30 s, 23 cycles at 95 ºC for 10 s and 68 ºC for 3 min. After agarose gel analysis, dot-blot arrays were prepared by spotting each amplified insert in duplicate into separate nylon membranes. Probing of the cDNA arrays was performed as described in DIG High Prime DNA Labeling and Detection Starter Kit II (Roche) using labeled forward and reverse SSH cDNA pools as probes. Clones displaying differential hybridization between forward and reverse probes were interpreted as differentially expressed and selected for insert sequencing.

Genomic DNA extraction

Grapevine leaves (1 cm² per sample) were ground in liquid nitrogen and homogenized in 1.5 mL tubes containing 300 μL of extraction buffer (0.35 M sorbitol, 0.1 M Tris-HCl pH 8.2, 5 mM EDTA, 2% (v/v) β-mercaptoethanol). Homogenates were supplemented with 300 μL of nuclei lysis buffer (2% (m/v) CTAB, 2 M NaCl, 0.2 M Tris-HCl pH 7.5, 50 mM EDTA) and 120 μL 5% (w/v) Sarkosil, vigorously shaken and incubated at 65 ºC for 15 min. Samples were extracted with 600 μL of chloroform:isoamylic alcohol (24:1) and centrifuged at 12,000 *g* during 10 min. Ice-cold isopropanol (0.65 vol.) was added to the recovered aqueous phases and the tubes were gently inverted several times. Nucleic acids were collected through centrifugation at 12,000 *g* during 5 min, resuspended in 100 μL of RNase containing buffer (50 mM Tris-HCl pH 8.0, 10 mM EDTA) and incubated for 15 min at room temperature. Samples were again extracted with chloroform:isoamylic alcohol (24:1) and precipitated with isopropanol. Following 70% (v/v) ethanol washing, the pellet was resuspended in 50 μL TE (10 mM Tris-HCl pH 8.0, 1 mM EDTA).

Real time PCR

Reverse transcription reactions for gene expression studies were performed using ThermoScript RT-PCR System (Invitrogen) as described by the manufacturer. cDNA was synthesized from 1.5 μg of total RNA and oligo(dT)$_{20}$ primed. RT reactions were carried at 55 ºC for 60 min.

All PCR primers were designed with Beacon Designer software (Premier Biosoft International) to target amplicons between 80 and 300 bps. qPCR was performed with iQ SYBR Green supermix (Bio-Rad) using iCycler equipment (Bio-Rad). cDNA for gene expression studies was diluted to 15-30 ng/μL. Genomic DNA to determine *DIR* copy number was diluted to 10 ng/μL. Reaction mixtures (20 μL) were prepared according to the following methodology: 1 μL of the diluted template, 1 μL primer mix (10 μM each), 10 μL iQ SYBR Green supermix (Bio-Rad), 8 μL H_2O. Thermal cycling was composed of an initial denaturation step for 3 min at 95 ºC, 40 cycles at 95 ºC for 10 s, 55 ºC for 30 s and 72 ºC for 30 s. Relative gene expression analysis was performed using *UBC* and *VAG* as normalization genes. The experiments were carried out using four biological replicates for SSH-detected transcripts and two biological replicates for coniferyl alcohol branching enzymes. All reactions were performed in triplicate and amplification specificity was assessed through melting curve analysis.

Results

SSH and cDNA library screening

To identify differentially expressed genes between symptomatic (S) and asymptomatic leaves (A) from powdery-mildew infected grapevines, SSH technique was used to generate cDNA pools enriched in both up and downregulated transcripts. Forward and reverse subtractions were performed using S and A samples as testers, respectively.

Prior to the cDNA library construction, SSH efficiency was confirmed through electrophoretic analysis of the resulting cDNA pools – subtracted and unsubtracted (Figure 4a).

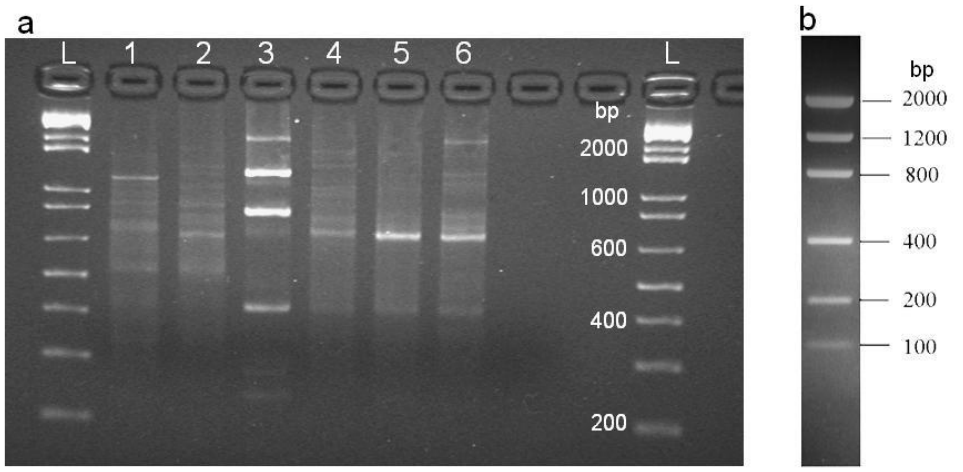

Figure 4. Suppression subtractive hybridization. (a) 2% (m/v) agarose electrophoresis of subtracted and unsubtracted grapevine cDNA samples: Lane L – DNA ladder Lane 1 – forward subtraction, Lane 2 – reverse subtraction, Lane 3 – control subtraction, Lane 4 – forward tester unsubtracted, Lane 5 – reverse tester unsubtracted, Lane 6 – control tester unsubtracted. (b) Illustration of an electrophoretic analysis of the Low DNA Mass Ladder supplemented to the control tester.

A control subtraction, performed simultaneously with the experimental samples, was also analyzed. The control consisted in the “subtraction” of equal samples (driver and tester) where the tester was supplemented with a residual amount of foreigner DNA (Low DNA Mass Ladder, Invitrogen) to simulate the presence of upregulated transcripts.

Analysis of the electrophoretic profiles present in Figure 4a, in particular the ones referring to the control subtraction and the corresponding unsubtracted pool (Lanes 3 and 6), are indicative that the "subtraction" process was accomplished. As expected, the foreigner DNA present in the tester sample was preferentially amplified over the cDNAs that were common to the tester and driver. Nevertheless, the efficiency of the method appears to be dependent on the size of the amplicons.

Two cDNA libraries were created from the forward and the reverse subtraction cDNA pools. While the first is expected to be enriched in upregulated genes, the second should hold genes that are repressed upon infection.

A total of 273 clones from both subtractions were screened for relative transcript abundance in the subtracted cDNA pools (Figure 5).

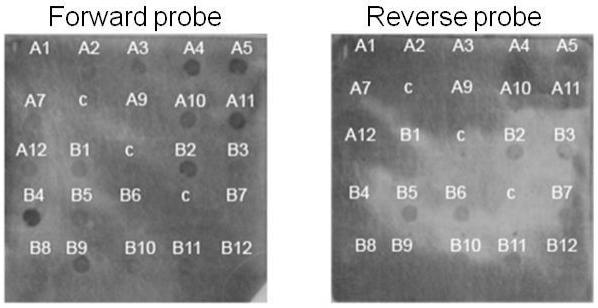

Figure 5. Representative dot-blot autoradiogram used for SSH library screening. Colony PCR products (A1 to B12) originated from the forward subtraction were hybridized with forward and reverse DIG-labelled probes. c – negative hybridization control.

Significant dot-blot hybridization differences were observed for 62 clones for which the corresponding cDNA inserts were sequenced. Sequence analysis revealed 28 non-redundant grapevine transcripts (Table 3) and three *E. necator* transcripts. Most inserts ranged from 300 to 800 bps.

Table 3. Differentially expressed transcripts detected by SSH of symptomatic (S) and asymptomatic leaves (A) from powdery-mildew infected grapevines.

Clone ID (Accession number)	Subtraction Library [a]	Predicted function	tBLASTx	E value
F1B5 (KC748395)	**Forward**	Glycerol-3-phosphate dehydrogenase-like	XM_002284443	9E-141
F1C5 (KC748400)	**Forward**	Beta-amyrin synthase / Triterpene synthase	XM_002269309	1E-24
F1A11 (KC748406)	**Forward**	Resveratrol O-methyltransferase	XM_002281445	8E-39
F1D5 (KC748408)	**Forward**	Mitogen-activated protein kinase	XM_003633911	1E-149
F1E6 (KC748418)	**Forward**	Dirigent-like protein	XM_002276412	2E-80
F1A12 (KC748407)	**Forward**	Calcium-binding EF hand family protein	AM476824	2E-142
F2C4 (KC748411)	**Forward**	Tyrosine kinase	XM_003635112	2E-70
F2C6 (KC748412)	**Forward**	Wall-associated kinase	XM_003631669	4E-82
F1C7 (KC748413)	**Forward**	Potassium transporter	XM_002264915	1E-75
F1A3 (KC748403)	**Forward**	Ribosomal protein s15a	XM_003632560	4E-95
F1D11 (KC748415)	**Forward**	*Vitis vinifera* - unknown / uncharacterized	XM_002277671	4E-94
F2A4	**Forward**	*Vitis vinifera* - unknown / uncharacterized	XM_003632258	6E-98
F2A5 (KC748404)	**Forward**	*Vitis vinifera* - unknown / uncharacterized	XM_003631832	8E-112
F1A2	**Forward**	*Vitis vinifera* contig VV78X174488.4	AM441276	1E-87
F1C2 (KC748409)	**Forward**	*Vitis vinifera* contig VV78X257382.43	AM476899	6E-136
F1C11	**Forward**	*Vitis vinifera* contig VV78X054516.4	AM482143	3E-36
F2D1 (KC748414)	**Forward**	*Vitis vinifera* contig VV78X057541.5	AM441985	2E-102
F1E5 (KC748417)	**Forward**	*Vitis vinifera* contig VV78X104455.3	AM484817	6E-112
R1D10 (KC748416)	**Reverse**	Oligopeptide transporter protein	XM_002274130	7E-130
R2C3 (KC748410)	**Reverse**	Hormone-sensitive lipase / Gibberellic acid	XM_002265728	8E-59
R1C7 (KC748397)	**Reverse**	Cinnamoyl-CoA reductase, putative	XM_002272413	1E-138
R1D7 (KC748401)	**Reverse**	Zinc finger RING-type protein-like	XM_002285229	1E-154
R1C11 (KC748402)	**Reverse**	Oligouridylate binding protein	XM_002276972	3E-151
R2A10 (KC748405)	**Reverse**	Carbohydrate transporter	XM_002278696	1E-62
R1A8 (KC748398)	**Reverse**	GPI-anchored protein	XM_002272370	8E-119
R1C2	**Reverse**	MYB/MYC transcription factor	XM_002282950	9E-120
R1B11 (KC748399)	**Reverse**	ATPase alpha subunit	GQ220323	9E-155
R1C1 (KC748396)	**Reverse**	*Vitis vinifera* contig VV78X123770.2	AM425900	4E-126

a – Forward and reverse SSH were performed using S and A samples as testers, respectively.

High-quality cDNA sequences obtained for 24 transcripts were deposited and made accessible in the dbEST NCBI database. tBLASTx analysis allowed us to assign a predicted function to 19 transcripts due to their very high similarity with known function genes from other plant species.
Three of the selected transcripts revealed homologies with grapevine predicted proteins of unknown function. Six sequences showed no significant similarity to known or putative function genes but were homologues to grapevine genomic sequences. The presence of poly(A) tails in the latter confirms they represent grapevine transcripts and thus, new uncharacterized genes.

Optimal number of reference genes for qRT-PCR

As highlighted in the previous chapter, an appropriate selection and validation of reference genes is a fundamental requirement to obtain reliable quantification results in gene expression studies. Given that our earlier expression stability analysis involved the particular experimental conditions here addressed, we used that information to select the reference genes for this part of the work. However, the previous consensus stability rank integrating the results for all the different methods was not used. Even though it represents the best agreement between geNorm, NormFinder and BestKeeper, the individual rankings for each of the methods were highly inconsistent for some of the genes. Thus, despite being aware that none of the software has been universally accepted as better over the other, we relied on geNorm results for the subsequent quantifications. geNorm is the most widely used software, its pairwise comparison algorithm depends on the intuitive principle that the expression ratio of two ideal reference genes should always remain constant across all samples, and it allows the determination of the optimal number of genes to be used for sample normalization. It calculates the

pairwise variation ($V_{n/n+1}$) between two sequential normalization factors (NF_n and NF_{n+1}) reflecting the accuracy changes accompanying the inclusion of a (n+1)th gene as internal control. The lower the V value, the more stable is the corresponding normalization factor. As suggested by the software developers, a cut-off threshold was set at V = 0.15 below which an additional control gene has no significant effect in data normalization.

As shown in Figure 6, under our experimental conditions, V2/3 was 0.13, indicating that the addition of a third control gene has negligible effects on the normalization factor. Therefore, only the two most stable genes as indicated by geNorm were used for sample normalization (*UBC* and *VAG*).

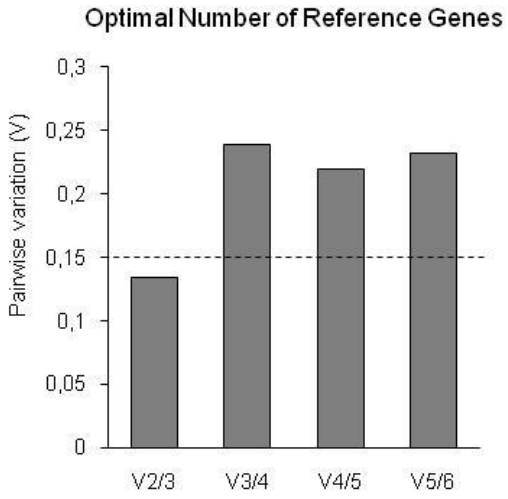

Figure 6. Determination of the optimal number of control genes for normalization using pairwise variation analysis ($V_{n/n+1}$) between the normalization factors NF_n and NF_{n+1}. A cut-off threshold of 0.15 indicates that the addition of a third control gene has no significant effect in data normalization.

Differential gene expression quantification by real-time RT-PCR

To confirm and quantify the differential gene expression levels detected by SSH, relative transcript quantification between S and A samples was performed using qRT-PCR. PCR primers were designed for all 19 transcripts (Table 4) for which a predicted function could be established.

Table 4. qRT-PCR primers

Gene		Sequence 5' to 3'
Triterpene synthase	Fw	TCACTCCATCAACCTCAGAAG
	Rv	CCCAGAAGAGCGAGAAGAG
Resveratrol *O*-methyltransferase	Fw	TGAGGTTCAAGGTTGGAATATG
	Rv	TGGTTGTGGATGATGTCTGG
DIR	Fw	CCAGCACTCATACAACTTAATATCAAC
	Rv	CTCAACAGCACAGACTTTCAGG
Glycerol-3-phosphate dehydrogenase	Fw	GCAACACGCTCAAG
	Rv	TGGCTGACACCTATG
MAPK	Fw	CAACTATGACACAAAGGAAGAAG
	Rv	CATTTACTGAAGAGAATATCAAAGAAC
Oligopeptide transporter	Fw	TATTGGAATAATCTACAGCGTGATAGTG
	Rv	GAAGACGAAGGCGAGCAGAG
Gibberellic acid receptor	Fw	AGTAGAAGCCGATTGTTGC
	Rv	AGAGTCTTGTTGTGGTTGC
Inositol transporter	Fw	GTAATAAGGTATCCAGTTGTTCAATG
	Rv	CTTCCTCTCAAATTCAGTCTATCG
Cinnamoyl-CoA reductase	Fw	GGTTGGAGATGGTGAGATG
	Rv	CTTGACGAGAGAAACTGGAG
Oligouridylate binding protein	Fw	AAGGTGCTGGAGGTAACG
	Rv	ATGTCGGTGGAGGTCAAC
Zinc-finger RING-type protein	Fw	TGAGATAGCCAGACAAGTAG
	Rv	TTGCCTCCACCATTGC
ACT (XM_002282480)	Fw	GACTACCTACAACTCCATCAT
	Rv	TCATTCTGTCAGCAATACCA
L2 (AJ441290.2)	Fw	TCTACTTCAACCGATATGC
	Rv	CCACCTGTCCGACTG
PEP (AF236126.1)	Fw	CCTCCTCCTCCAGATTGC
	Rv	GGCTTGCTTGATTCCATTATC
UBC (EE253706)	Fw	CATAAGGGCTATCAGGAGGAC
	Rv	TGGCGGTCGGAGTTAGG
CYP (ES880796)	Fw	ACAGCCAAGACCTCGTG
	Rv	GCCTTCACTGACCACAAC
VAG (XM_002281110.1)	Fw	TTGCCTGTGTCTCTTGTTC
	Rv	TCAATGCTGCCAGAAGTG
EF1 (GU585871.1)	Fw	GAACTGGGTGCTTGATAGGC
	Rv	AACCAAAATATCCGGAGTAAAAGA
UFGT (JF522535.1)	Fw	GGTGGTTTTACCTGCTAATTTGTT
	Rv	GTGAGAAGAGCGAGTTTAGGTTTC
DFR (AY780886.1)	Fw	TCATCACTATCATACCGACTCTTGT
	Rv	CCTGCCGTATAATTGAATGAGC
*AR (*XM_002282806.1*)*	Fw	TCTATCAGCACCATCACAGCCAAGG
	Rv	CCAACCACCCACTCTCGTCTTCC
ConGlu (XM_002264642.2)	Fw	TCTCTTGGAGTCAACAGCTACCG
	Rv	TCACTTCTCCAAATCTCCCTTCGG
*PRR**	Fw	TTCTTGTDGTGGGTGGVACAGGSTA
	Rv	ACCAYATYTACTTTCTTCACWGCTT
*CaOMT**	Fw	TCSMCCRGTATGAYCCCARMAACTA
	Rv	TGGKGAYCTKAGCAGCAATCT
*CAD**	Fw	AAATGSGTAGCCTTGRGACTGA
	Rv	TCYGATCCCACCTCCACC
UDP-GT (XM_002273320.1)	Fw	ACTCCTCATCTCCCTAACTTGCTG
	Rv	TTCATGGCCGAGATTGCAGAG
F5H (XM_002272608.2)	Fw	TCCGACTCCACCCACCTATT
	Rv	GCCCGCTTTGAGAAACCTTG

* Degenerate primer

Amplification specificity for each primer pair was evaluated by both BLASTn and melting curve analysis. Yet, eight genes were excluded from the study either due to unspecific amplifications or primer-dimer formation. In addition to the selected genes, the relative expression levels of actin and ribosomal protein L2 were also measured to evaluate the potential bias being introduced in the quantification due to inappropriate reference gene selection.

The relative gene expression levels between S and A mRNA samples are represented in Figure 7.

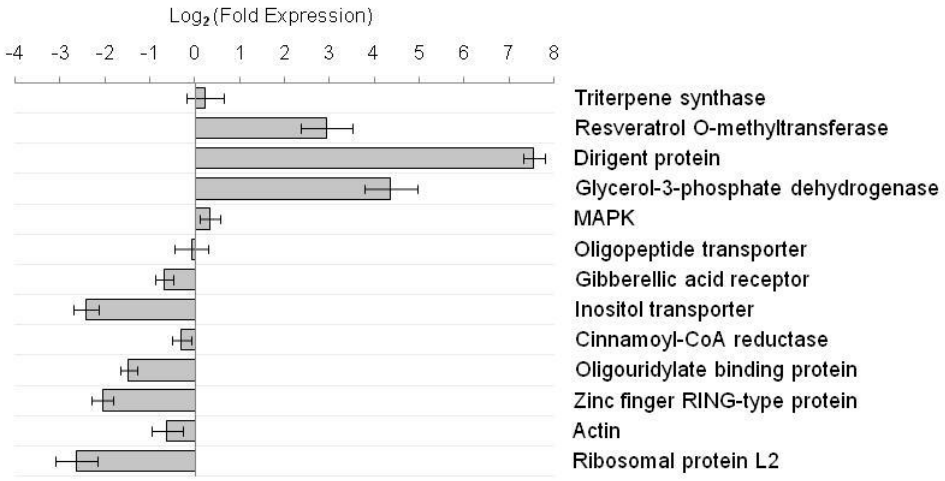

Figure 7. qRT-PCR analysis of the SSH detected transcripts and two commonly used normalization genes (Actin, L2 ribosomal protein). Relative gene expression quantification between symptomatic and asymptomatic grapevine leaves was calculated based on triplicated PCR reactions from four biological replicates, using *UBC* and *VAG* as normalization genes.

With the exception of KC748416, representing an oligopeptide transporter, all SSH detected transcripts were found to be present in significantly different amounts in symptomatic and asymptomatic samples. The agreement observed in all cases between the cDNA library, from where the transcripts were identified (forward or reverse SSH), and their correspondent up or downregulation also validates the subtraction process

(Table 3, Figure 7). Overall, the analyzed genes present slightly moderate levels of differential expression with $\log_2$(fold change) values ranging from -2.65 to 4.36 for L2 ribosomal protein and glycerol-3-phosphate dehydrogenase, respectively. Among all the transcripts, the dirigent-like protein (*DIR*) (KC748418) stands out of the remaining due to the magnitude of overexpression in symptomatic leaves when compared to asymptomatic ones. Its upregulation reaches over 180 fold change, representing a variation 10 to 150 times larger than that observed for the remaining transcripts.

Genomic *DIR* copy number determination in *Vitis vinifera* cultivars

To assess whether *DIR* gene dosage could be somehow relevant in *V. vinifera – E. necator* interaction, qPCR was used to determine the *DIR* copy number in three *V. vinifera* cultivars with different powdery mildew susceptibilities. Genomic DNA from the cultivars Carignan, Fernão Pires and Touriga Nacional was used as template for *V. vinifera* cultivars with high, moderate and low powdery mildew susceptibility, respectively. The powdery mildew susceptibility degree of each cultivar was assessed according to the empirical ranking provided by Dr. Antero Martins and co-workers (ISA/PORVID), which is based on their wide viticulture experience and field observations.

Given the individual DNA quality patterns obtained from the three *V. vinifera* cultivars, accurate spectrophotometric DNA quantification was not feasible and thus absolute quantification of *DIR* gene copy number was not carried out. Instead, a relative quantification procedure was selected using cultivar Pinot Noir genomic DNA as calibrator and three single copy genes as reference. According to the grapevine genome sequence available at Genoscope (http://www.genoscope.cns.fr/spip/), *DIR* is a two-copy gene in Pinot Noir, while UDP-glucose:flavonoid 3-*O*-

glucosyltransferase (*UFGT*), dihydroflavonol reductase (*DFR*) and anthocyanidin reductase (*AR*) are products of single-copy genes. *DIR* copy number was calculated (Figure 8) based on the $E^{-\Delta Ct}$ ratios between *DIR* and single-copy genes according to the following equation:

$$\text{DIR copy number} = \frac{E_{DIR}^{\Delta\text{Ct(calibrator–cultivar)}}}{E_{ref}^{\Delta\text{Ct(calibrator–cultivar)}}} \times 2$$

where *E* = amplification efficiency of the gene (*DIR* or *reference*) and ΔCt = calibrator Ct – cultivar Ct from the respective gene.

No significant differences in the determined $E^{-\Delta Ct}$ ratios were observed for each of the three cultivars (Figure 8), indicating that *DIR* is a two-copy gene in the genomes of the cultivars Carignan, Fernão Pires and Touriga Nacional.

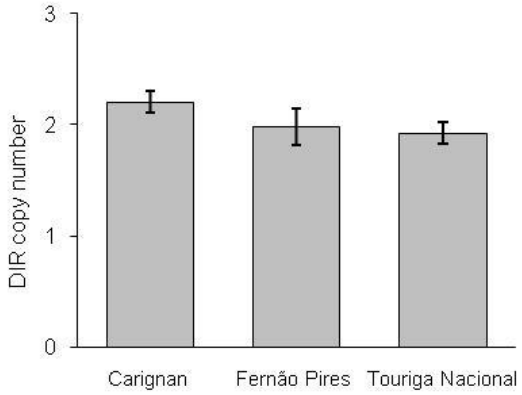

Figure 8. Genomic *DIR* copy number from grapevine cultivars with different powdery mildew susceptibilities. Absolute copy number was determined through qPCR using the relative quantification method where the genomic DNA of Pinot Noir was used as calibrator. Three Pinot Noir single copy genes were used for normalization.

Coniferyl alcohol branching genes

Up to date, almost all the described DIR assisted reactions involve coniferyl alcohol dimerization to afford (+)-pinoresinol [20]. Given the substantial *DIR* upregulation in *E. necator*-infected symptomatic grapevine leaves, a transcriptomic approach was applied to analyze the "metabolic neighbourhood" directly concerned with, or centred in coniferyl alcohol (Figure 9).

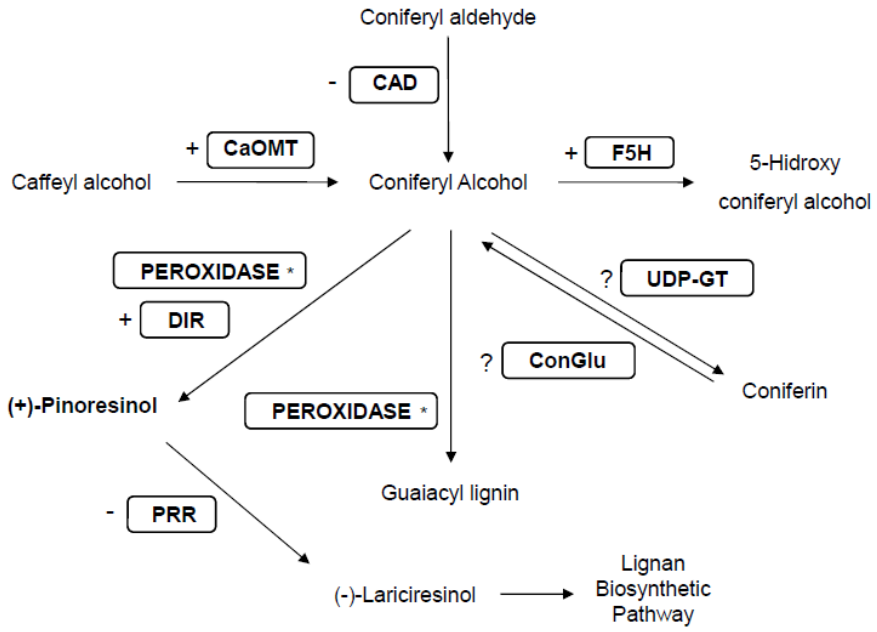

Figure 9. Coniferyl alcohol branching enzymes. Overview of *V. vinifera* genes directly involved in coniferyl alcohol metabolism and their determined up (+)/downregulation(-) in *E. necator* symptomatic leaves.
* - Spontaneous peroxidase activity.

The metabolic pathway information was obtained through KEGG database [21,22]. The main objective was to investigate whether the differential transcription observed for SSH-identified *DIR* was consistent with the ones from the remaining branching genes, regarding the reported coniferyl alcohol metabolic fate (*i.e.* yield of (+)-pinoresinol). According to the

phenylpropanoid metabolic pathway described for several plant species, which is illustrated in Figure 9, a study on the relative expression of the genes encoding caffeic acid *O*-methyltransferase (*CaOMT*), coniferyl-alcohol dehydrogenase (*CAD*), ferulate-5-hydroxylase (*F5H*), coniferyl-alcohol glucosyltransferase (*UDP-GT*), coniferin beta-glucosidase (*ConGlu*) and pinoresinol reductase (*PRR*) was conducted. The *V. vinifera* genome database was searched for each of the previous gene orthologues and PCR primers were designed (Table 4) within the conserved regions of each orthologue family. Melting curve analysis for both *UDP-GT* and *ConGlu* amplicons consistently revealed non-specific amplifications, a result which did not allow data gathering concerning the interconversion between coniferyl-alcohol and coniferin. Relative transcription $\log_2$(fold values) determined for the remaining coniferyl-alcohol branching genes is shown in Figure 10.

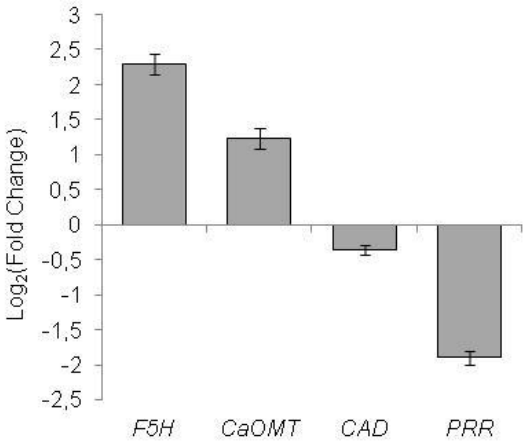

Figure 10. qRT-PCR analysis of the coniferyl alcohol related genes. Relative gene expression quantification between symptomatic and asymptomatic grapevine leaves was calculated based on triplicated PCR reactions from two biological replicates, using *UBC* and *VAG* as normalization genes.

Discussion

SSH cDNA libraries

In contrast to conventional transcriptomic studies, regarding plant-pathogen interactions, where the experimental design is set to identify early or midterm host responses induced by the pathogen, the experimental approach followed in the present work emphasises long term transcriptional modifications. Moreover, it focuses on differential expression patterns occurring within the host tissues (*V. vinifera* leaves) due to prolonged and successful fungal colonization when compared to tissues that, although having been exposed to *E. necator* spores, remain asymptomatic. PAMP-triggered immunity (PTI) and systemic acquired resistance (SAR) constitute key elements in plant defence mechanisms [23]. However, PTI relies on the recognition of highly conserved epitopes among pathogens and thus, comprises, along with pre-formed chemical and physical barriers, a non-host resistance mechanism [24]. Conversely, SAR is based on much higher degree of specificity towards pathogens and is mediated by the products of disease resistance (*R*) genes after the plant is locally infected by the pathogen [25]. Nevertheless, apart from the initial recognition process, both PTI and SAR seem to share downstream signalling machinery and essentially differ from one another by the extent of the pathogen-induced responses, transient in PTI and prolonged in SAR [26].

By applying the SSH technique to determine differentially expressed genes between symptomatic (S) and asymptomatic (A) leaves from powdery mildew infected grapevine (*V. vinifera*, cv. Touriga Nacional), the genes exclusively involved in PTI are expected to be overlooked. Given that, in this study, S and A samples were both collected from plants exposed to the same initial external stimulus and subsequently grown for 30 days with generalized powdery mildew infection, it is reasonable to

assume that at least some of the detected transcript changes will be a consequence of an activated SAR mechanism. Moreover, the detection of mRNA variations reflecting host attempts to maintain homeostasis is expected while excessive nutrient consumption is occurring due to the pathogen presence. In addition, the pathogen also exerts pressure to modulate the host gene expression to its own benefice. In other words, this experimental approach accounts for the permanent host genetic manipulation by the pathogen to fulfill its nutritional needs and to suppress the host specific recognition mechanisms. Anyhow, without additional data, the SSH detected transcripts (Table 3) can only be assigned to standard functional classes: signalling processes and secondary metabolite biosynthetic pathways, which for the most part concern genes associated with defence-related mechanisms.

The apparently reduced number of SSH identified genes may be tentatively explained by the premise that the cDNA library screening process, namely the use of non-radioactive labelled probes, did not show enough sensitivity to discriminate between the individual relative transcript abundance of both cDNA subtraction pools. Thus, despite the positive evidence on the subtraction efficiency, an unknown number of the overall "subtracted" transcripts may not have been detected in this study.

Reference gene selection for qRT-PCR studies

To become aware of the possible bias magnitude generated by the use of an inadequate reference gene selection, the relative transcription levels of the genes encoding actin and the ribosomal protein L2 were measured. The poor stability of the former had already been shown for biotic stress in potato [27], whereas the latter was shown to be the worst ranked candidate in the previous chapter. Both actin and ribosomal protein L2 are downregulated in symptomatic leaves (when compared to asymptomatic

ones), with approximate fold-change values of -1.5 and -6.3, respectively (Figure 7). These data confirm the study of Derveaux and colleagues, who reported that small changes in expression levels should not be based on single non-validated reference genes to prevent significantly biased results [28].

Differential gene expression quantification by qRT-PCR

Regarding the SSH identified transcripts and independently of the relative expression quantification accuracy, one cannot get into profound considerations about their role in plant defense. Still it is possible to correlate our results with others described in the literature as far as plant pathogen interactions are concerned. It was interesting to notice that none of the detected genes had correspondence with the ones detected by Fekete *et al*. (2009) which performed a similar gene expression study during the early stages (up to 48h) of *E. necator* infection in grapevine leaves [29]. Such observation highlights the infection process dynamics evidencing distinct host transcriptional responses/modifications during the course of infection. Moreover, within the time lapse Fekete and colleagues carried their experiments, significant differential expression changes were also observed along the first 48h of infection. We therefore consider that the present study provides novel and valuable information about *V. vinifera* - *E. necator* interaction in the sense that it describes transcriptomic changes occurring long after the infection is established and possibly illustrates host manipulation by the pathogen and the systemic acquired resistance mechanism developed by the asymptomatic leaves of the plant.

As mentioned before, the majority of the detected genes in the present study belong to signalling pathways or to secondary metabolite biosynthetic routes. The most relevant genes are discussed.

F1B5 EST (KC748395), coding for a glycerol-3-phosphate dehydrogenase, was found to be upregulated in powdery mildew symptomatic leaves, with a fold-change value of +20.6 when compared to asymptomatic leaves. Glycerol-3-phosphate was recently reported as a regulator of plant defense signalling. Although the mechanisms underlying this signalling pathway remain unexplored, it has been shown that *Arabidopsis thaliana* mutants in glycerol-3-phosphate synthesizing genes, such as glycerol kinase or glycerol-3-phosphate dehydrogenase, display enhanced susceptibility to *Colletotrichum higginsianum*, a hemibiotrophic ascomycete responsible for anthracnose disease in *Brassica* sp. [30].

Clone R2A10 (KC748405), codes for an inositol transporter, which was observed to be downregulated (-5.38 fold-change) in symptomatic leaves. Myo-inositol plays an important role as the structural basis for a number of secondary messengers in the signal transduction pathways which modulate intracellular events through free Ca^{2+} level regulation [31]. Though ubiquitous in biochemical pathways, myo-inositol metabolism is regarded to intervene in elicitor-induced phytoalexin production and programmed cell death [32,33]. This makes sense as part of the overall fungal strategy in keeping the host defenses low during the long-time it operates as a parasite of grapevine leaves.

R2C3 EST (KC748410) codes for a hormone sensitive lipase (downregulated: -1.60 fold change) with high homology for a gibberellic acid receptor. Besides playing an important role in plant growth and development, gibberellic acid hormonal signalling is also involved in plant defense mechanisms. Moreover, it has been reported as a potential manipulation target in host-microbe compatible interactions [34].

Concerning clone F1D5 (KC748408), coding for a mitogen activated protein kinase (MAPK), a slight powdery mildew-induced upregulation (+1.26 fold change) was observed. MAPK cascade-mediated signalling is an essential step in the establishment of resistance to pathogens [4].

Within the MAPK family, F1D5 displays the highest homology with MAPK4, which negatively regulates biotic stress signalling, namely systemic acquired resistance [35].

According to our results, R1C7 transcript (KC748397), highly similar to cinnamoyl-CoA reductase (CCR), was weakly repressed in symptomatic leaves. Being a key enzyme in lignin biosynthetic pathway, its regulation directly affects lignin deposition patterns in plants [36]. Several genes encoding CCR have already been shown to be associated to both developmental stages and biotic/abiotic stresses [36-38]. The lignification process can be an important step towards pathogen resistance, either through lignin deposition or formation of lignin-like compounds [39,40]. Thus, the observed CCR downregulation, in this case, can hypothetically be perceived as host manipulation by the pathogen.

An overexpression in symptomatic leaves regarding clone F1C5 (triterpene synthase), F1A11 (resveratrol *O*-methyltransferase) and F1E6 (DIR) was also observed. The corresponding genes are directly involved in the synthesis of secondary metabolites exhibiting antimicrobial properties. Triterpene synthases are oxidosqualene cyclases catalyzing the cyclization of 2,3-oxidosqualene to afford triterpenoid compounds such as lupeol, betulinic acid or beta-amyrin [41]. The SSH detected oxidosqualene cyclase (KC748400) has the highest homology with beta-amyrin synthase. *trans*-Resveratrol, a trihidroxystilbene phytoalexin is, *per se*, an antifungal compound reported to be produced in plants in response to pathogen attack [42]. Nevertheless, subsequent *trans*-resveratrol metabolic modifications, like dimerization or *O*-methylation, can yield products with enhanced antifungal activity [43]. *O*-Methylation of *trans*-resveratrol to afford pterostilbene, a highly toxic metabolite, is catalized by resveratrol-*O*-methyltransferase, whose expression was observed to increase in grapevine leaves upon downy mildew infection [44]. This correlates well with the present work where the SSH detected resveratrol-

O-methyltransferase (KC748406) is upregulated in grapevine leaves (+7.68 fold change) due to *E. necator* colonization. Dirigent proteins, although devoid of enzymatic activity, play an important role as chiral auxiliaries to direct the stereochemistry of the reactions in which they participate [15,45]. Up to date, most of the functionally characterized dirigent proteins were shown to participate in lignan biosynthesis, namely in the dimerization of coniferyl alcohol to afford (+)-pinoresinol, a key step in lignan biosynthesis [16]. Lignans constitute an abundant class of phenylpropanoid dimers, well recognized for their antifungal properties [46,47]. Among the SSH detected transcripts, the gene encoding the dirigent protein (KC748418) displayed by far the highest differential transcription level between symptomatic and asymptomatic leaves from powdery mildew infected grapevine. Its upregulation magnitude in symptomatic leaves reached fold-change values up to 150 times higher than the remaining SSH detected transcripts, highlighting a great potential relevance in plant defense mechanisms.

Dirigent Proteins

Genes encoding dirigent proteins have been described as being constitutively expressed at very low levels but rapidly induced in response to biotic stress [48,49]. This is consistent with the observed upregulation intensity for the detected dirigent protein encoding gene. Considering the potentially important role of DIR in plant protection against pathogens and the low constitutive expression level of the gene encoding it, the transcriptional rate, and thus the speed at which the plant reacts to stress, could be limited by gene dosage. Therefore, since no data could be gathered about *E. necator*-induced *DIR* transcription in grapevine cultivars with different powdery mildew susceptibilities, *DIR* gene copy number was determined for three *V. vinifera* cultivars (Carignan, Fernão Pires, and

Touriga Nacional). All three cultivars were shown to possess an equal number of *DIR* copies in their genome, which was the same as that contained in Pinot Noir. Thus, it is possible to conclude that powdery-mildew susceptibility in *V. vinifera* cultivars is not directly correlated to *DIR* gene copy number, despite the apparent great potential importance played by DIR in plant protection against pathogens.

Considering the genes differentially transcribed between symptomatic and asymptomatic leaves from *E. necator*-infected *V. vinifera* and the putative reaction assisted by the DIR protein (dimerization of coniferyl alcohol to afford (+)-pinoresinol), the transcription levels of the genes whose products operate in the metabolic neighbourhood of coniferyl alcohol were analyzed (Figure 9). The main objective of such an experiment was trying to correlate the expression level of those genes involved in the metabolism of the monolignol with the observed, fungal-induced upregulation of the *DIR* gene. Even though this analysis is not representative of the extremely intricate cellular metabolism, it may provide clues indicative of major metabolic flux alterations. When the transcription rate of most enzymes depicted in Figure 9 was determined under the conditions originating 180 fold upregulation of the *DIR* gene, it was interesting to note that pinoresinol reductase (PRR), described as the enzyme metabolizing the product of the DIR-assisted reaction, undergoes downregulation. Alternative explanations include divergent branching of lignan biosynthetic pathway, in which pinoresinol is converted into metabolites other than lariciresinol, or the involvement of the DIR in the stereochemical control of other reactions.

In the absence of the DIR protein under study, three isomers are formed by dimerization of coniferyl alcohol molecules, in an oxidative reaction which occurs either spontaneously or in the presence of peroxidases [15]: pinoresinol, dehydrodiconiferyl alcohol (DDCA) and guaiacylglycerol 8-*O*-4'-coniferyl ether (GGCE), in the thermodynamic-dependent relative

proportions of 26 to 28%, 52 to 57% and 17 to 19%, respectively. In a different study, Halls (2004) confirmed similar proportions as 0.5:1.0:0.3. However, only (+)-pinoresinol is formed when the DIR protein is present [50]. Furthermore, the complete stereoselectivity is preserved as long as the oxidative capacity does not exceed a point where the DIR protein becomes saturated [15].

Knowing that both DDCA [51] and GGCE [52] have been reported as lignin precursors, a different hypothesis may be formulated to explain the >180 fold increase in *DIR* gene transcription in symptomatic grapevine leaves infected with powdery mildew: to ensure that neither of the two isomers other than (+)-pinoresinol is formed under such conditions. If this hypothesis is correct, a low level of DIR during the initial stages of *E. necator* infection may allow lignin biosynthesis to build up physical barriers, whereas a potent, lignan dependent antifungal activity is considered a host priority at later stages of infection.

References

1. Glawe DA (2008) The powdery mildews: A review of the world's most familiar (yet poorly known) plant pathogens. Annual Review of Phytopathology 46: 27-51.
2. Carisse O, Bacon R, Lefebvre A (2009) Grape powdery mildew (*Erysiphe necator*) risk assessment based on airborne conidium concentration. Crop Protection 28: 1036-1044.
3. Ferreira RB, Monteiro S, Freitas R, Santos CN, Chen Z, et al. (2007) The role of plant defence proteins in fungal pathogenesis. Molecular Plant Pathology 8: 677-700.
4. Pitzschke A, Schikora A, Hirt H (2009) MAPK cascade signalling networks in plant defence. Current Opinion in Plant Biology 12: 421-426.
5. Jones JDG, Dangl JL (2006) The plant immune system. Nature 444: 323-329.

6. Nicaise V, Roux M, Zipfel C (2009) Recent advances in PAMP-triggered immunity against bacteria: pattern recognition receptors watch over and raise the alarm. Plant Physiology 150: 1638-1647.
7. Chisholm ST, Coaker G, Day B, Staskawicz BJ (2006) Host-microbe interactions: Shaping the evolution of the plant immune response. Cell 124: 803-814.
8. Mendgen K, Hahn M (2002) Plant infection and the establishment of fungal biotrophy. Trends in Plant Science 7: 352-356.
9. Panstruga R (2003) Establishing compatibility between plants and obligate biotrophic pathogens. Current Opinion in Plant Biology 6: 320-326.
10. O'Connell RJ, Panstruga R (2006) Tete a tete inside a plant cell: establishing compatibility between plants and biotrophic fungi and oomycetes. The New phytologist 171: 699-718.
11. Mullins MG, Bouquet A, Williams LE (1992) Biology of the grapevine; Press CU, editor. New York.
12. Fung R, Qiu W, Su Y, Schachtman D, Huppert K, et al. (2007) Gene expression variation in grapevine species *Vitis vinifera* L. and *Vitis aestivalis* Michx. Genetic Resources and Crop Evolution 54: 1541-1553.
13. Fung RWM, Gonzalo M, Fekete C, Kovacs LG, He Y, et al. (2008) Powdery mildew induces defense-oriented reprogramming of the transcriptome in a susceptible but not in a resistant grapevine. Plant Physiology 146: 236-249.
14. Caldo RA, Nettleton D, Peng J, Wise RP (2006) Stage-specific suppression of basal defense discriminates barley plants containing fast- and delayed-acting Mla powdery mildew resistance alleles. Molecular Plant-Microbe Interactions 19: 939-947.
15. Davin LB, Wang H-B, Crowell AL, Bedgar DL, Martin DM, et al. (1997) Stereoselective bimolecular phenoxy radical coupling by an auxiliary (Dirigent) protein without an active center. Science 275: 362-367.
16. Umezawa T (2003) Diversity in lignan biosynthesis. Phytochemistry Reviews 2: 371-390.
17. MacRae WD, Towers GHN (1984) Biological activities of lignans. Phytochemistry 23: 1207-1220.
18. Akiyama K, Maruyama M, Yamauchi S, Nakashima Y, Nakato T, et al. (2007) Antimicrobiological activity of lignan: Effect of benzylic oxygen and stereochemistry of 2,3-dibenzyl-4-butanolide and 3,4-

dibenzyltetrahydrofuran lignans on activity. Bioscience, Biotechnology, and Biochemistry 71: 1745-1751.
19. Chang S, Puryear J, Cairney J (1993) A simple and efficient method for isolating RNA from pine trees. Plant Molecular Biology Reporter 11: 113-116.
20. Ralph SG, Jancsik S, Bohlmann J (2007) Dirigent proteins in conifer defense II: Extended gene discovery, phylogeny, and constitutive and stress-induced gene expression in spruce (*Picea* spp.). Phytochemistry 68: 1975-1991.
21. Kanehisa M, Goto S (2000) KEGG: Kyoto Encyclopedia of Genes and Genomes. Nucleic Acids Research 28: 27-30.
22. Kanehisa M, Goto S, Sato Y, Furumichi M, Tanabe M (2012) KEGG for integration and interpretation of large-scale molecular data sets. Nucleic Acids Research 40: D109-D114.
23. Liu P-P, Bhattacharjee S, Klessig DF, Moffett P (2010) Systemic acquired resistance is induced by R gene-mediated responses independent of cell death. Molecular Plant Pathology 11: 155-160.
24. Mishina TE, Zeier J (2007) Pathogen-associated molecular pattern recognition rather than development of tissue necrosis contributes to bacterial induction of systemic acquired resistance in *Arabidopsis*. The Plant Journal 50: 500-513.
25. Vlot AC, Klessig DF, Park S-W (2008) Systemic acquired resistance: the elusive signal(s). Current Opinion in Plant Biology 11: 436-442.
26. Tsuda K, Katagiri F (2010) Comparing signaling mechanisms engaged in pattern-triggered and effector-triggered immunity. Current Opinion in Plant Biology 13: 459-465.
27. Nicot N, Hausman J-F, Hoffmann L, Evers D (2005) Housekeeping gene selection for real-time RT-PCR normalization in potato during biotic and abiotic stress. Journal of Experimental Botany 56: 2907-2914.
28. Derveaux S, Vandesompele J, Hellemans J (2010) How to do successful gene expression analysis using real-time PCR. Methods 50: 227-230.
29. Fekete C, Fung RWM, Szabó Z, Qiu W, Chang L, et al. (2009) Up-regulated transcripts in a compatible powdery mildew–grapevine interaction. Plant Physiology and Biochemistry 47: 732-738.
30. Venugopal SC, Chanda B, Vaillancourt L, Kachroo A, Kachroo P (2009) The common metabolite glycerol-3-phosphate is a novel

regulator of plant defense signaling. Plant signaling & behavior 4: 746-749.

31. Shigaki T, Bhattacharyya MK (2000) Decreased inositol 1,4,5-trisphosphate content in pathogen-challenged soybean cells. Molecular Plant-Microbe Interactions 13: 563-567.
32. Zhao J, Davis LC, Verpoorte R (2005) Elicitor signal transduction leading to production of plant secondary metabolites. Biotechnology Advances 23: 283-333.
33. Meng PH, Raynaud C, Tcherkez G, Blanchet S, Massoud K, et al. (2009) Crosstalks between myo-Inositol metabolism, programmed cell death and basal immunity in *Arabidopsis*. PLoS ONE 4: e7364.
34. Schäfer P, Pfiffi S, Voll LM, Zajic D, Chandler PM, et al. (2009) Manipulation of plant innate immunity and gibberellin as factor of compatibility in the mutualistic association of barley roots with *Piriformospora indica*. The Plant Journal 59: 461-474.
35. Petersen M, Brodersen P, Naested H, Andreasson E, Lindhart U, et al. (2000) *Arabidopsis* MAP Kinase 4 negatively regulates systemic acquired resistance. Cell 103: 1111-1120.
36. Lauvergeat V, Lacomme C, Lacombe E, Lasserre E, Roby D, et al. (2001) Two cinnamoyl-CoA reductase (CCR) genes from *Arabidopsis thaliana* are differentially expressed during development and in response to infection with pathogenic bacteria. Phytochemistry 57: 1187-1195.
37. Escamilla-Trevino LL, Shen H, Uppalapati SR, Ray T, Tang YH, et al. (2010) Switchgrass (*Panicum virgatum*) possesses a divergent family of cinnamoyl CoA reductases with distinct biochemical properties. New Phytologist 185: 143-155.
38. So HA, Chung E, Cho CW, Kim KY, Lee JH (2010) Molecular cloning and characterization of soybean cinnamoyl CoA reductase induced by abiotic stresses. Plant Pathology Journal 26: 380-385.
39. Tang X, Xie M, Kim YJ, Zhou J, Klessig DF, et al. (1999) Overexpression of Pto activates defense responses and confers broad resistance. Plant Cell 11: 15-29.
40. Kawasaki T, Koita H, Nakatsubo T, Hasegawa K, Wakabayashi K, et al. (2006) Cinnamoyl-CoA reductase, a key enzyme in lignin biosynthesis, is an effector of small GTPase Rac in defense signaling in rice. Proceedings of the National Academy of Sciences of the United States of America 103: 230-235.

41. Hayashi H, Huang P, Takada S, Obinata M, Inoue K, et al. (2004) Differential expression of three oxidosqualene cyclase mRNAs in *Glycyrrhiza glabra*. Biological & pharmaceutical bulletin 27: 1086-1092.
42. Chang X, Heene E, Qiao F, Nick P (2011) The phytoalexin resveratrol regulates the initiation of hypersensitive cell death in *Vitis* cell. PLoS ONE 6: e26405.
43. Schnee S, Viret O, Gindro K (2008) Role of stilbenes in the resistance of grapevine to powdery mildew. Physiological and Molecular Plant Pathology 72: 128-133.
44. Schmidlin L, Poutaraud A, Claudel P, Mestre P, Prado E, et al. (2008) A stress-inducible resveratrol *O*-methyltransferase involved in the biosynthesis of pterostilbene in grapevine. Plant Physiology 148: 1630-1639.
45. Liu J, Stipanovic RD, Bell AA, Puckhaber LS, Magill CW (2008) Stereoselective coupling of hemigossypol to form (+)-gossypol in moco cotton is mediated by a dirigent protein. Phytochemistry 69: 3038-3042.
46. Apers S, Vlietinck A, Pieters L (2003) Lignans and neolignans as lead compounds. Phytochemistry Reviews 2: 201-217.
47. Saleem M, Kim HJ, Ali MS, Lee YS (2005) An update on bioactive plant lignans. Natural Product Reports 22: 696-716.
48. Zhu L, Zhang X, Tu L, Zeng F, Nie Y, et al. (2007) Isolation and characterization of two novel dirigent-like genes highly induced in cotton *(Gossypium barbadense* and *G-hirsutum*) after infection by Verticillium dahliae. Journal of Plant Pathology 89: 41-45.
49. Ralph S, Park J-Y, Bohlmann J, Mansfield S (2006) Dirigent Proteins in Conifer Defense: Gene Discovery, Phylogeny, and Differential Wound- and Insect-induced Expression of a Family of DIR and DIR-like Genes in Spruce (*Picea* spp.). Plant Molecular Biology 60: 21-40.
50. Halls SC, Davin LB, Kramer DM, Lewis NG (2004) Kinetic study of coniferyl alcohol radical binding to the (+)-pinoresinol forming dirigent protein. Biochemistry 43: 2587-2595.
51. Takeda H, Kotake T, Nakagawa N, Sakurai N, Nevins DJ (2003) Expression and function of cell wall-bound cationic peroxidase in *Asparagus* somatic embryogenesis. Plant Physiology 131: 1765-1774.

52. Nord FF (1964) The formation of lignin and its biochemical degradation. Geochimica et Cosmochimica Acta 28: 1507-1522.

Chapter IV: Study on *Vv*DIR1 Function and Physiological Role

This chapter presents unpublished data

Author contribution:

AFB performed the majority of the experimental work

Abstract

Dirigent proteins are proteins devoid of catalytic activity which can act as chiral auxiliaries in reactions performed by other proteins. They were first reported as participating in lignan biosynthesis where they were shown to regio-stereochemically control the monolignol radical coupling reactions, namely the dimerization of coniferyl alcohol to afford (+)-pinoresinol. Being involved in the synthesis of compounds potentially relevant for plant defence, corroborated with reported gene overexpression upon biotic and abiotic stresses, they are annotated as disease-responsive proteins. In *Vitis vinifera*, *Vv*DIR1 gene was earlier observed as displaying a significant upregulation in powdery mildew infected leaves. To confirm its putative role in lignan biosynthesis or potential involvement in lignin formation, several experimental approaches were attempted. Lignin quantification using acetyl bromide assay was performed for diseased and healthy *V. vinifera* leaves. Infected leaves displayed higher contents of lignin when compared to healthy leaves. *Arabidopsis thaliana* T-DNA mutants with disrupted *At*DIR5 and *At*DIR6 genes, as well as a double mutant were intended for reverse genetic studies. The inability to generate/detect homozygous individuals for T-DNA insertion in *At*DIR5 may suggest the presence of a lethal phenotype possibly affecting seed development. *Vv*DIR1 heterologous expression was performed using a *P. pastoris* expression system. Recombinant protein production was achieved at very low levels with yields of approximately 2.2 mg per litre of yeast culture. *In vitro* coniferyl alcohol coupling reactions in the presence of *Vv*DIR1 generated increased amounts of pinoresinol over the remaining products, confirming a stereoselective control of the radical coupling.

Introduction

Dirigent proteins (DIR) were discovered in 1997 in *Forsythia* species by Davin and colleagues, where they were found to actively participate in one of the first steps of the lignan biosynthetic pathway [1]. Lignans are secondary metabolites belonging to the vast class of phenylpropanoids, for which a major role in plant defence is acknowledged [2-4]. Their broad range of biological functions and activities, not only to the plant itself but also to other symbiotic or parasitic organisms, make them a particularly attractive class of natural compounds with potential agronomic importance. Nevertheless, the widespread interest in these compounds arose mainly due to their promising application in the fields of pharmacy and nutrition. Relevant activities for human health include antioxidant, antimicrobial, antitumor, antimitotic and antiviral properties [2,5-7].

With several thousand known lignans, isolated from a number of species, a remarkably rich structural variation is observed. In the strict sense, the term lignan refers only to phenylpropanoid dimers linked through a C-C bond between the carbons 8 and 8' of their side chains [8]. However, a broader definition has been suggested in which higher oligomers (dilignans and sesquilignans) and dimers with other C-C bonds (neolignans) are included [9,10]. Hence, according to Davin and Lewis (2003) suggestion, all coupling products of hydroxycinnamoyl-derived compounds, regardless of their molecular size or interunit linkages, should be termed lignans [11]. A few examples of lignans frequently encountered in plants are depicted in Figure 11. Soon after their structure elucidation, researchers inferred that the building blocks of those compounds would be C_6C_3 phenylpropanoids and that their formation would occur through oxidative coupling reactions mediated by peroxidases

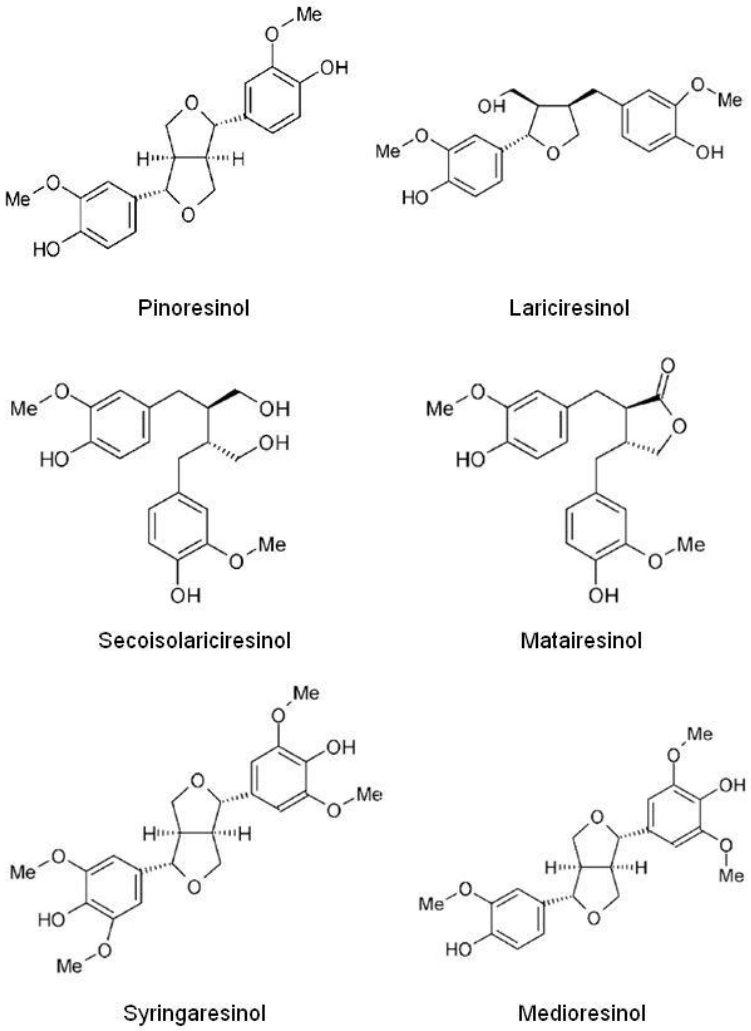

Figure 11. Commonly occurring lignans in plants

or laccases. Though this was later confirmed, the biosynthetic pathway of lignans remained an enigmatic and controversial process as the exact precursors for each lignan could not always be assigned and, moreover, these metabolites exhibited optical activity when isolated from plant extracts whereas the ones obtained *in vitro* were racemic [12-14]. Among the numerous hydroxycinnamic acid derivatives, the commonly suggested precursors for lignan synthesis were ferulic acid, coniferaldehyde, coniferyl

alcohol, sinapyl alcohol and *p*-coumaryl alcohol (Figure 12) [11]. For instance, (+)-pinoresinol isolated from *Forsythia* species was believed to result from the oxidative coupling of two molecules of coniferyl alcohol [14].

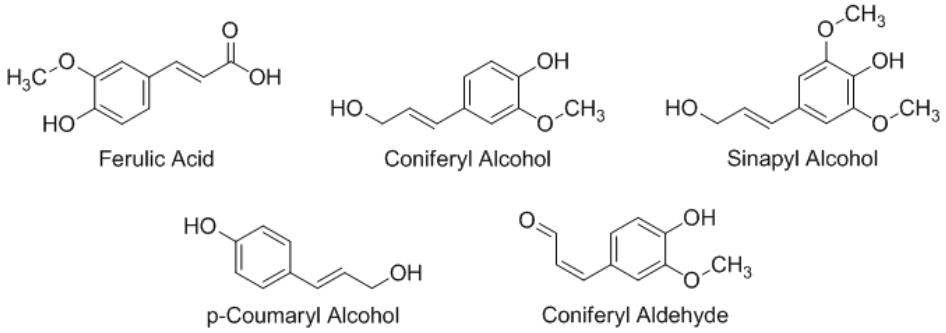

Figure 12. Hydroxycinnamic acid derivatives potentially involved in the synthesis of lignans.

In fact, *in vitro* coupling of coniferyl alcohol using peroxidase-H_2O_2 or laccase-O_2 systems, could originate pinoresinol. Yet, both its antipodes were consistently formed in equal amounts [2]. Further investigations along the rationale that, *in vivo*, a stereoselective control of the phenypropanoid coupling would have to be operative, led Davin and Lewis to the isolation and identification of the first DIR protein in *Forsythia intermedia* [1]. Being inactive *per se*, this protein had the ability to act as an enantioselective auxiliary in the dimerization of coniferyl alcohol to afford (+)-pinoresinol. The proposed mechanism in which such dimerization occurs is illustrated in Figure 13. Two separate reactions are involved: the first is the one electron oxidation of coniferyl alcohol promoted by laccases or peroxidases. In open solution, radicals undergo nonspecific coupling yielding several racemic products. The second is the radical sequestering by the DIR, guiding the dimerization process towards the exclusive formation of enantiomerically pure pinoresinol [1,15,16].

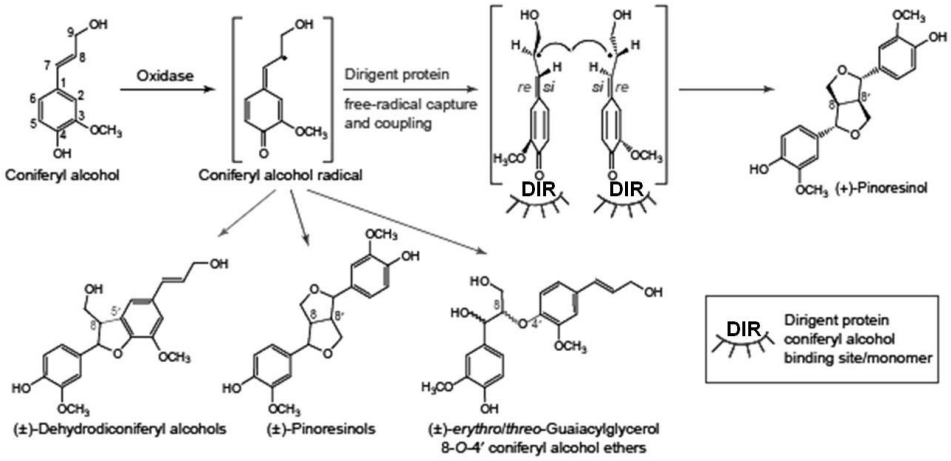

Figure 13. Formation of DIR-mediated (stereoselective) *versus* non-specific coniferyl alcohol coupling products (adapted from Davin and Lewis, 2005).

The discovery of this DIR protein, followed by the detection of other DIR homologues displaying the same activity in other species, and the observation that (+)-pinoresinol could be further metabolized to afford other lignans, partially unravelled the intriguing process of lignan biosynthesis [5,17]. Despite their large diversity and the occurrence of species-specific lignans, several studies have shown the existence of a common lignan biosynthetic pathway according to which the DIR-mediated coniferyl alcohol dimerization is a branching step from the general phenylpropanoid metabolism [16,18-21]. It is during this first reaction, the formation of pinoresinol, that the enantioselective character of lignan biosynthesis is acquired. The pathway then continues using pinoresinol as substrate to generate other ubiquitous lignans as lariciresinol, secoisolariciresinol and matairesinol. The enzymes responsible for these reactions, pinoresinol/lariciresinol reductase and secoisolariciresinol dehydrogenase, may also play an important role during the enantioselective synthesis of other downstream lignans as they can display differential affinity for each of the substrate enantiomers [5].

In addition to the major contribution to enlighten lignan biosynthesis, DIR discovery also brought up a series of questions concerning the formation of lignin [22]. In a sense, both biosynthetic processes could be related to each other. Not only are their products formed in a similar fashion, through radical-coupling reactions, but also they share the same monolignol precursors.

The synthesis of lignin has long been presumed to occur through random radical coupling of monolignols [23,24]. However, some biological aspects of lignification could not be explained under the light of this model: in native lignins 8-*O*-4' linkages are the most abundant, whereas *in vitro* a higher percentage of 8-8' and 8-5' linkages are observed; during the lignification process, targeting of specific monolignols into discrete regions of the cell is observed [22,25]. Arguably, according to these observations, the potential involvement of DIR proteins in lignin assembly was hypothesized. Additional evidence supporting this hypothesis was provided by immunolocalization and *in situ* hybridization studies where both mRNA and DIR epitopes were detected along lignin formation sites [26,27].

In this chapter, an attempt was made to elucidate the biological role of the previously identified DIR, designated *Vv*DIR1, from *V. vinifera* (Chapter III), investigating its possible connection to the lignin formation process and/or confirming its involvement in the stereoselective formation of coniferyl alcohol dimers.

Materials and Methods

Plant material and growth conditions

Vitis vinifera – Healthy cuttings (cultivar Touriga Nacional), with three buds each, were rooted in water and then transferred to soil (1 L pot per plant). Plants were maintained in a growth chamber at 25 ºC with a photoperiod of 16 h (480 $\mu mol.m^{-2}.s^{-1}$). After acclimatization, all plants were simultaneously inoculated with *E. necator* by direct contact with naturally infected grapevine leaves. The primary inoculum was collected from a vineyard at Instituto Superior de Agronomia, Lisbon, Portugal and passed on to a set of grapevines in a greenhouse which provided the experimental inoculum source. Leaves from the greenhouse plants were used to inoculate all the plants in the growth chamber. Plants were allowed to grow with generalized powdery mildew infection for 30 days prior to sample collection. After the infection stage, fully expanded leaves (fourth and fifth positions from the tip of each shoot) with and without *E. necator* infection symptoms (visible mycelia on the upper leaf surface) were randomly harvested and frozen in liquid nitrogen.

Arabidopsis thaliana – Seeds for wild-type and the selected T-DNA mutants, Mutant A (GK-022D05-018341) and B (WiscDsLox442B7), disrupting *At*DIR6 and *At*DIR5, respectively, were obtained from Nottingham Arabidopsis Stock Centre. Seeds were sterilized by immersion in 70% (v/v) ethanol (1 min), 10 % (v/v) household bleach (10 min) and washed five times in sterile water. Following sterilization, seeds were sown in Murashige & Skoog (MS) basal medium [28] containing 1 % (w/v) sucrose, 0.05 % (w/v) MES, 0.7 % (w/v) agar and were vernalized during 3 to 5 days at 4 ºC in the dark. Germination, selection and growth of the plants were carried in a growth chamber at 23 ºC with a photoperiod of 16 h (200 $\mu mol.m^{-2}.s^{-1}$). Selection of mutants was performed either by

incorporation of the selective agent in the growth medium (10 μg/mL sulfadiazine - mutant A) or daily pulverization (0.1 % (w/v) BASTA herbicide – mutant B). After the selection period, resistant plants were transferred to soil in individual pots. Following few days growth in soil (6 leaves) a small leaf sample was collected to confirm T-DNA presence and determine the corresponding genotype. Positive mutants (heterozygous or homozygous for the insertion) were maintained in the growth chamber through its lifecycle, watered every two days, for seed collection. To avoid cross-pollination the floral shoots of each plant were isolated with a paper bag as soon as floral buds appeared (until silique maturation). Seeds were collected by harvesting and crushing the floral shoots, releasing the seeds from the siliques. Seeds were cleaned by gentle tapping and blowing of the samples and were stored in the dark, at room temperature, in sealed tubes.

Cell wall isolation

Method A – Cell walls were extracted using a modification of the Uppsala method [29,30]. Leaf samples (c.a. 1 g) were ground in liquid nitrogen using a mortar and pestle and sonicated in 80 % (v/v) ethanol (40 mL/g) during 15 min. Samples were centrifuged (3000 *g*, 15 min) and the supernatant discarded. This procedure was repeated four times followed by a similar sonication/wash step using chloroform:methanol (2:1; 40 mL/g) and an acetone wash step (40 mL/g). Samples were air dried, resuspended in phosphate buffer (10 mM potassium phosphate (pH 6.0), 0.02 % (w/v) NaN_3; 30 mL/g) and incubated at 90 ºC during 2 h to gelatinize starch. After cooling to 55 ºC, samples were treated, first with 2 U of α-amylase (Sigma A3403) during 2 h and then with 2 U of α-amiloglucosidase (Sigma A7095) during 2.5 h. The solid residue was recovered by centrifugation (3000 *g,* 15 min) and washed 4 times with

water (40 mL/g). Following lyophilization, samples were used for lignin quantification.

Method B - Leaf samples (c.a. 1 g) were ground in liquid nitrogen using a mortar and pestle and sonicated in 100 mM potassium phosphate buffer, pH 7.0 (10 mL/g), during 15 min. Samples were centrifuged (3000 *g*, 15 min) and the supernatant discarded. This procedure was repeated and the samples were resuspended in 10 mM potassium phosphate, pH 7.0. The suspension was incubated for 2 h at 90 ºC and cooled to 55 ºC. After cooling, samples were treated, first with 2 U of α-amylase (Sigma A3403) during 2 h and then with 2 U of α-amiloglucosidase (Sigma A7095) during 2.5 h. Samples were centrifuged (3000 *g*, 15 min) and washed with water (3x), acetone (3x), methanol:chlorophorm (1:1) (3x) and diethyl ether (2x). Samples were air-dried, lyophilized and used for lignin quantification.

Lignin quantification - Acetyl bromide assay

Cell wall samples were weighted (20 to 25 mg) into glass tubes fitted with Teflon-lined caps and were supplemented with 2.5 mL of freshly prepared 25 % (v/v) acetyl bromide in glacial acetic acid. The samples were incubated at 50 ºC during 3 h after which they were transferred to 50 mL volumetric flasks containing 10 mL of 2 M NaOH and 12 mL of glacial acetic acid. Hydroxylamine (0.5 M, 1.75 mL) was added to each flask and the volume was adjusted to 50 mL using glacial acetic acid. The absortion spectra were obtained for each sample (250 to 350 nm) and lignin content was determined as Abs_{280nm}/g cell wall. Quantification experiments were performed in triplicate from four biological replicates

***A. thaliana* genotype analysis**

A one-step DNA extraction was used to obtain genomic DNA templates for the PCR screening. Using a plastic rod, a small leaf was crushed inside a microcentrifuge tube containing 200 μL of extraction buffer diluted 10-fold

in TE buffer. Extraction buffer: 200 mM Tris-HCl (pH 7.5), 250 mM NaCl, 25 mM EDTA, 0.5% (w/v) SDS. TE buffer: 10 mM Tris-HCl (pH 8.0), 1 mM EDTA. The extraction solution (1 μL) was used as template in 20 μL PCR reactions containing 2 μL of 10X PCR Buffer (Invitrogen), 13.8 μL H_2O, 0.6 μL of 50 mM $MgCl_2$, 0.4 μL of 10 mM dNTPs, 1 μL of 10 μM primer fw, 1 μL of 10 μM primer rv and 0.2 μL of *Taq* DNA polymerase (Invitrogen). Thermal cycling was composed of an initial denaturation step for 5 min at 95 ºC, 30 cycles at 95 ºC for 20 s, 60 ºC for 20 s and 72 ºC for 1 min. For each mutant, two primer pairs were used as indicated in Figure 18 and Table 5.

A. thaliana germination rate

Seed sterilization and germination were performed under the same conditions as described above. For each line, wildtype and mutant B, a set of 50 seeds was used in each replicate. Germination rates were determined 6 days after vernalization using 4 replicates for each line.

Expression vector construction of _VvDIR1_

Native and optimized gene sequences were used for *P. pastoris* transformation. The coding region of native *VvDIR1* gene (excluding the signal peptide) was obtained by PCR amplification using genomic DNA from grapevine leaves as template (genomic DNA was extracted as described in chapter III). PCR amplification was performed with Platinum *Pfx* polymerase (Invitrogen) in 25 μL reactions (2.5 μL 10X Amplification buffer, 0.75 μL of 10 mM dNTPs, 0.5 μL of 50 mM $MgSO_4$, 0.75 μL of 10 μM primer – each, 1 μL template, 0.2 μL of *Pfx* polymerase and 18.55 μL H_2O) using the primer sense: 5'-GAGAGAATTCTATCAGGGCAAGAAGAAG-3' and antisense: 5'-GAGATCTAGAGCCCAGCACTCATACAACTT-3' and a thermal cycling composed of an initial denaturation step for 5 min at 94 ºC, 30 cycles at 94

ºC for 15 s, 65 ºC for 30 s and 68 ºC for 1min. The primers were designed to contain *Eco*RI and *Xba*I restriction sites (underlined). *VvDIR1* optimized gene was obtained from EurofinsMWG as a synthetic gene cloned into pEX-A, also with the same flanking *Eco*RI and *Xba*I restriction sites. PCR products or pEX-A-*VvDIR1* were double digested using 2 units of *Eco*RI and *Xba*I (Roche) during 2 h at 37 ºC and the fragments of interest were gel purified using the Wizard SV Gel and PCR Clean-Up System (Promega) according to manufacturer's instructions.

The recombinant expression of native and synthetic *VvDIR1* was performed using the EasySelect Pichia Expression Kit (Invitrogen). All vectors were maintained and propagated in *E. coli* DH5α competent cells. Vector pPICZαA was linearized by double digestion (*Eco*RI and *Xba*I, 2 units, 2 h, 37 ºC), gel purified and ligated to the insert (1:3 vector:insert molar ratio) overnight at 16 ºC. Ligation mixtures were transformed into *E. coli* and positive transformants were selected in 1.5 % (w/v) agar low salt LB medium (1% (w/v) tryptone, 0.5% (w/v) yeast extract, 0.5% (w/v) NaCl, pH 7.5) containing 25 µg/mL zeocin. Randomly picked zeocin-resistant colonies were grown in liquid low salt LB (with zeocin) for vector isolation using the Wizard Plus SV Minipreps DNA Purification System (Promega). Vectors were sequenced and analysed for the presence and correct ORF of the insert. Correct constructs, bearing α-factor secretion signal, target gene and His-tag in frame, were propagated in *E. coli* using 100 mL cultures (low salt LB, 25 μg/mL zeocin) to isolate transforming DNA (JetStar 2.0 Plasmid Midiprep Kit, Genomed). The expression vector (10 μg) was linearized using 5 units of *Sac*I (Roche) during 3 h at 37 ºC and was used for *P. pastoris* transformation.

Transformation and recombinant expression of *VvDIR1*

P. pastoris cells (strains X-33, GS115 and KM71H) were prepared for transformation as follows: 5 mL liquid YPD (1% yeast extract, 2% peptone, 2% dextrose) were inoculated and grown overnight (30 ºC, 150 rpm). Forty μL of the previous culture was used to inoculate 50 mL of fresh YPD and grown overnight to an OD of 1.3-1.5. Cells were collected and washed (1500 *g*, 5 min, 4 ºC) twice with ice cold water (50 and 25 mL) and once with ice cold 1 M sorbitol (20 mL). Final resuspension was made in 1 mL of ice cold 1 M sorbitol.

Forty μL of the cell suspension were mixed with 10 μg of linearized plasmid in a cold 0.2 cm electroporation cuvette and kept in ice (5 min). Electroporation was performed using the preset protocol for *Saccharomyces cerevisiae* from the electroporation system (Gene Pulser XCell, Biorad) and 1 mL of ice cold 1 M sorbitol was added to the cuvette. The mixture was transferred to a sterile tube and incubated for 1 h at 30 ºC without agitation. Transformation mixtures were plated in 2 % agar YPDS (YPD + 1 M sorbitol) containing 100 μg/mL zeocin and incubated at 30 ºC until colonies were formed (3 to 6 days). 20 to 25 *Pichia* transformants were screened by direct PCR for genome integration using *AOX* primers, according to Linder [31] and were evaluated for their differential resistance to zeocin by patching them in 1.5 % agar YPDS plates with increasing concentrations of zeocin (500, 1000 and 2000 μg/mL). Mut phenotypes were determined (GS115 and X33) by patching the selected colonies in 1.5 % agar plates with MMH (1.34 % yeast nitrogen base, 4×10^{-5} % biotin, 0.5 % methanol) or MDH (1.34 % yeast nitrogen base, 4×10^{-5} % biotin, 2 % dextrose) medium. Following a 2 day incubation period at 30 ºC, Mut^+ should grow normally in both plates and Mut^S should grow normally in MDH but slower in MMH. Mut^+ transformants were selected for recombinant expression.

Recombinant expression was induced as follows. A single colony was inoculated in BMGY (1% yeast extract, 2% peptone, 100 mM potassium phosphate, pH 6.0, 1.34% yeast nitrogen base, 4 × 10^{-5} % biotin, 1% glycerol) medium (50 mL for Mut^s; 5 mL for Mut^+) and incubated at 28 ºC, 150 rpm until a 2 to 6 OD was reached. Cells were recovered (1500 *g*, 5 min) and resuspended in BMMY (BMGY without glycerol and 0.5 % methanol instead) medium (10 to 20 mL for Mut^s ; to an OD of 1 for Mut^+). Cultures were incubated under the same conditions, adding daily methanol to a final concentration of 0.5 to 1 %, during a period of 6 days. One mL aliquots were collected every 24 h and the respective supernatants were analysed by SDS-PAGE and western blotting.

Coniferyl alcohol coupling assays

Reactional mixtures with a total volume of 250 μL were prepared in 100 mM potassium phosphate buffer, pH 5.9 containing 5 μL of 75 mM coniferyl alcohol, and 1.5 mU of *Trametes versicolor* laccase (Sigma-51639). For *Vv*DIR activity assays, 60 μg of total protein from *P. pastoris* culture supernatants were incorporated in the mixture. Reactions were initiated by the addition of laccase and were incubated at 25 ºC during 1.5 h. The reaction mixture was extracted once with two volumes of ethyl acetate and evaporated to dryness. The residue was resuspended in methanol and analysed by reverse phase HPLC (280 nm) in a Luna PFP(2) C18 column (Phenomenex) using a 0.1% TFA (A):acetonitrile (B) linear gradient at a flow rate of 1 mL/min: 0 min - 0 % B, 4 min - 31 % B, 27 min - 40 % B, 29 min - 100 % B, 31 min - 100 % B, 34 min - 0 % B, 37 min - 0 % B.

Purification of recombinant *Vv*DIR1

The supernatant of a 200 mL *P. pastoris* culture was precipitated using 80 % saturation of ammonium sulphate and resuspended in a minimum volume (c.a. 2 mL) of binding buffer (20 mM potassium phosphate buffer, pH 7.4, 500 mM NaCl, 15 mM imidazole). Purification was performed using a HisTrap FF crude 1 mL column (GE Healthcare) at a flow rate of 1 mL/min. Sample was loaded into the column and washed with 20 mL of binding buffer. Elution was performed with 7 mL of elution buffer (20 mM potassium phosphate, pH 7.4, 500 mM NaCl, and 500 mM imidazole).

SDS-PAGE and western blot analysis

Polyacrylamide gel electrophoresis (PAGE) was performed according to Laemmli [32] in handcast 10 cm x 7 cm mini gels using a 15 % polyacrilamide separation gel. Concentrated supernatant samples (equivalent to 10-30 μL of supernatant) were boiled for 5 min in sample buffer containing 2 % SDS and 100 mM β-mercaptoethanol prior to electrophoresis. Gel staining was performed with Coomassie Brilliant Blue (CBB-R250 or CBB-G250) or silver staining protocol [33]. Western blotting was performed by transferring the electrophoresis products onto a PVDF membrane using a semi-dry system (BioRad). The membranes were probed with 1:5000 diluted anti-HisTag antibodies (Invitrogen, R931-25) and detected by enhanced chemiluminescence (Thermo Scientific SuperSignal West Femto Maximum Sensitivity Substrate) according to manufacturer's instructions.

Sequence analysis

Multiple sequence alignments were performed by ClustalW in BioEdit program. Homologue database search was performed by BLAST (http://blast.ncbi.nlm.nih.gov/Blast.cgi). Potential glycosylation sites and signal peptide prediction was performed by NetNGlyc 1.0 and SignalP 4.1 using the CBS server prediction tools (http://www.cbs.dtu.dk/). Conserved

domains regions were determined with the CD search tool from NCBI (http://www.ncbi.nlm.nih.gov/Structure/cdd/wrpsb.cgi). Codon adaptation index (CAI) was calculated using GenScript rare codon analysis tool (http://www.genscript.com/cgi-bin/tools/rare_codon_analysis) and the codon optimization was performed by Genart optimization tool (Invitogren).

Results and Discussion

Lignin quantification in healthy and *E. necator*-infected *V. vinifera* leaves

Given the results from the previous chapter, where the significant upregulation of a *V. vinifera* DIR gene, named *VvDIR1*, could not be correlated, at a transcriptomic level, with the expression of the putative gene encoding the next enzyme in lignan biosynthetic pathway, an attempt was made to investigate whether *DIR* overexpression and lignin content in leaves infected with *E. necator* could be associated.

Sequence analysis shows that the predicted *Vv*DIR1 (XM_002276412) is highly homologous to DIR-a proteins already characterized as (+)-pinoresinol-forming in other plants (Figure 14).

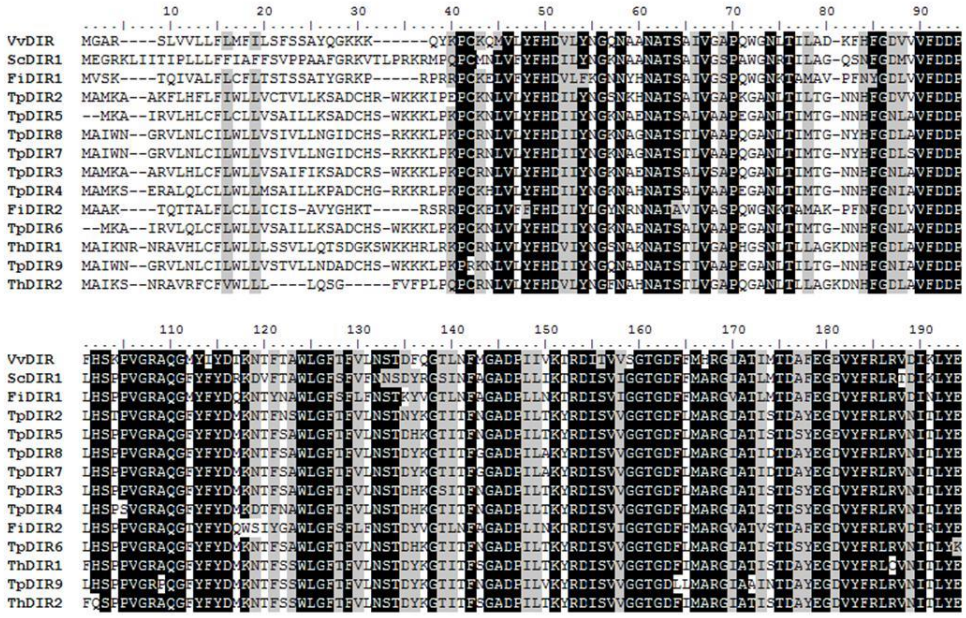

Figure 14. Predicted aminoacid alignment of DIR-a members participating in (+)-pinoresinol formation and *Vv*DIR1 responsive to *E.necator* infection. Identity, similarity and difference are indicated on black, grey or white backgrounds, respectively.

Predicted aminoacid identities between *Vv*DIR1 and the selected DIR-a members range from 67 to 74% for *Fi*DIR2 and *Th*DIR2, respectively. Though the previous transcriptomic studies can indicate that *VvDIR1* may not be involved in pinoresinol formation, its high degree of conservation strongly suggests that this protein would be likely to participate in coniferyl alcohol metabolism, either in lignan or lignin biosynthesis.

Addressing this issue, we used acetyl bromide assay to determine the lignin content of healthy and diseased *V. vinifera* leaves. This method was preferred over gravimetric methods as it has been reported to be a rapid and simple procedure, suitable for small sized samples [34]. It relies on lignin solubilization followed by a derivatization reaction which allows a quantification methodology based on absorption at 280 nm [35]. Though the quantification is performed at 280 nm, the acquisition of UV spectrum (250 to 400 nm) is advisable to assess sample quality. Derivatized lignin

should possess a fairly sharp maximum at 280 nm. The presence of interferents such as proteins and carbohydrates or excessive sample degradation could be indicated by peak broadening and increased absorbance at higher wavelengths [35,36]. Since this method was developed for woody tissues and later adapted to other samples, a preliminary test involving two different cell wall isolation protocols (A and B; see Materials and Methods) was performed. Examples of lignin UV spectra obtained for both methods are presented in Figure 15. One disadvantage of acetyl bromide assay, if absolute lignin values are required, is the necessity of specific lignin standards. Alternatively, a good estimate can be achieved if extinction coefficients are available from previously performed studies on the same species. In this case, given the absence of standards and of literature information, we processed the results in absorbance units (280 nm) per gram of cell wall, which is suitable for comparison purposes between samples.

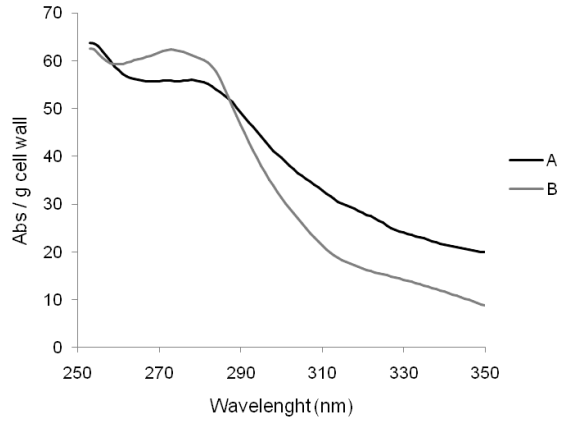

Figure 15. Comparison of representative UV spectra from acetyl bromide treated lignin obtained from *V. vinifera* cell walls isolated according to methods A and B described in the methods section.

Neither method, A or B, produced the desirable UV spectra. According to the previous considerations, method B should have been preferred over method A. However, those spectra could not be reproduced for all the samples. On the other hand, despite its inferior quality, method A was

reproducible for all the samples. For this reason, and considering that for this assay we were only interested in a comparison between samples, the lignin quantification was carried out using the cell wall isolation protocol A (Figure 16).

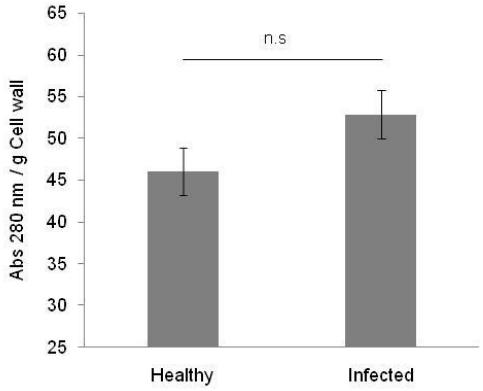

Figure 16. Lignin quantification using acetyl bromide assay ($Abs_{280\ nm}$ / g cell wall) of healthy and *E. necator* infected *V. vinifera* leaves. Data are means (n = 4) ± SD. n.s – not significantly different ($P < 0.05$)

As demonstrated by the results, presented in Figure 16, the lignin content is slightly higher in diseased leaves than in healthy leaves (52.9 and 46.0 Abs units/ g cell wall, respectively). However, the observed differences are not statistically significant. Considering the hypothesis that the 180 fold upregulation of *VvDIR1* could be related with coniferyl alcohol recruitment to the synthesis of lignin, one would expect a much higher difference in lignin content to be observed. Yet, even if such had been observed, we are aware that we could not attribute it to *Vv*DIR1 solely based on this experiment, as many other factors could be influencing the production of lignin. In fact, these results only confirm the already known feature of plant defence against these and other fungal pathogens: the localized deposition of lignin to provide cell wall reinforcement [37,38].

VvDIR1 homologues in *Arabidopsis thaliana*

Following the previous inconclusive results concerning the physiological role of *Vv*DIR1, a reverse genetics approach was adopted using *A. thaliana* as the experimental system. The main goals initially proposed for this study involved the assessment of susceptibility to powdery mildew and of lignin content for wild type and a DIR-disrupted T-DNA mutant of *A. thaliana*. However, sequence database analysis revealed that *A. thaliana* possessed two genes (*At4G23690* and *At1G64160*) coding for *At*DIR6 and *At*DIR5 proteins with high degree of homology to *Vv*DIR1, sharing 58% and 55% aminoacid identity, respectively, and 70% similarity (Figure 17). Mutants for both genes were ordered from the Nottingham Arabidopsis Stock Centre. Polymorphism selection was based on T-DNA insertion in the coding region (exon) of the gene: Mutant A - *At*DIR6 (GK-022D05-018341); Mutant B – *At*DIR5 (WiscDsLox442B7). A double mutant, bearing both polymorphisms, was also intended to be obtained for this part of the work.

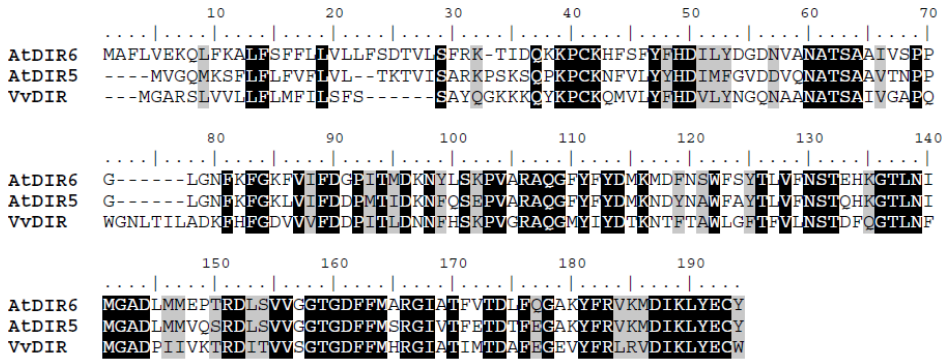

Figure 17. Predicted aminoacid sequence alignment of *Vv*DIR1 (XM_002276412) with its *A. thaliana* homologues *At*DIR6 and *At*DIR5. Identity, similarity and difference are indicated on black, grey or white backgrounds, respectively.

In the absence of any reported information concerning the dominance or recessiveness of DIR genes, it was mandatory that any mutants involved in further tasks were homozygous for T-DNA. The genotype screening of

both mutants was assessed though PCR using two sets of primers for each mutant according to the following scheme (Figure 18, Table 5).

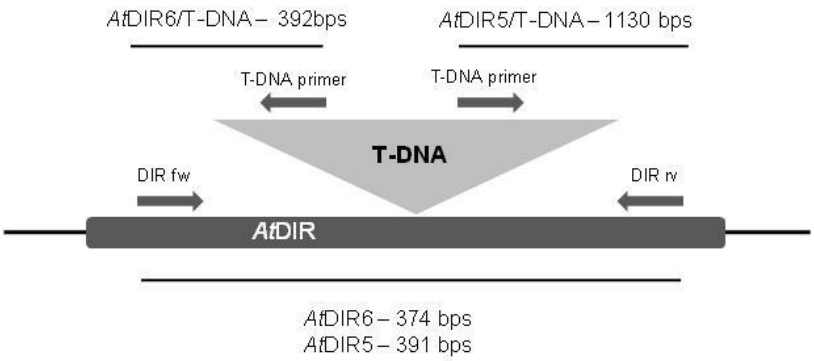

Figure 18. Diagram displaying PCR primer pair location and corresponding amplicon sizes used for genotype analysis of *A. thaliana* mutants.

Table 5. Primer sequences used for *A. thaliana* mutant screening (see Figure18).

Primer	Sequence 5' - 3'
AtDIR6fw	CTCTTCTCCGATACCGTCTTATCTT
AtDIR6rv	AGATCTCTTGTTGGCTCCATCATCA
T-DNAprimerAtDIR6	TTATAATAACGCTGCGGACATCTAC
AtDIR5fw	CTCTCTCATTATCCACTCTCACATT
AtDIR5rv	GTACGCGAACCATGCATTGTAGTCA
T-DNAprimerAtDIR5	TGCTGCTCTTGCCTCTGTAATAGTG

Following the preliminary plant selection with the appropriate selective marker for each mutant (sulfadiazine for mutant A and glufosinate ammonium for mutant B), PCR screening using the above primer sets was performed for the remaining plants to isolate T-DNA transformants. In both cases, no homozygous individuals were detected for T-DNA. Heterozygous transformants were used as a parental line for the next generation. For the mutant A, we were able to obtain and isolate individuals homozygous for the T-DNA insertion. Seeds from those individuals were collected and stored to perform the forthcoming studies, including the creation of the double mutant. However, for the second mutant, mutant B, T-DNA-homozygous individuals were never obtained,

even after two sequential generations originated from the selected heterozygous individuals (Figure 19). Such event suggested that *At*DIR5 loss-of-function could produce a lethal phenotype, for instance affecting seed germination or seedling development. To evaluate the previous hypothesis a germination assay was conducted to assess whether the mutant seeds would display a reduced germination capacity when compared to wild type plants. Interestingly, no differences were observed between plant lines, both displaying germination rates close to 97 % six days after sowing.

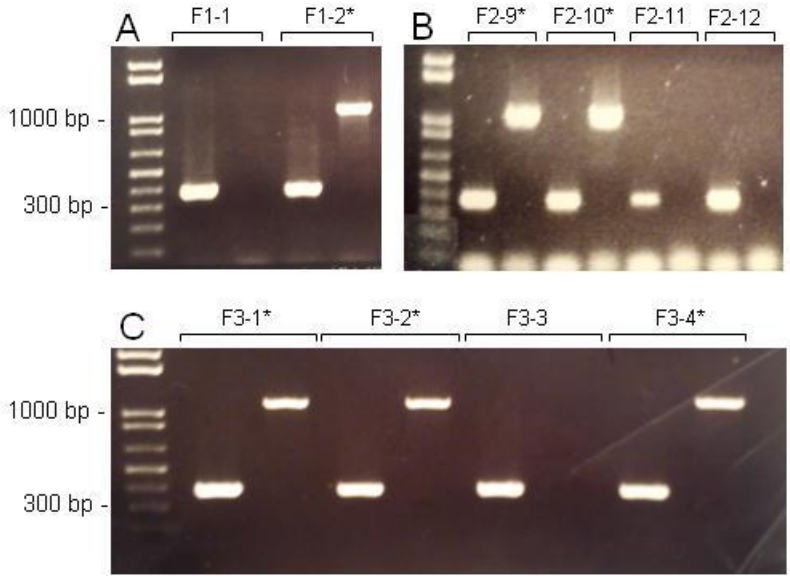

Figure 19. Representative genotype PCR screening of the (**A**) first, (**B**) second and (**C**) third generation of B mutants. PCR primer sets: AtDIR5fw/rv – left lane; T-DNA/AtDIR5rv – right lane. * Heterozygous for T-DNA insertion serving as parents for the next generation.

A possible explanation for these observations remains: a lethal phenotype could be generated in earlier stages where the mutation would interfere with seed/embryo formation rather than germination; the formation of defective seeds, which in some cases can display significant morphological differences (i.e. very small size) that could have caused

those seeds to be overlooked during the collection process. A new, yet to be performed, thorough analysis of mutant siliques and seeds, with increased awareness concerning this matter, will be necessary to confirm the previous hypothesis.

Despite the inability to obtain the homozygous T-DNA mutant B, with one of the possible causes being the formation of a lethal phenotype, the recently published study by Kim and coworkers [39], reporting *At*DIR5 recombinant production, activity, and spatiotemporal expression, led us to believe that a lethal loss-of-function mutant would be unlikely in this case. According to Kim's work, both *At*DIR6 and *At*DIR5 are responsible for the stereoselective coupling of coniferyl alcohol into (-)-pinoresinol [39]. *At*DIR6 was first characterized by Pickel and colleagues [40]. Though an opposite stereoselectivity is observed, such observation was expectable given the optical rotation of lignans isolated from *A. thaliana* [41]. While *At*DIR6 was constitutively expressed in all plant organs during the observed developmental stages, *At*DIR5 was mainly expressed only in the shoot meristem (3 days after germination) and in the vascular region of cotyledons (3 weeks after germination) [39]. In view of its proven participation in lignan biosynthesis or the plausible involvement in lignin assembly, *At*DIR5 disruption would not be likely to produce a lethal phenotype, at least at the embryo development stage. Although both lignans and lignin are present in seeds, namely in the coat, they are not perceived as essential for seed formation or viability [42-44].

Considering the previous comments, a possibility exists that the B mutant screening process has been carried inappropriately. Due to the failure to detect this mutant, together with other incidents such as the suitability of the acetyl bromide assay for *A. thaliana* leaves or the lack of readily available *Erysiphe cichoracearum* spores, we decided to arrest this line of work.

Heterologous expression of *VvDIR1*

In a further attempt to gather direct evidence of *Vv*DIR1 function, we decided to produce its recombinant form as a mean to confirm its "activity" towards coniferyl alcohol. As mentioned, its high homology to other DIR proteins from the subfamily-a suggests that *Vv*DIR1 could mediate the stereoselective formation of pinoresinol, namely its (+)-antipode. Predicted *VvDIR1* is a single exon gene of 755 nucleotides containing an ORF coding for a 185 amino acid peptide with an expected molecular weight of ca. 21 kDa (Figure 20).

```
VvDIR1

2    CTC ACA AGT CCA AGC TGA TCA GTC ATC TAT AGC TTT TAC AAT TTT CTT CTC CTC CTT TTT TAG GGT TTT AGA GAG
77   TAA AGG AGA AGA ATG GGA GCC AGG AGT TTG GTA GTT CTT CTC TTC CTG ATG TTC ATC CTC TCT TTT TCT TCT GCC
1                    M   G   A   R   S   L   V   V   L   L   F   L   M   F   I   L   S   F   S   S   A

152  TAT CAG GGC AAG AAG AAG CAA TAC AAA CCA TGT AAG CAA ATG GTC TTG TAT TTC CAT GAT GTT CTC TAC AAT GGC
22    Y   Q   G   K   K   K   Q   Y   K   P   C   K   Q   M   V   L   Y   F   H   D   V   L   Y   N   G

227  CAA AAT GCA GCT AAT GCC ACT TCT GCA ATT GTG GGT GCA CCC CAA TGG GGA AAC CTT ACC ATC TTG GCA GAT AAG
47    Q   N   A   A   N   A   T   S   A   I   V   G   A   P   Q   W   G   N   L   T   I   L   A   D   K

302  TTC CAT TTT GGT GAT GTG GTG GTG TTT GAT GAC CCC ATT ACT CTT GAC AAC AAC TTC CAC TCC AAA CCA GTT GGT
72    F   H   F   G   D   V   V   V   F   D   D   P   I   T   L   D   N   N   F   H   S   K   P   V   G

377  AGA GCA CAA GGC ATG TAC ATA TAT GAC ACC AAA AAC ACC TTC ACT GCT TGG CTG GGG TTC ACA TTT GTT CTC AAC
97    R   A   Q   G   M   Y   I   Y   D   T   K   N   T   F   T   A   W   L   G   F   T   F   V   L   N

452  AGC ACA GAC TTT CAG GGC ACC TTG AAC TTC ATG GGA GCT GAC CCC ATT ATA GTG AAG ACC AGG GAC ATT ACT GTG
122   S   T   D   F   Q   G   T   L   N   F   M   G   A   D   P   I   I   V   K   T   R   D   I   T   V

527  GTG AGT GGG ACA GGA GAC TTC TTC ATG CAT AGG GGA ATT GCC ACT ATT ATG ACT GAT GCA TTT GAA GGT GAA GTA
147   V   S   G   T   G   D   F   F   M   H   R   G   I   A   T   I   M   T   D   A   F   E   G   E   V

602  TAT TTC AGG CTT AGG GTT GAT ATT AAG TTG TAT GAG TGC TGG TGA AGA TAA GAA AAA ACT ATG AAA AAA TAA GGA
172   Y   F   R   L   R   V   D   I   K   L   Y   E   C   W   *

677  GTG TGT GGT TTA TTT CAT TAT GAA TGT ACT GAT GAT CAG CAT ATG CTT AGT AAA TAA AGG TTT TCA ACT TCT CAT
752  TTA A
```

Figure 20. *Vv*DIR1 full length cDNA and predicted amino acid sequence. Signal peptide (1-21) is underlined. Stop codon is indicated by an asterisk and the potential *N*-glycosylation sites (Asn51, Asn64 and Asn121) are in bold underlined.

Amino acid sequence analysis using CBS server prediction tools (http://www.cbs.dtu.dk/) shows that, like the already characterized DIR proteins, *Vv*DIR1 displays an N-terminal region typical of a signal peptide, with cleavage site between the residues 21 and 22 (SignalP 4.1), and potential *N*-glycosylation sites (Asn51, Asn64 and Asn121; NetNGlyc 1.0). Due to the predicted post translational modifications, it was essential that a eukaryotic expression system was used. Heterologous expression of

functional DIR proteins has been successfully achieved in several systems including *Spodoptera*/baculovirus, *Drosophila,* plant-cell cultures and *Pichia pastoris*. With the latter presenting several advantages over the others, including higher protein yields, it was chosen for the recombinant expression of *Vv*DIR1. The coding region of *Vv*DIR1, without secretory signal sequences, was obtained by PCR amplification, using genomic DNA as template, and cloned into the expression vector pPICZαA in frame with α-factor secretion signal and the C-terminal polyhistidine tag. Following pPICZαA-*VvDIR1* genome integration in *P. pastoris* KM71H strain and clone screening for positive insertion and differential resistance to zeocin, the recombinant expression was induced for the selected transformants using daily methanol supplementation during a six day period. SDS-PAGE analysis was used to monitor the protein content of the culture supernatant during induction (Figure 21). The assembled construct used for transformation coded for a ~21 kDa protein (*Vv*DIR1+His-tag) which could possibly be glycosylated. Glycosylation is known to affect protein behaviour during electrophoresis causing inaccurate molecular weight estimation [45]. In this case, building an analogy with the previous works, where the glycosylation of DIR proteins increased their apparent size, we would estimate a possible shift of 2 to 12 kDa in SDS-PAGE gels. However, as seen in figure 21, no detectable expression was observed in the supernatant during the induction period as the band at 45 kDa was shown to be a native protein from *P. pastoris*.

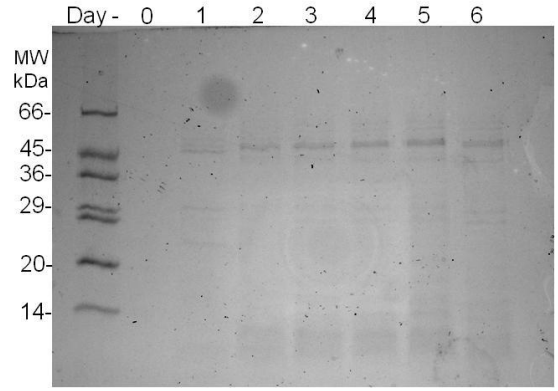

Figure 21. SDS-PAGE (CBB-R250 stained) analysis of *P. pastoris* (KM71H transformant K15) culture supernatant 0 to 6 days post-induction. Growth conditions for Mut^S phenotype at 28ºC with daily addition of 0.5% methanol.

To assess whether *Vv*DIR1 expression was completely inexistent or a problem during secretion was occurring, we analyzed the yeast cell lysis protein content (Figure 22).

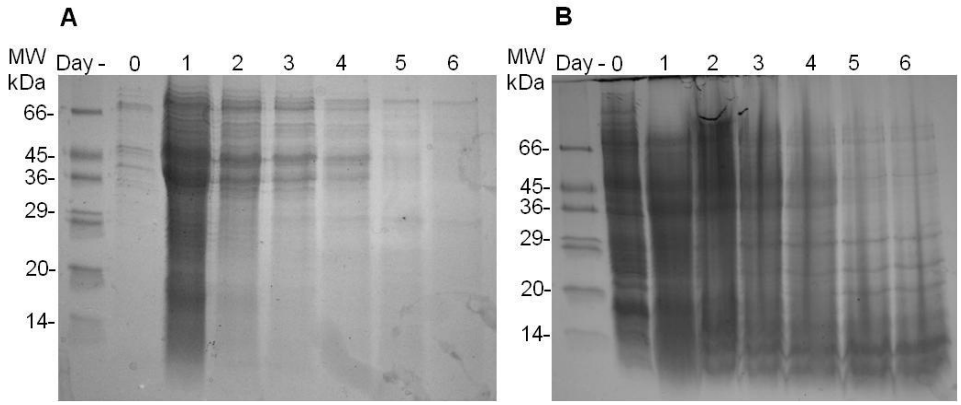

Figure 22. SDS-PAGE (CBB-R250 stained) analysis of *P. pastoris* (KM71H transformant K15) cell lysis (**A**) supernatant and (**B**) pellet 0 to 6 days post-induction. Growth conditions for Mut^S phenotype at 28ºC with daily addition of 0.5% methanol.

Even though we lacked information concerning the apparent size of our recombinant target protein, the SDS-PAGE profiles show no evidence of successful *Vv*DIR1 expression. When performing western blot analysis (anti-His-tag) of the previous samples we were able to observe, for the

culture supernatant, faint bands within the expected molecular weight range for the recombinant protein (Figure 23).

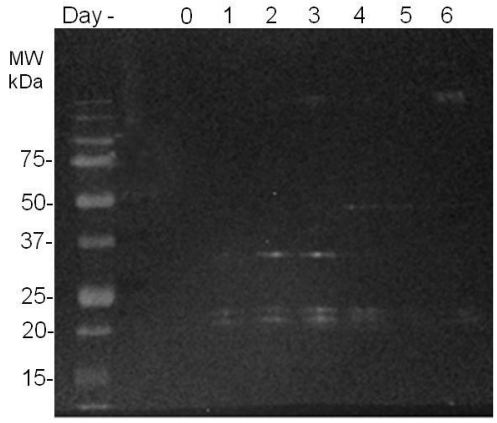

Figure 23. Western blot (Anti-His-tag) of *P. pastoris* (KM71H transformant K15) culture supernatant 0 to 6 days post-induction. Growth conditions for Mut^S phenotype at 28ºC with daily addition of 0.5% methanol.

The two bands between 20 and 25 kDa, detected from day 1 to 4, could possibly represent *Vv*DIR1 in its apo and glycosylated forms, respectively. The third band, 25 to 37 kDa range (days 2 and 3) could also represent the protein of interest except with a higher degree of glycosylation. According to this, *Vv*DIR1 recombinant expression could be occurring but at very low levels, not suitable for the following experiments (*in vitro* coupling of coniferyl alcohol). To address this issue, several subsequent attempts were performed to increase the recombinant protein yields. Tested variables included manipulation of growth conditions, such as temperature, initial OD for induction and methanol concentration, and also the analysis of other transformants from different *P. pastoris* strains (GS115 and X33). For all the tested conditions the result was invariably the same with little or no *Vv*DIR1 expression displayed. Considering the several reasons, some already addressed, behind the unsuccessful expression of *Vv*DIR1 in *P. pastoris*, we hypothesized that codon usage differences between the native and the host species could lie on the basis of the problem. So far, a reasonable number of studies dealing with

heterologous protein expression have reported variations in codon frequency as one of the main factors affecting foreigner protein expression levels in the host organism. In most cases, sequence optimization replacing the low frequency codons resulted in a dramatic expression increase [46]. Accordingly, we decided to evaluate our native *Vv*DIR1 sequence for its expression suitability in *P.pastoris* by determining its codon adaptation index (CAI), a measure of its codon resemblance to the host species preferences which can be used as a parameter to assess the likely success of heterologous gene expression [47,48]. Genscript rare codon analysis tool (www.genscript.com/) was used to calculate the CAI of native *Vv*DIR1 and hypothetically optimized sequences (Figure 24).

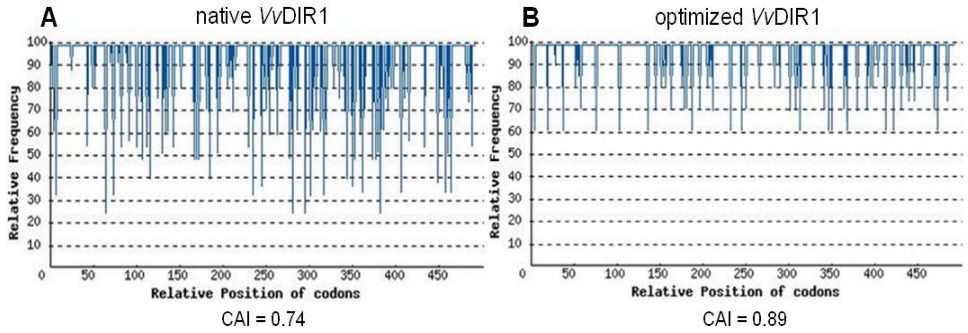

Figure 24. *Pichia pastoris* Codon Adaptation Index (CAI) of the (**A**) native and (**B**) codon optimized *Vv*DIR1 sequence as calculated by Genescript rare codon analysis tool. Optimized sequence was generated using GeneArt tool (Invitrogen).

Overall, native *Vv*DIR1 CAI score for *P. pastoris* (0.74) does not appear as a critical factor for the previous unsuccessful expression. Although it falls below the CAI threshold, indicative of a good expression level sequence (CAI > 0.8) as suggested by the software developers, such a small difference may not explain the extremely low expression level of *Vv*DIR1 in *P. pastoris*. In fact, many of *P. pastoris* native genes can display a CAI score below 0.8. On the other hand, according to *P. pastoris* codon usage frequency table, native *VvDIR1* sequence bears several low frequency codons including four below 30% relative frequency (Figure 24A). The

presence of those codons is likely to restrict the expression efficiency. Thus, in an additional attempt to improve our expression yields, we optimized *Vv*DIR1 sequence according to *P. pastoris* codon usage (Figure 24B). The new sequence (CAI = 0.89) was obtained as a synthetic gene and integrated in *P. pastoris* genome using an identical expression cassette as before. Again, all three *P. pastoris* strains were transformed. Best performing transformants for zeocin resistance were tested for protein expression. Despite the sequence optimization, we were not able to reach the desired expression level. However, a reasonable improvement was achieved as most of the transformants were producing the target protein in easily detectable amounts using western blot analysis. The best results were obtained for X33 strain, transformants XA2 and XA6 (Figure 25).

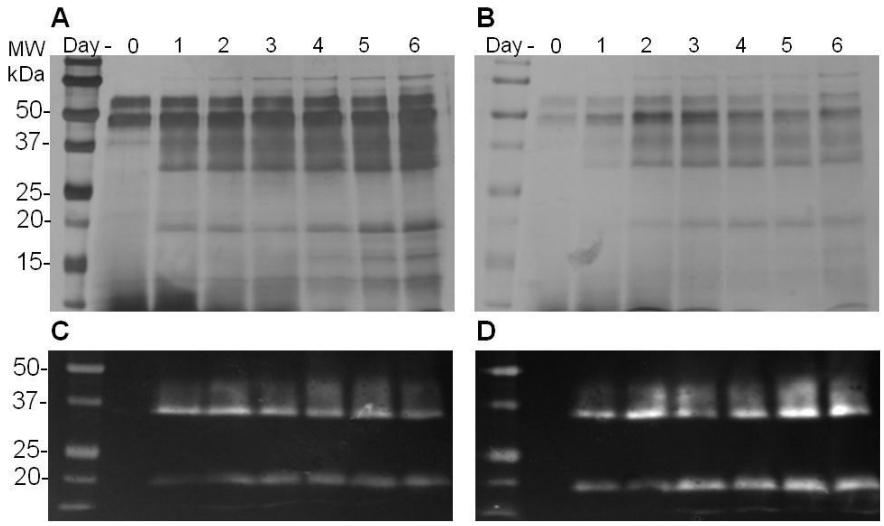

Figure 25. (**A**; **B**) SDS-PAGE (silver stained) and (**C**; **D**) western blot (anti-His-tag) analysis of *P. pastoris* (X-33) (**A**; **C**) XA2 and (**B**, **D**) XA6 culture supernatants 0 to 6 days post-induction. Growth conditions for Mut$^+$ phenotype at 28ºC with daily addition of 0.5% methanol.

According to the previous results (Figure 25), and as already hypothesized, the target protein could be present in the growth media in its apo and glycosylated forms. For the two transformants, XA2 and XA6, the western blot analysis evidences a sharp band at ~20 kDa, the

expected size for the mature protein, and a smear within the 37 kDa region which indicates that a high heterogeneity may exist in the glycosylated population of polypeptides. When observing the SDS-PAGE total protein profile from *P. pastoris* supernatants, it is noticeable that the relative amount of recombinant *Vv*DIR1 is considerably lower than could be expected. Still, given its undoubted presence in the supernatants, we tested its putative activity by evaluating any "dirigent" effect upon coniferyl alcohol oxidative coupling reactions. *In vitro* reactions were adapted from the work performed by Pickel and optimized according to our experimental conditions [40]. The typical HPLC profile obtained for the coniferyl alcohol dimerization experiments is shown in Figure 26.

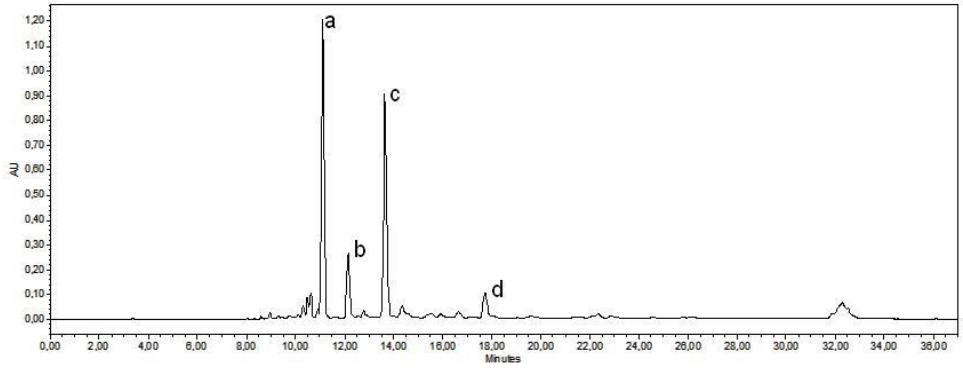

Figure 26. Reverse phase HPLC profile of coniferyl alcohol *in vitro* oxidative coupling monitored at 280 nm. **a**-coniferyl alcohol, **b/c**-unknown reaction products, **d**-pinoresinol.

As previously mentioned, dimerization of coniferyl alcohol radicals in open solution generates three main products as racemic mixtures: dehydrodiconiferyl alcohol, guaiacylglycerol 8-*O*-4'-coniferyl ether and pinoresinol. Peaks a and d, were identified based on their retention times and UV spectra using reference standards chemically synthesized by the organic chemistry group at FCT/UNL. The remaining peaks were not identified but were initially assigned as potential reaction products by monitoring the reactional mixture profile at several time points of the reaction. However, ambiguous information was collected for peak b as its

formation was not consistently observed for all the reactions. Hence, the potential DIR effect on the reactions was evaluated by determining the ratio changes between product **c** and pinoresinol (**d**). Product c was not identified and, therefore, the ratios were calculated using the chromatogram peak areas at 280 nm. To cope with the low amount of recombinant protein for the assays, the base reaction (buffered system with coniferyl alcohol and laccase) was tuned to the lowest initial concentrations of substrate, still allowing for HPLC detection, and diminished laccase amounts. By doing so, we aimed at maximizing any effect the growth media could have on the coupling reactions. Both XA2 and XA6 supernatants were tested for their activity during the induction period. XA6 showed the greater activity at day 4 post-induction (Figure 27).

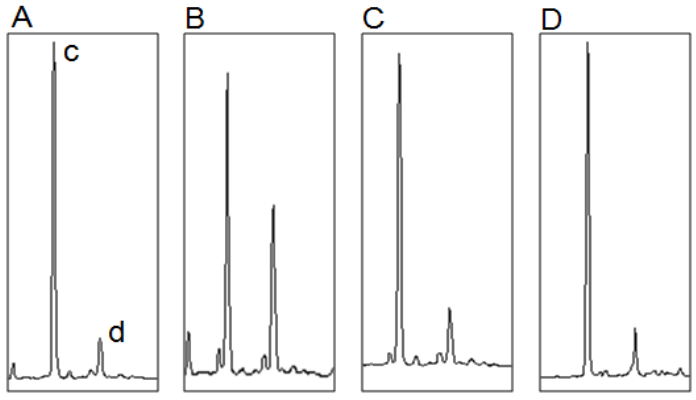

	Ratio (relative peak area at 280 nm)			
product c	87.7 %	58.8 %	81.9 %	88.1 %
pinoresinol	12.3 %	41.2 %	18.1 %	11.9 %

Figure 27. HPLC analysis of coniferyl alcohol *in vitro* coupling products in the (**A**) absence or presence of (**B**) XA6 *P. pastoris* growth media, (**C**) previously boiled XA6 *P. pastoris* growth media and (**D**) empty transformant (X-33 strain) growth media. Compounds **c** and **d** represent product c and pinoresinol, respectively as in Figure 26. All reactions were performed using 60 μg of total protein ($V_{reaction}$ = 250 μL) – day 4 post-induction.

As observed from the previous DIR activity screening results, *Vv*DIR1 is able to affect the product ratio of coniferyl alcohol coupling reactions. Even though the selected monitoring method is not ideal, in the sense that it

does not allow accurate estimation of substrate conversion rate to each of the products, it was suitable to confirm the preferential synthesis of pinoresinol in the presence of our target protein. In theory, had the recombinant expression in *P. pastoris* been higher, only pinoresinol would be formed during the oxidative coupling reactions. This sample limitation restricted our ability to produce and isolate enough quantity of "DIR-guided" pinoresinol to determine its optical activity and enantiomeric excess. Additional efforts to obtain increased amounts of *Vv*DIR1 for the required assays included the scale-up of XA6 *P. pastoris* induction cultures to a volume of 200 mL. Nevertheless, monitored relative activity of those cultures was considerably lower than the obtained for the previous assays (Figure 28). Also, the post translational process of glycosylation seemed affected by scaling-up *Vv*DIR1 recombinant production.

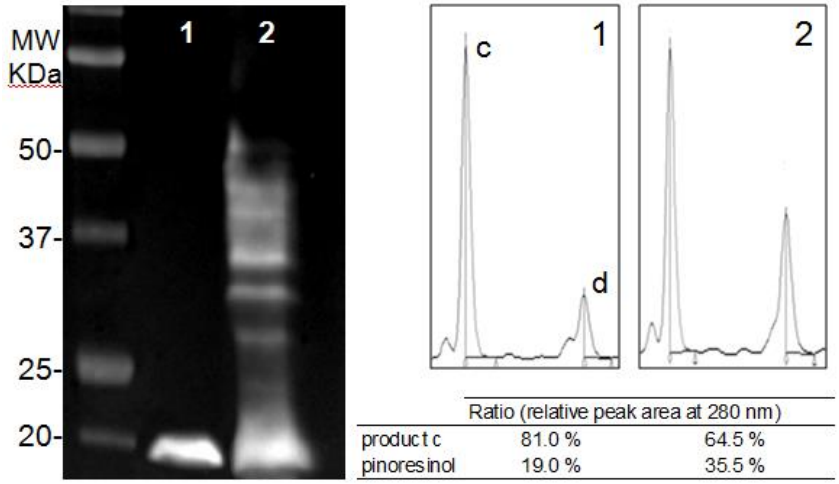

	Ratio (relative peak area at 280 nm)	
product c	81.0 %	64.5 %
pinoresinol	19.0 %	35.5 %

Figure 28. Western blot analysis (anti-His-tag) of XA6 *P. pastoris* culture supernatants from two identical scale-up procedures (lanes 1 and 2) and the corresponding HPLC profiles of *in vitro* reactions. Peaks **c** and **d** are the unknown product c and pinoresinol, respectively as in Figure 26. Reactions were performed using 60 μg of total protein ($V_{reaction}$ = 250 μL) collected 4 days post-inoculation.

For two similar cultures of XA6 transformants, grown under the same conditions, distinct western blot profiles were observed, with one of them

secreting only the unglycosylated form of *Vv*DIR1, and the other secreting both forms, including a highly heterogeneous population of glycosylated *Vv*DIR1 (Figure 28). HPLC profiles of *in vitro* reactions using both supernatants as guiding agents show that only one of the cultures displayed activity (lane 2 – Figure 28). This observation is in agreement with the recent work performed by Kazenwadel and collaborators [49] where *At*DIR6 glycosylation was demonstrated to play a crucial role in the structure and function of the protein. The removal of *N*-glycans from *At*DIR6 results in a complete loss of function [49]. In view of the latter, it is reasonable that no DIR activity was observed for the *P. pastoris* culture producing the unglycosylated form of *Vv*DIR1 (lane 1 – Figure 28). The XA6 *P. pastoris* supernatant containing the glycosylated forms of *Vv*DIR1 was further processed using Ni-IMAC as a mean to increase the targets protein purity for improved *in vitro* coupling reactions (Figure 29).

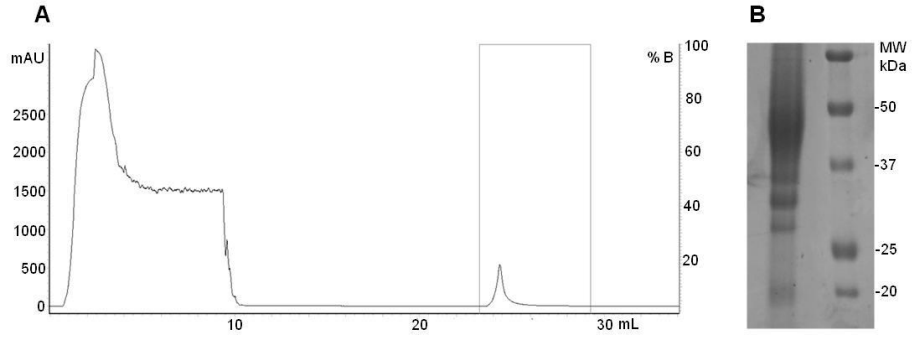

Figure 29. Purification of recombinant *Vv*DIR1 from XA6 *P. pastoris* culture supernatants. **(A)** IMAC-Ni (HisTrap FF crude-1mL) elution profile (Abs 280 nm) of concentrated total proteins from growth media of XA6 transformant using a one-step gradient of 100% B buffer (500 mM imidazole). (**B**) SDS-PAGE (CBB-G250 stained) analysis of *Vv*DIR1 eluted pool.

All the recombinant forms of *Vv*DIR1 were successfully recovered from the total protein extracts. However, very low yields (c.a. 450 μg) were observed for the scale-up process, roughly 2.2 mg of recombinant protein per litre of *P. pastoris* culture. These low amounts were additionally aggravated by the presence of several forms of the target protein, some of

which possibly not active towards coniferyl alcohol radicals. Even so, a final attempt to increase DIR-mediated pinoresinol formation was performed. As before, preferential formation of pinoresinol occurred in the presence of *Vv*DIR1 protein. Although, to some extent, a proportional relation between the amount of formed pinoresinol and *Vv*DIR1 concentration was observed, at higher concentrations a diminished effect was shown possibly due to interferents. As a result of the oxidizing capacity being higher than the practical saturation point of *Vv*DIR1, complete reaction stereoselectivity was never achieved. As for, still with the limitation of reduced pinoresinol amounts, we could not characterize *Vv*DIR1 enantioselectity. Further efforts concerning optimization of *Vv*DIR1 heterologous expression as well as *in vitro* reaction adjustments would be required to accomplish the proposed objective.

References

1. Davin LB, Wang HB, Crowell AL, Bedgar DL, Martin DM, et al. (1997) Stereoselective bimolecular phenoxy radical coupling by an auxiliary (dirigent) protein without an active center. Science 275: 362-366.
2. Pare PW, Wang HB, Davin LB, Lewis NG (1994) (+)-Pinoresinol synthase - a stereoselective oxidase catalyzing 8,8'-lignan formation in *Forsythia intermedia*. Tetrahedron Letters 35: 4731-4734.
3. Bagniewska-Zadworna A, Barakat A, Łakomy P, Smoliński DJ, Zadworny M (2014) Lignin and lignans in plant defence: Insight from expression profiling of cinnamyl alcohol dehydrogenase genes during development and following fungal infection in *Populus*. Plant Science 229: 111-121.
4. Harmatha J, Dinan L (2003) Biological activities of lignans and stilbenoids associated with plant-insect chemical interactions. Phytochemistry Reviews 2: 321-330.
5. Umezawa T (2003) Diversity in lignan biosynthesis. Phytochemistry Reviews 2: 371-390.

6. Willför SM, Smeds AI, Holmbom BR (2006) Chromatographic analysis of lignans. Journal of Chromatography A 1112: 64-77.
7. Russell GB, Singh P, Fenemore PG (1976) Insect-control chemicals from plants. III. Toxic lignans from *Libocedrus bidwillii*. Australian Journal of Biological Sciences 29: 99-103.
8. Haworth RD (1942) The chemistry of the lignan group of natural products. Journal of the Chemical Society (Resumed): 448-456.
9. Davin L, Lewis N (1992) Phenylpropanoid metabolism: Biosynthesis of monolignols, lignans and neolignans, lignins and suberins. In: Stafford H, Ibrahim R, editors. Phenolic Metabolism in Plants: Springer US. pp. 325-375.
10. Dewick PM (1989) Biosynthesis of lignans. In: Atta-ur-Rahman, editor. Studies in natural products chemistry. Amsterdam: Elsevier. pp. 459-503.
11. Davin L, Lewis N (2003) An historical perspective on lignan biosynthesis: Monolignol, allylphenol and hydroxycinnamic acid coupling and downstream metabolism. Phytochemistry Reviews 2: 257-288.
12. Freudenberg K (1965) Lignin: Its constitution and formation from p-hydroxycinnamyl alcohols: lignin is duplicated by dehydrogenation of these alcohols; intermediates explain formation and structure. Science 148: 595-600.
13. Goodwin TW, Mercer EI (1983) Introduction to plant biochemistry. Oxford ; New York: Pergamon Press. ix, 677 p., 677 leaves of plates p.
14. Umezawa T, Davin LB, Yamamoto E, Kingston DGI, Lewis NG (1990) Lignan biosynthesis in *Forsythia* species. Journal of the Chemical Society, Chemical Communications: 1405-1408.
15. Halls SC, Davin LB, Kramer DM, Lewis NG (2004) Kinetic study of coniferyl alcohol radical binding to the (+)-pinoresinol forming dirigent protein. Biochemistry 43: 2587-2595.
16. Davin LB, Lewis NG (2005) Dirigent phenoxy radical coupling: advances and challenges. Current Opinion in Biotechnology 16: 398-406.
17. Kim M, Jeon J-H, Fujita M, Davin L, Lewis N (2002) The western red cedar (*Thuja plicata*) 8-8′ DIRIGENT family displays diverse expression patterns and conserved monolignol coupling specificity. Plant Molecular Biology 49: 199-214.

18. Xia Z-Q, Costa MA, Proctor J, Davin LB, Lewis NG (2000) Dirigent-mediated podophyllotoxin biosynthesis in *Linum flavum* and *Podophyllum peltatum*. Phytochemistry 55: 537-549.
19. Suzuki S, Sakakibara N, Umezawa T, Shimada M (2002) Survey and enzymatic formation of lignans of *Anthriscus sylvestris*. Journal of Wood Science 48: 536-541.
20. Okunishi T, Umezawa T, Shimada M (2001) Isolation and enzymatic formation of lignans of *Daphne genkwa* and *Daphne odora*. Journal of Wood Science 47: 383-388.
21. Takaku N, Choi D-H, Mikame K, Okunishi T, Suzuki S, et al. (2001) Lignans of *Chamaecyparis obtusa*. Journal of Wood Science 47: 476-482.
22. Gang DR, Costa MA, Fujita M, Dinkova-Kostova AT, Wang H-B, et al. (1999) Regiochemical control of monolignol radical coupling: A new paradigm for lignin and lignan biosynthesis. Chemistry & Biology 6: 143-151.
23. Higuchi T (1957) Biochemical studies of lignin formation. Physiologia Plantarum 10: 633-648.
24. Freudenberg K (1959) Biosynthesis and constitution of lignin. Nature 183: 1152-1155.
25. Davin LB, Lewis NG (2000) Dirigent proteins and dirigent sites explain the mystery of specificity of radical precursor coupling in lignan and lignin biosynthesis. Plant Physiology 123: 453-462.
26. Kwon M, Burlat V, Davin L, Lewis N (1999) Localization of dirigent protein involved in lignan biosynthesis: Implications for lignification at the tissue and subcellular level. In: Gross G, Hemingway R, Yoshida T, Branham S, editors. Plant Polyphenols 2: Springer US. pp. 393-411.
27. Burlat V, Kwon M, Davin LB, Lewis NG (2001) Dirigent proteins and dirigent sites in lignifying tissues. Phytochemistry 57: 883-897.
28. Murashige T, Skoog F (1962) A revised medium for rapid growth and bio assays with tobacco tissue cultures. Physiologia Plantarum 15: 473-497.
29. Theander O, Westerlund EA (1986) Studies on dietary fiber. 3. Improved procedures for analysis of dietary fiber. Journal of Agricultural and Food Chemistry 34: 330-336.
30. Theander O (1991) Chemical analysis of lignocellulose materials. Animal Feed Science and Technology 32: 35-44.

31. Linder S, Schliwa M, Kube-Granderath E (1996) Direct PCR screening of *Pichia pastoris* clones. Biotechniques 20: 980-982.
32. Laemmli UK (1970) Cleavage of structural proteins during the assembly of the head of bacteriophage T4. Nature 227: 680-685.
33. Blum H, Beier H, Gross HJ (1987) Improved silver staining of plant proteins, RNA and DNA in polyacrylamide gels. Electrophoresis 8: 93-99.
34. Dence CW (1992) The determination of lignin. In: Lin S, Dence C, editors. Methods in lignin chemistry: Springer Berlin Heidelberg. pp. 33-61.
35. Hatfield R, Fukushima RS (2005) Can lignin be accurately measured? Lignin and Forage Digestibility Symposium, 2003 CSSA Annual Meeting, Denver, CO. Crop Sci 45: 832-839.
36. Hatfield RD, Grabber J, Ralph J, Brei K (1999) Using the acetyl bromide assay to determine lignin concentrations in herbaceous plants: some cautionary notes. Journal of Agricultural and Food Chemistry 47: 628-632.
37. Ferreira RB, Monteiro S, Freitas R, Santos CN, Chen Z, et al. (2006) Fungal Pathogens: the battle for plant infection. Critical Reviews in Plant Sciences 25: 505-524.
38. Underwood W (2012) The plant cell wall: A dynamic barrier against pathogen invasion. Frontiers in Plant Science 3.
39. Kim K-W, Moinuddin SGA, Atwell KM, Costa MA, Davin LB, et al. (2012) Opposite stereoselectivities of dirigent proteins in *Arabidopsis* and *Schizandra* species. Journal of Biological Chemistry 287: 33957-33972.
40. Pickel B, Constantin M-A, Pfannstiel J, Conrad J, Beifuss U, et al. (2010) An enantiocomplementary dirigent protein for the enantioselective laccase-catalyzed oxidative coupling of phenols. Angewandte Chemie International Edition 49: 202-204.
41. Nakatsubo T, Mizutani M, Suzuki S, Hattori T, Umezawa T (2008) Characterization of *Arabidopsis thaliana* pinoresinol reductase, a new type of enzyme involved in lignan biosynthesis. Journal of Biological Chemistry 283: 15550-15557.
42. Venglat P, Xiang D, Qiu S, Stone S, Tibiche C, et al. (2011) Gene expression analysis of flax seed development. BMC Plant Biology 11: 74.

43. Bonawitz ND, Kim JI, Tobimatsu Y, Ciesielski PN, Anderson NA, et al. (2014) Disruption of mediator rescues the stunted growth of a lignin-deficient *Arabidopsis* mutant. Nature 509: 376-380.
44. Liang M, Davis E, Gardner D, Cai X, Wu Y (2006) Involvement of AtLAC15 in lignin synthesis in seeds and in root elongation of *Arabidopsis*. Planta 224: 1185-1196.
45. Durchschlag H, Christl R, Jaenicke R (1991) Comparative determination of the particle weight of glycoproteins by SDS-PAGE and analytical ultracentrifugation. In: Borchard W, editor. Progress in Analytical Ultracentrifugation: Steinkopff. pp. 41-56.
46. Gustafsson C, Govindarajan S, Minshull J (2004) Codon bias and heterologous protein expression. Trends in Biotechnology 22: 346-353.
47. Sharp PM, Li W-H (1987) The codon adaptation index-a measure of directional synonymous codon usage bias, and its potential applications. Nucleic Acids Research 15: 1281-1295.
48. Puigbo P, Bravo I, Garcia-Vallve S (2008) E-CAI: a novel server to estimate an expected value of codon adaptation index (eCAI). BMC Bioinformatics 9: 65.
49. Kazenwadel C, Klebensberger J, Richter S, Pfannstiel J, Gerken U, et al. (2013) Optimized expression of the dirigent protein *At*DIR6 in *Pichia pastoris* and impact of glycosylation on protein structure and function. Applied Microbiology and Biotechnology 97: 7215-7227.

Chapter V: *Vitis vinifera* DIR family – Possible Putative Players in Stilbenoid Biosynthesis

This chapter presents unpublished data

Author contribution:

AFB performed the majority of the experimental work

Abstract

Resveratrol and other stilbenes comprise an essential group of *Vitis vinifera* secondary metabolites with important roles in plant defence and also of much interest in the field of medicine. Despite the number of studies published on these compounds, for most of them, the biosynthetic pathway remains unknown. However, a possible involvement of DIR during the first stages of oligomerization has been suggested. In this study an attempt was made to investigate the potential participation of *Vv*DIR in the dimerization of resveratrol. Database analysis revealed that *V. vinifera* DIR family is amongst the largest described, encoding 42 putative *Vv*DIR from different subfamilies (DIR-a, DIR-b/d, DIR-e and DIR-g). As a mean to choosing plausible candidates for the study, 16 *Vv*DIR transcripts were analyzed for their presence in different organs of the plant and response to *Phaeomoniella chamydospora* infection. Most genes were expressed ubiquitously but evidence of tissue specific expression was also observed, with *Vv*DIR25 and *Vv*DIR27 being expressed in the trunk and leaves, whereas *Vv*DIR36 and *Vv*DIR37 being root specific. Differential expression profile upon *P. chlamydospora* infection was partially obtained for four *Vv*DIR genes. No fungal induced expression was detected. Instead, *Vv*DIR25 and *Vv*DIR30 were responsive to wounding during the inoculation process. Four *Vv*DIR protein candidates were recombinantly expressed in *Pichia pastoris* and evaluated for their activity towards resveratrol dimerization. No influence was observed during the *in vitro* reactions. In a final attempt to detect guiding activity in resveratrol dimerization, protein extracts from leaves and canes were analyzed. While leaves showed no influence in the reaction, the canes displayed regioselective activity during dimerization, preventing the spontaneous formation of δ-viniferin and inducing the synthesis of a novel symmetric resveratrol dimer never described before.

Introduction

Dirigent proteins are believed to play an important role in plant secondary metabolism due to their role in the stereochemical guidance of oxidative coupling reactions. Their functional characterization and the recognized bioactivity of the metabolites they “help” to synthesize, illustrates well the level of sophistication plants have acquired to cope with external aggression factors [1]. Because the enantioselectivity feature of many of these metabolites is often related to their bioactivity, correct configuration in their synthesis must be accomplished for proper function in the host organism [2,3].

In oxidative coupling reactions, the laccases and peroxidases responsible for radical formation can display wide substrate specificity [4,5]. While their active centres may, in part, influence the regioselectivity of radical coupling, they lack the ability to control the enantiomeric composition of the products which, in the case of coniferyl alcohol, is performed by dirigent proteins [6-9]. Although the most documented dirigent-mediated reaction is the dimerization of coniferyl alcohol to afford (+)-pinoresinol, dirigent proteins may also be involved in the synthesis of other metabolites in reactions yet to be described [10].

So far, cDNA and genomic ORF database analyses allowed a reasonable number of DIR and DIR-like genes to be further identified in several plants, establishing a *DIR* multigene family [11]. The three largest known *DIR* families have been reported in *Arabidopsis thaliana* (25 genes), *Picea* spp (35 genes) and *Oryza sativa* (54 genes). A high degree of heterogeneity can be observed among family members. In *Picea*, predicted amino acid identity between two *DIR* cDNAs can range from as high as 99.5% to as low as 17.6% [12]. According to their predicted amino acid sequence and phylogenetic analysis, they are grouped into six distinct subfamilies (DIR-a, DIR-b/d, DIR-c, DIR-e and DIR-f) (Figure 30).

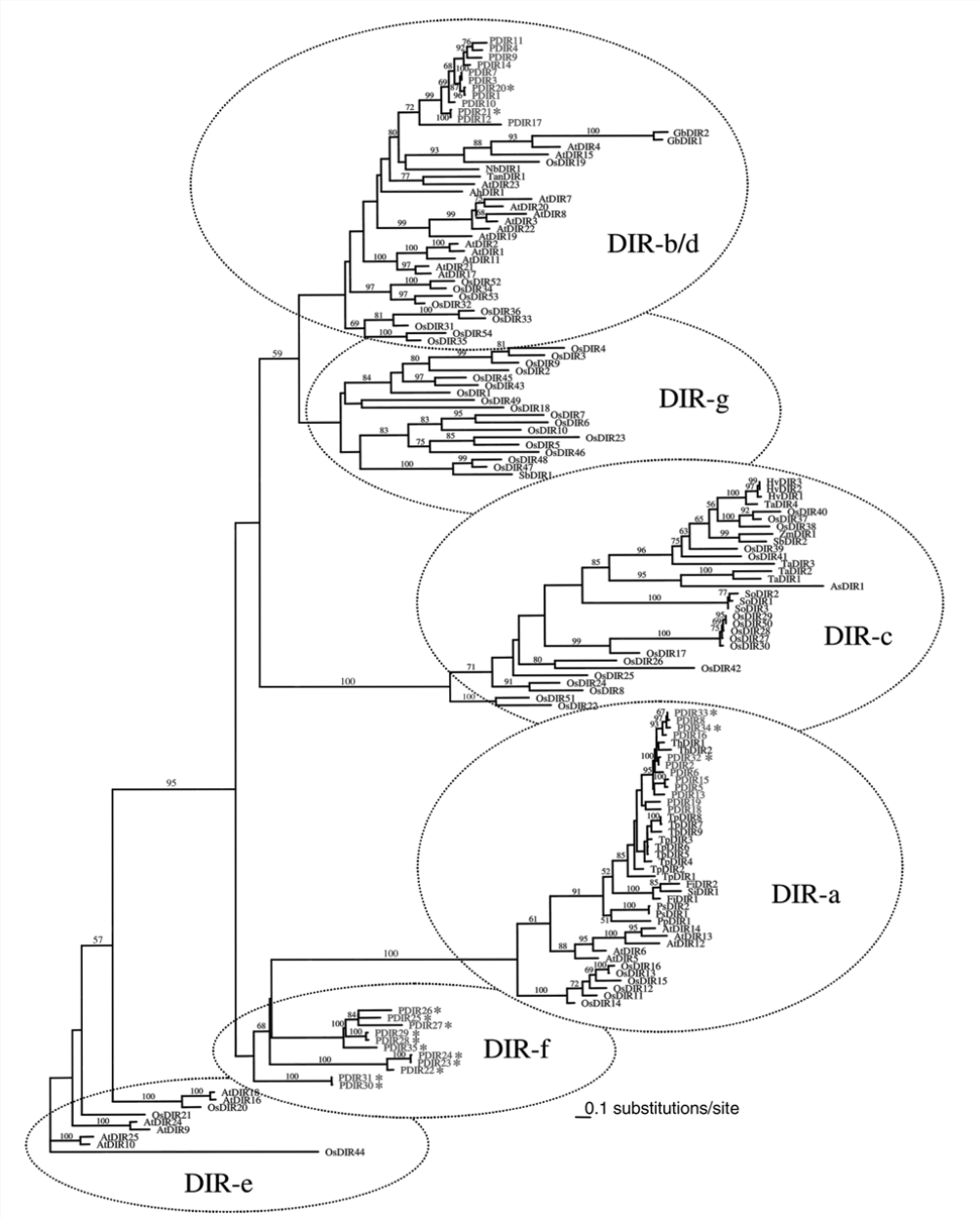

Figure 30. Phylogenetic tree of 150 dirigent protein sequences illustrating the existing subfamilies according to Ralph [12]. Adapted from Ralph, 2007.

With few exceptions, DIR biochemical/physiological functions have only been assigned to members of the DIR-a subfamily ((+)-pinoresinol formation) [12]. More recently, a DIR-a protein from *Arabidopsis thaliana*

(*At*DIR6), was shown to possess opposite stereoselectivity towards coniferyl alcohol coupling, mediating the formation of (-)-pinoresinol [13]. Additional reactions involving DIR participation were only reported for a member of DIR-b/d subfamily in cotton, where a dirigent protein was shown responsible for the enantioselective dimerization of hemigossypol into (+)-gossypol, a defense-related terpenoid [14]. As for the remaining proteins and subfamilies, though some evidence exist that they might participate in plant defense, little is known about the type or the number of reactions they can assist [12,15].

Given the size number and heterogeneity of DIR superfamily, together with the widespread occurrence of radical coupling steps in pathways leading to enantiomerically pure compounds, there is great potential for the general involvement of DIR proteins in the control of secondary metabolism [10]. The fact the DIR transcripts are often reported as differentially expressed during numerous biotic and also abiotic stresses, indirectly supports the previous assumption. They are now associated to a wide variety of stimuli affecting plants which can range from abiotic stresses such as wound, drought, temperature and salinity, to biotic stresses including herbivore insect and fungal pathogen attacks [11,15-19].

On the other hand, quite direct evidence of DIR alternative reactions can be gathered from metabolites detected in plants. Lignans isolated from *Larrea tridentata* are thought to be derived from oxidative coupling of allylphenol units instead of monolignols [20]. Resembling coniferyl alcohol dimerization, *in vitro* coupling of *E*-*p*-anol using laccase as oxidixing agent affords racemic mixtures of 8-8', 8-5' and 8-*O*-4' lignans. Isolated lignans from this species are exclusively 8-8'-linked, some being present as pure enantiomers [21]. Another example refers to *Eucommia ulmoides,* where cell-wall preparations were demonstrated to exert diastereoselective control in the synthesis of 8-*O*-4'- linked sinapyl units and cross-coupling

of sinapyl and coniferyl alcohol radicals yielding the corresponding lignans at specific *erythro/threo* ratios displaying several degrees of optical activity [22,23]. The case of (+)-syringaresinol synthesis in *Liriodendron tulipifera* also provides evidence of additional enantioselective control during monolignol coupling. According to the proposed biosynthesis, syringaresinol, a central precursor to other syringyl lignans, can be formed from sinapyl moieties. Feeding experiments using *L. tulipifera* shoots suggest that sinapyl alcohol dimerization is under stereoselective control to afford (+)-syringaresinol [24]. Several other cases exist, such as the formation of (-)-blechnic acid from caffeic acid coupling or the intramolecular oxidation of (7*E*, 7'*E*) 4-coumaryl 4-coumarate to generate hinokiresinol [25,26].

Apart from the previous examples, literature reports also point the stilbenoid biosynthetic pathway as a potential site of action for DIR proteins [27]. Stilbenoids are hydroxylated derivatives of stilbene originated from the general phenylpropanoid pathway [28]. Unlike lignans, which are ubiquitous in plants, stilbenoids can only occur in a restricted group of plant families expressing the key enzyme for the stilbene structure formation (stilbene synthase (STS)) [29]. Stilbene units are characterized for their 1,2-diphenylethylene backbone and are formed through a single multi-step reaction involving three malonyl-CoA molecules and one CoA-ester of a cinnamic acid derivative. Depending on the nature of the CoA-ester, different primary stilbenes can be formed (Figure 31) [30]. Although a single enzyme can metabolize different subtrates, it generally shows much higher affinity to a specific starter molecule [31,32]. That will likely be an important factor defining the type and features of stilbenoids synthesized by different plants. In *Vitis* species, as in the *Vitaceae* family, the predominant form of STS seems to be the *p*-coumaroyl-CoA-type (resveratrol synthase). For this reason, resveratrol, perhaps the most well known and extensively studied stilbene, can be

easily found in almost all members of this family and is thought to be the major precursor in the formation of other stilbenoid metabolites [33].

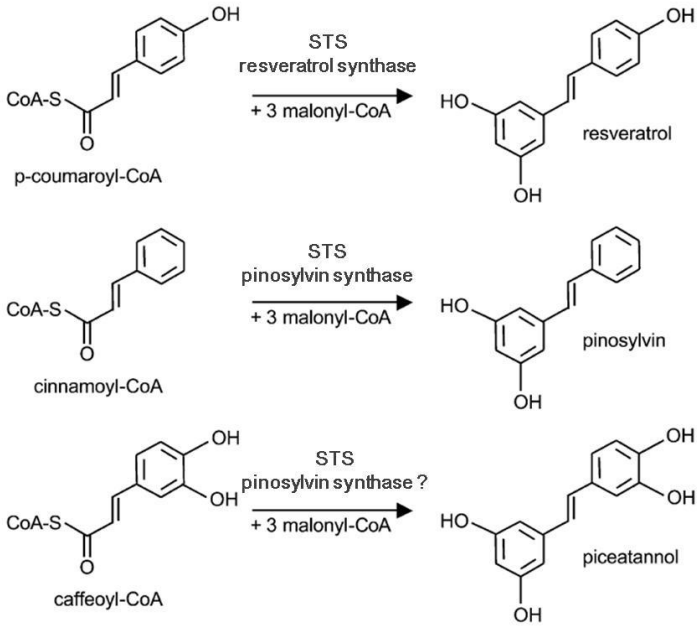

Figure 31. Examples of different reactions catalyzed stilbene synthases to afford stilbenes commonly occurring in *Vitis* (resveratrol), *Pinus* (pinosylvin) and *Picea* (piceatannol) species. Adapted from [29].

Stilbenoids are notorious for the great complexity and diversity of their structures. From the relatively simple basic unit of resveratrol, plants evolved several mechanisms of upstream modifications which, when combined, allow for the synthesis of an endless set of possible compounds (Figure 32). These can include simple rearrangements of the hydroxyls whereby they become substituted by methyl, methoxy and sugar groups or the addition of new substituent groups. Prenylated and geranylated stilbenes are also known. Moreover, they can undergo oxidative coupling, originating compounds with several degrees of oligomerization [29,33-35]. So far, in *V. vinifera*, over 60 stilbenoids have

been isolated and identified [33]. A few of them are depicted in the following figure.

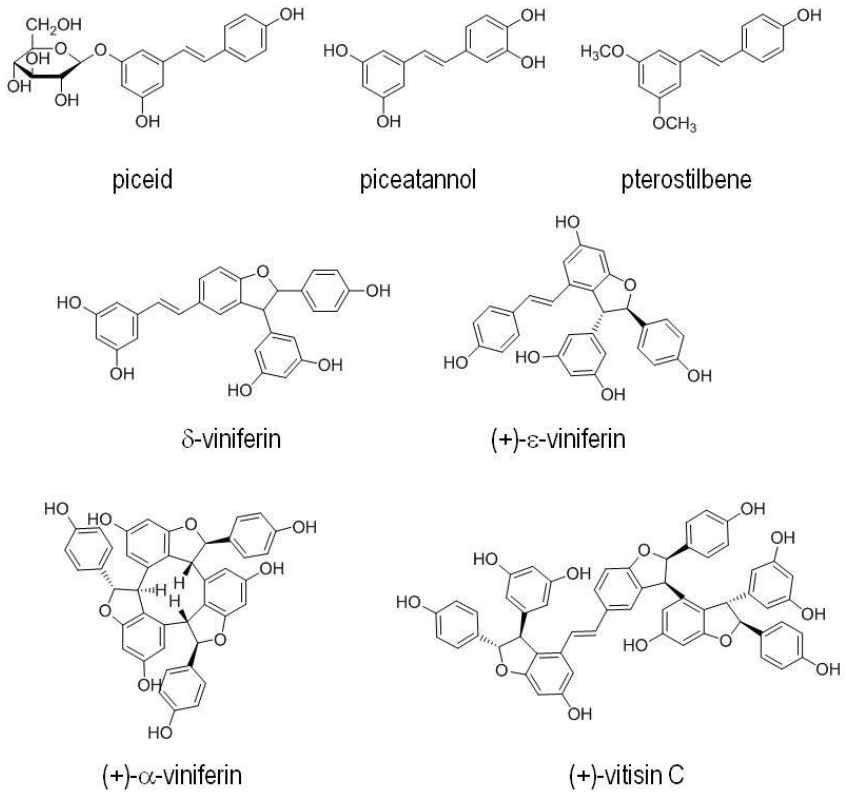

Figure 32. Representatives of stilbenoid metabolites detected in *V. vinifera* illustrating oligomerization levels and resveratrol modifications.

It is during the oligomerization process, occurring through oxidative coupling reactions, that DIR proteins are thought to intervene, namely in the dimerization of resveratrol to afford ε-viniferin [10,27]. This distilbenoid occurs in *Vitis* species and other Vitaceaous plants as the (+)-antipode but has also been detected in other plants as the (-)-enantiomer [33,36,37]. While their presence in different plants as opposite enantiomerically pure compounds does not provide sufficient evidence of a DIR-mediated reaction, the several attempts to mimetize this dimerization *in vitro* strongly suggest that a regiostereochemical control must be operative *in*

vivo. To date, a few studies exist on *in vitro* resveratrol coupling and the characterization of its products using several different oxidative enzymes (peroxidases or lacases) either from plant or fungal origin. Neither was able to detect the formation of ε-viniferin [38-44]. The only work reporting the successful *in vitro* production of ε-viniferin was performed by Takaya and co-workers where, using inorganic oxidants they were able to synthesize the distilbenoid in the form of racemate [41].

Taken together, the previous studies strongly indicate that DIR or DIR-like proteins may be acting upon the stilbenoid biosynthetic pathway, at least in the formation of the enantiomerically pure forms of ε-viniferin. Structure analysis of more complex stilbenoids also suggests that this resveratrol dimer would likely serve as monomer for higher degrees of polimerization [45]. If that is the case, the stereoselective control during its synthesis would also explain the optical activity observed for many other stilbenoid compounds.

In this chapter, an attempt was made to identify additional DIR and DIR-like proteins encoded in *V. vinifera* genome, evaluate its expression in different plant tissues and possibly identify new DIR-mediated reactions either in lignan or stilbene biosynthetic pathways.

Materials and Methods

Plant material and treatments

Healthy *Vitis vinifera* cuttings, with three buds each, were rooted in water and then transferred to soil (1 L pot per plant). Plants were maintained in a growth chamber at 25 ºC with a photoperiod of 16 h (480 $\mu mol.m^{-2}.s^{-1}$). After one month of acclimatization period, whole plants or detached leaves were subjected to the different treatments.

For the *Phaeomoniella chlamydospora* treatment, a pure fungal isolate was obtained from CBS (CBS 239.74) and propagated in PDA medium at

23ºC in the dark. Inoculation was performed at the base of the primary shoot by removing a small section of the bark with a scalpel and placing a 5 mm inoculation plug (cut from the actively growing margin of the colony) into the wound (mycelium side down). Each wound was then covered with moist cotton wool and sealed with parafilm. The same procedure was followed for negative control plants using non inoculated PDA plugs. Plants were maintained under the above described conditions up to one week with samples being harvested at 2, 4, 8, 12, 24 and 192 h post inoculation. All samples were immediately frozen in liquid nitrogen and used for total RNA extraction.

For the UV irradiation treatment, leaves were detached and their undersides were exposed to UV-C radiation (Philips TUV 30 W, 92 μW cm^{-2} at 253 and 7 nm) at a distance of 15 cm from the source during 10 min. Following irradiation, treated and control samples were incubated in a dark wet chamber at room temperature for 48h. After that period, samples were collected for methanolic and protein extraction.

Sequence analysis

Multiple sequence alignments were performed by ClustalW in BioEdit program. Homologue database search was performed by BLAST (http://blast.ncbi.nlm.nih.gov/Blast.cgi). Potential glycosylation sites and signal peptide prediction was performed by NetNGlyc 1.0 and SignalP 4.1 using the CBS server prediction tools (http://www.cbs.dtu.dk/). Conserved domain regions were determined with the CD search tool from NCBI (http://www.ncbi.nlm.nih.gov/Structure/cdd/wrpsb.cgi). Identity matrix was obtained using T-Coffee (http://www.ebi.ac.uk/Tools/msa/tcoffee/). Mega 5.0 was used to construct *Vv*DIR phylogenetic tree using BIONJ algorithm with 75 bootstrap replicates. Codon adaptation index (CAI) was calculated using GenScript rare codon analysis tool (http://www.genscript.com/cgi-

bin/tools/rare_codon_analysis) and the codon optimization was performed by Genart optimization tool (Invitogren).

DNA extraction

Whole grapevine plants were harvested from the growth chamber. Leaves, canes and roots were collected, ground and used for genomic DNA extraction as described in chapter III.

RNA extraction and cDNA synthesis

Total RNA extraction was performed as described in chapter III using the Rapid CTAB (hexadecyltrimethyl ammonium bromide) method. Prior to reverse transcription, samples were treated with RQ1 RNase-Free DNAse (Promega) according to the manufacturer's protocol.

All samples were reverse transcribed using ThermoScript RT-PCR System (Invitrogen) as described by the manufacturer. cDNA was synthesized from 600 ng of total RNA and oligo$(dT)_{20}$ primers. RT reactions were carried at 55 ºC for 60 min.

Primer design and qPCR

PCR primers were designed with Primer-BLAST (http://www.ncbi.nlm.nih.gov/tools/primer-blast/) and Primer Premier 5 (Premier Biosoft International) to target amplicons between 80 and 300 bp. Amplification specificity was first assessed through BLAST and Primer-BLAST using *V. vinifera* database as template. qPCR was performed with iQ SYBR Green supermix (Bio-Rad) using iCycler equipment (Bio-Rad). Prior to use, cDNA samples were diluted to 20 ng/μL. Reaction mixtures (20 μL) were prepared as follows: 5 μL of the diluted template, 1 μL primer mix (10 μM each), 10 μL iQ SYBR Green

supermix (Bio-Rad), 4 μL H_2O. Thermal cycling was composed of an initial denaturation step for 3 min at 95 ºC, 40 cycles at 95 ºC for 10 s, 55 ºC for 30 s and 72 ºC for 30 s. All reactions were performed in triplicate and amplification specificity was confirmed through melting curve analysis.

Expression vector construction and recombinant expression of *Vv*DIR

Recombinant expression of the selected VvDIR was performed as described in chapter IV. Briefly, *VvDIR* optimized genes were obtained from EurofinsMWG as synthetic genes and were cloned into pPICZαA vector, in frame with *Pichia pastoris* native α-secretion signal and a C-terminal Histag. Linearized expression vectors were transformed into KM71H strain and the transformants were evaluated for increased zeocin resistance in YPDS containing 500 to 2000 μg/mL zeocin. Selected transformants were tested for recombinant expression induction as follows: a single colony was inoculated in 50 mL BMGY medium and incubated at 28 ºC, 150 rpm until a 2 to 6 OD was reached. Cells were recovered and reinoculated in 10 to 20 mL BMMY medium. Cultures were incubated under the same conditions, adding daily methanol to a final concentration of 0.5 to 1 %, during a period of 4 days. 1 mL aliquots were collected every 24 h and the respective supernatants were analysed by SDS-PAGE and western blotting as described in chapter IV.

Methanolic extractions

Samples were ground to a fine powder (6 g dw leaves or 1.5 g dw canes) and were stirred in n-hexane (30 mL/g) during 1h. The solid residue was recovered by filtration and extracted twice with methanol (10 mL/g) by stirring (30 min), sonicating (15 min) and stirring (30 min). The methanolic

fractions were evaporated to dryness and resuspended again in 3 mL methanol for HPLC analysis.

Grapevine protein extractions

Leaves – Samples were macerated together with 30 % (w/w) PVPP in liquid nitrogen using a mortar and pestle. Extraction buffer (0.35 M Tris-HCl, pH 8, 20 mM EDTA, 11 mM sodium diethyldithiocarbamate, 15 mM cysteine and freshly added 200 μM PMSF) was added to the samples (10 mL/g) and stirred during 15 min at 4 ºC. Samples were centrifuged (15000 *g*, 15 min, 4 ºC) and the supernatant was collected. Samples were desalted to water, lyophilised and resuspended in phosphate buffer to perform *in vitro* reactions.

Wood – The extraction method was adapted from Halls [46]. Briefly, 20 g dw of grapevine canes were ground and extracted three times with cold acetone (10 mL/g) stirring at 4 ºC during 20 min. Solid residue was recovered by filtration, resuspended (10 mL/g) in buffer A (100 mM potassium phosphate, pH 5.5, 1% (v/v) Triton X-100, 0.1 % (v/v) β-mercaptoethanol) and stirred at 4 ºC for 1 h. The supernatant was collected (fraction Fa) and the solid residue was further extracted with buffer B (100 mM potassium phosphate, pH 5.5, 0.1 % (v/v) β-mercaptoethanol) and buffer C (100 mM potassium phosphate, pH 5.5, 1.5 M NaCl, 0.1 % (v/v) β-mercaptoethanol) as described above (fractions Fb and Fc, respectively). Resulting fractions were concentrated and the buffer exchanged to potassium phosphate buffer to perform the *in vitro* reactions.

Oxidative coupling reactions

For recombinant *Vv*DIR activity assays, 30 μg of total protein from *P. pastoris* culture supernatants were incorporated in the reactional mixtures. Coniferyl alcohol reactions were performed in a total volume of 125 μL in

100 mM potassium phosphate buffer, pH 5.9 containing 2.5 μL of 75 mM coniferyl alcohol and 0.75 mU of *T. versicolor* laccase (Sigma-51639). Reactions were initiated by the addition of laccase and were incubated at 25 ºC during 1.5 h. Resveratrol reactions were performed in a total volume of 150 μL of 100 mM potassium phosphate buffer, pH 5.9 containing 20 μL of 30 mM resveratrol and 5.7 mU of laccase. Reactions were incubated at 25 ºC during 4 h.

For the assays in the presence of protein extracts from grapevine leaves, reactions of 500 μL in potassium phosphate buffer were performed. Reaction mixtures contained the extracts (20, 100, 500 or 1000 μg of protein), 170 μL of 30 mM resveratrol and 50 mU of horseradish peroxidase (Sigma-P8375). Reactions were initiated with 5 μL of 700 mM hydrogen peroxide and incubated during 1 h at 25 ºC with further 5 μL of hydrogen peroxide being added passed 30 min.

For the assays with protein extracts from wood, resveratrol reactions were performed in a total volume of 300 μL of 100 mM potassium phosphate buffer, pH 5.9 containing 20 μL of 30 mM resveratrol, 11.4 mU of laccase and 30 μg of wood proteins. Reactions were incubated at 25 ºC during 30 min.

All the reaction mixtures were extracted once with two volumes of ethyl acetate and evaporated to dryness. The residue was resuspended in methanol and analysed by reverse phase HPLC (recorded at 280 nm or 310 nm) on a Luna PFP(2) C18 column (Phenomenex) using a 0.1% TFA (A):acetonitrile (B) linear gradient at a flow rate of 1 mL/min: 0 min - 0 % B, 4 min - 31 % B, 27 min - 40 % B, 29 min - 100 % B, 31 min - 100 % B, 34 min - 0 % B, 37 min - 0 % B. Due to technical reasons the gradient had to be modified and adjusted several times for different sets of injections. Peak identification was performed by chromophore comparison and re-injection of standards.

Isolation and identification of a new resveratrol dimer

Approximately 7 mg of resveratrol were used in a large scale *in vitro* reaction as described above (gravevine cane protein extracts as oxidizing agent). The reactions were performed during 1 h and the residue was extracted with ethyl acetate followed by evaporation and resuspension in methanol. The sample was separated by HPLC using a semi-preparative Luna PFP(2) column with a 0.1% TFA (A):acetonitrile (B) linear gradient at a flow rate of 4 mL/min: 0 min - 0 % B, 4 min - 29 % B, 15 min - 33 % B, 18 min - 100 % B, 22 min - 100 % B, 24 min - 0 % B, 28 min - 0 % B. Consecutive injections were made collecting the desired sample peak. Sample was evaporated (0.9 mg) and used for structural elucidation using 1D and 2D NMR:

^{1}H NMR (600 MHz; CD_3OD): 7.00 (d, J=2.0 Hz, H-10/H-10'); 6.91 (d, J=16.3 Hz, H-7/H-7'); 6.85 (dd, J=8.2 Hz, J=2.0 Hz, H-14/H-14'); 6.77 (d, J=16.1 Hz, H-8/H-8'); 6.76 (d, J=8.2 Hz, H-13/H-13'); 6.45 (d, J=2.1 Hz, H-2/H-2' and H-6/H-6'); 6.18 (t, J=2.1 Hz, H-4/H-4').

^{13}C NMR (150 MHz; CD_3OD): 159.6 (C-3/C-3', C-5/C-5'); 146.5 (C-12); 146.4 (C-12'); 141.3 (C-1); 131.1 (C-9 and C-11); 129,7 (C-8); 129,6 (C-8'); 127.0 (C-7); 126.9 (C-7'); 120.2 (C-14); 120.1 (C-14'); 116.5 (C-13); 116.4 (C-13'); 113.8 (C-10); 113.7 (C-10'); 105.9 (C-2 and C-6); 105.7 (C-2' and C-6'); 102.8 (C-4); 102.5 (C-4').

The assignments are interchangeable between the carbon signals of equivalent positions of each monomeric subunit.

ESI-MS *m/z*: 455.15 $[M+H]^+$

Results and Discussion

Vitis vinifera DIR superfamily

To identify potential DIR/DIR-like genes encoded by *V. vinifera* we performed a comprehensive search of publicly available databases retrieving cDNA and genomic ORF sequences homologous to the already known DIR genes in other plants. According to our analysis, *V. vinifera* genome encodes a family of 42 putative *DIR*/*DIR*-like genes (Table 6).

Table 6. Putative *DIR* genes encoded in *V. vinifera* genome.

DIR nomenclature	Accession number	cDNA length (bp)	ORF length (aa)
VvDIR1	XM_002276412	667	185
VvDIR2	XM_002276394	668	185
VvDIR3	XM_002276441	972	186
VvDIR4	XM_002272108	579	192
VvDIR5	XM_002285639	800	193
VvDIR6	XM_002285640	794	193
VvDIR7	XM_002285646	777	189
VvDIR8	XM_002285642	582	193
VvDIR9	XM_002285641	844	192
VvDIR10	XM_002285645	840	193
VvDIR11	XM_002283363	790	193
VvDIR12	XM_002283367	665	194
VvDIR13	XM_002285649	779	195
VvDIR14	XM_002285647	814	193
VvDIR15	XM_002285648	582	193
VvDIR16	XM_002280686	740	191
VvDIR17	XM_002280755	699	192
VvDIR18	XM_002280781	688	189
VvDIR19	XM_002280675	689	192
VvDIR20	XM_002276245	480	159
VvDIR21	XM_002280927	742	188
VvDIR22	XM_002276222	510	169
VvDIR23	XM_002276381	1029	342
VvDIR24	XM_002266416	672	153
VvDIR25	XM_002266789	707	178
VvDIR26	XM_002276686	828	184
VvDIR27	XM_002276705	692	185
VvDIR28	XM_002273774	321	106
VvDIR29	XM_002277446	507	168
VvDIR30	XM_002272476	850	186
VvDIR31	XM_002283643	2433	643
VvDIR32	XM_002282925	750	249
VvDIR33	XM_002285577	928	253
VvDIR34	XM_002276140	4044	1347
VvDIR35	XM_002276108	1105	362
VvDIR36	XM_002276081	729	242
VvDIR37	XM_002281449	954	317
VvDIR38	XM_002269361	534	177
VvDIR39	XM_002269312	384	127
VvDIR40	XM_002270627	684	179
VvDIR41	XM_002270451	684	179
VvDIR42	XM_002270552	691	179

The elevated number of predicted *DIR* genes in grapevine, constituting the second biggest family described to date, anticipates their potential

importance in this species. Most of the genes fit the general description for DIR proteins, coding for relatively small proteins of approximately 180 amino acid residues and being single exon genes. A few exceptions were observed with predicted ORF lengths ranging from 242 to 1347 amino acid residues for *Vv*DIR23 and *Vv*DIR31 to 37. All putative DIR sequences were analyzed against the conserved domain database (CDD) to identify/confirm their functional regions. Overall, the general protein architecture is comprised only of a single DIR domain (PF03018) preceded of the signal peptide sequence. Yet, for some of the above mentioned longer ORF genes (*VvDIR31*, *VvDIR34* and *VvDIR35*) additional conserved regions were detected (Figure 33).

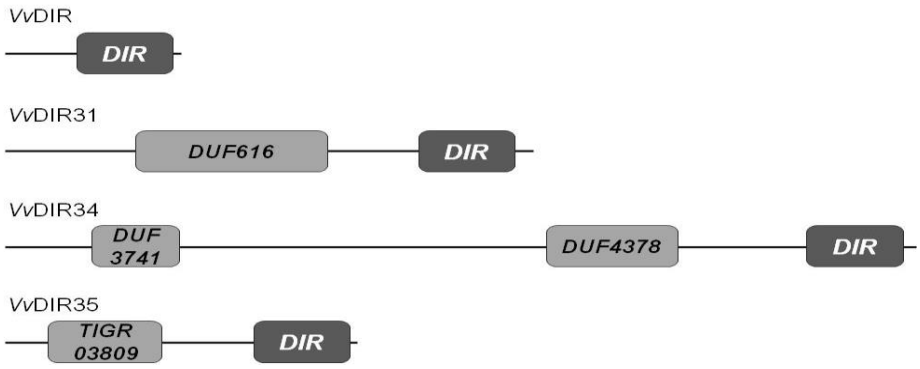

Figure 33. Schematic domain organization of grapevine predicted DIR genes. Common arquitecture (*Vv*DIR) and exceptions are depicted (*VvDIR31, 34* and *35*).

Though the presence of other domains could be useful to infer a function or locate the metabolic pathway where those DIR would act, in this case no information could be retrieved as all extra domains are annotated as domains of unknown function. A *Vv*DIR31 similar architecture was found for an *A. thaliana* protein while the remaining (*VvDIR34* and *VvDIR35*) seem exclusive of *V. vinifera.*

Multiple sequence alignment of the putative *VvDIR* was performed to evaluate general sequence similarities among all members of the family and generate a phylogenetic tree (Figures 34 and 35).

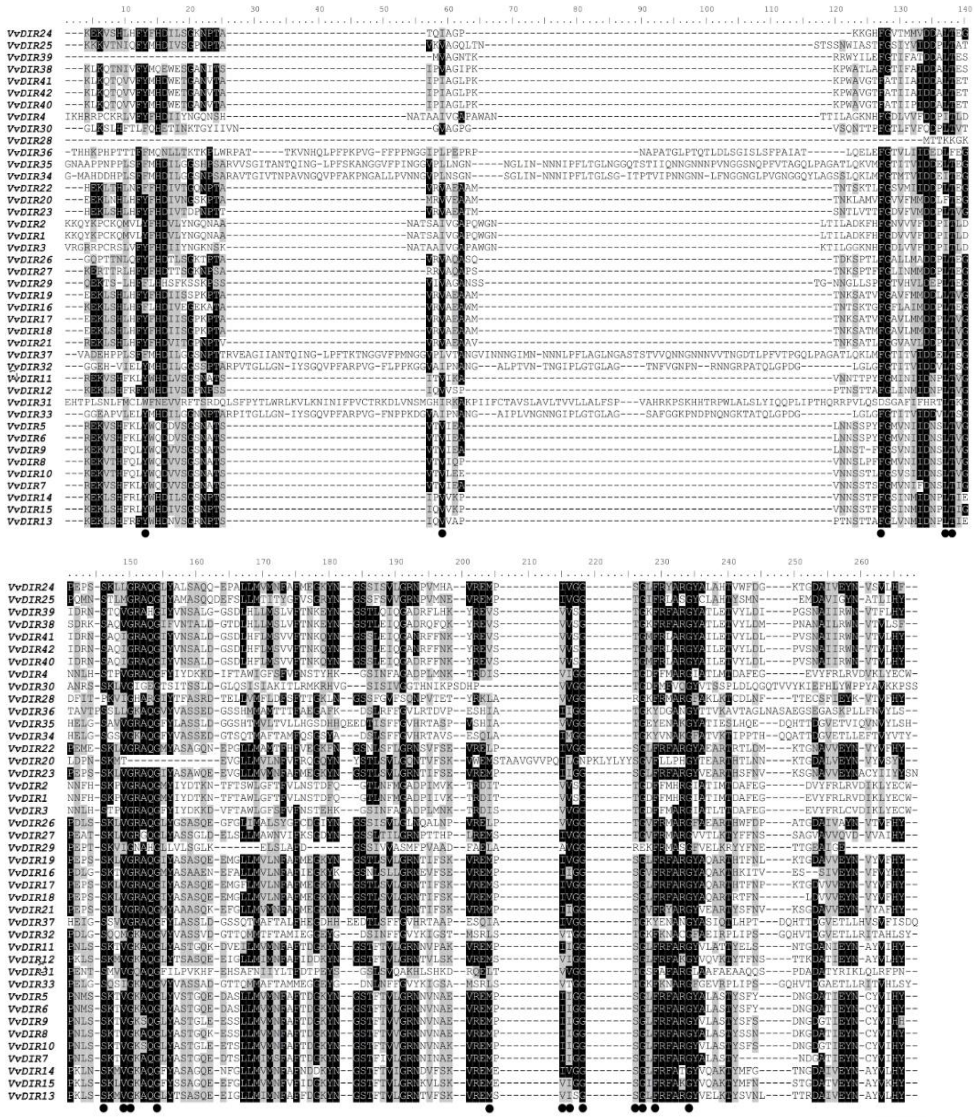

Figure 34. Amino acid sequence alignment of grapevine DIR family (only DIR domain of approximately 150 aa are displayed) using ClustalW. Conserved similarity shading is shown for 50% identity (black) and 50% similarity (grey). Highly conserved residues (identity or similarity) present in more than 95% of the sequences are marked with a black dot.

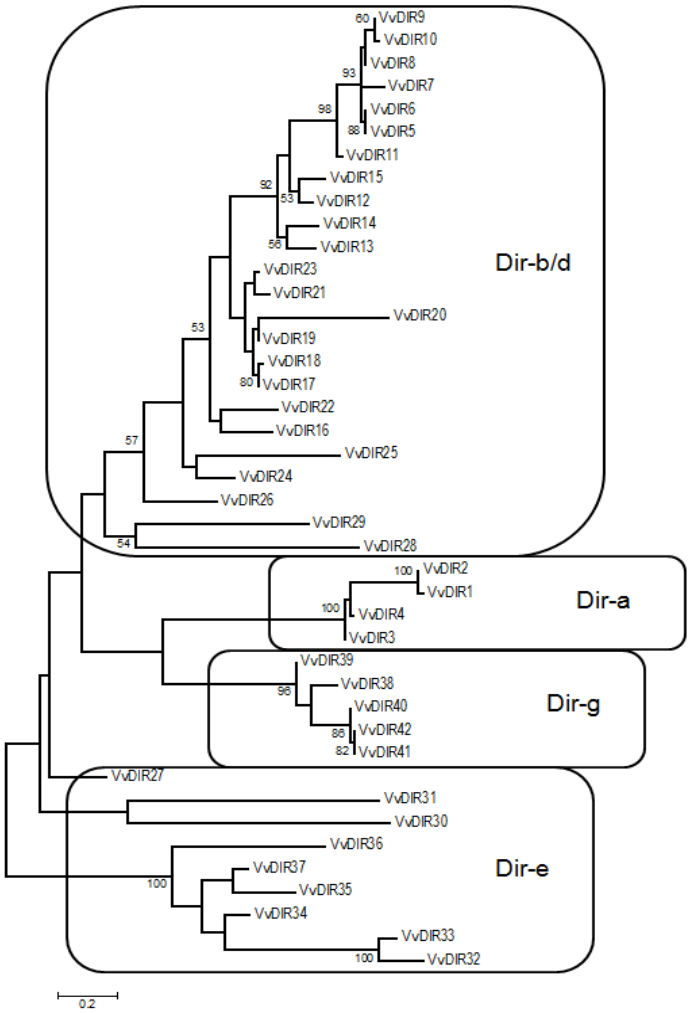

Figure 35. Phylogenetic tree of grapevine DIR/DIR-like protein sequences analyzed by maximum likelihood. The tree was generated by MEGA5 software using BioNJ algorithm. Branch lengths are measured in the number of substitutions per site.

Sequence analysis revealed the existence of several highly conserved residues that were present in more than 95 % of the sequences (one Ser at position 146 and four Gly residues at positions 150, 154, 218 and 234 of the alignment, respectively). Those amino acids can represent critical residues potentially involved in the function or regulation of DIR activity. Pairwise sequence similarities among *Vv*DIR, also evidences the previously mentioned high heterogeneity of DIR superfamily, with

identities between members ranging from as low as 15.09 %, for *Vv*DIR31 and *Vv*DIR36, to as high as 98.96 %, for *Vv*DIR5 and *Vv*DIR6. Following the previous work of Ralph and colleagues [11,12] where, according to phylogenetic analysis, DIR proteins (150 sequences from several plants) were divided into six distinct subfamilies, we attempted to assign the predicted *Vv*DIR into the already existing groups. We were able to merge all *Vv*DIR into four of those subfamilies (DIR-a, DIR-b/d, DIR-e and DIR-g). Reasonably, none of *Vv*DIR has been assigned into the DIR-c and DIR-f subfamilies, as the first was only found in monocotyledons, and the second seems to be exclusive of *Picea* species. Minimum intra-group variation was observed for the sub-family DIR-g with all the members of the group sharing between 74 % and 97 % sequence identity. As expected, the pinoresinol-forming *Vv*DIR1 fell into the DIR-a category. Three additional *Vv*DIR-a were encountered, *Vv*DIR2, 3 and 4, sharing 97.3, 67.4 and 68.1 % amino acid identity with *Vv*DIR1, respectively.

_Vv_DIR tissue-specific transcription

Having previously unveiled the grapevine DIR family we next aimed at determining how many and which encoded *Vv*DIR genes could we demonstrate as being transcribed in *V. vinifera*. A transcript screening approach using qRT-PCR was selected for this task. Although the objective was to analyze all the 42 transcripts, the existence of highly similar cDNA sequences for some of the genes, posed several constrains during the primer design process. In some of the cases, a compromise between the primer set specificity and reasonable amplification efficiency could not be easily achieved. For those cases, we assembled small groups of closely related genes and designed a specific primer pair for only one of the members, which was considered as representative of the group, but chosen solely based on its nucleotidic sequence for primer

design purposes. Therefore, some of the genes could have been ignored during the screening. Even considering similar functions for all genes within the same group, their expression could follow distinct spatiotemporal patterns. Regardless the limitations, we considered that this approach would be suitable for our initial analysis. We designed a set of 19 primers pairs (Table 7) and evaluated their amplification efficiency/specificity against genomic DNA prior to transcript screening (Table 8). *Vv*DIR7, *Vv*DIR26 and *Vv*DIR40 primer pairs did not generate any detectable products following PCR amplification, most likely due to bad primer design, and were not used for the transcript screening process.

Table 7. Primer pairs (forward – top, reverse – bottom) used for *Vv*DIR transcript screening

	Primer sequence 5' - 3'	Amplicon (bp)		Primer sequence 5' - 3'	Amplicon (bp)
VvDIR1*	CCAGCACTCATACAACTTAATATCAAC CTCAACAGCACAGACTTTCAGG	197	VvDIR28	ACCCCCAAGGTCATTGGTCA CCGCCAGCTTCCTGTAAGTC	169
VvDIR7*	TCAACTTACAACGATGGCGCC CGTGAACTAAAGCTCCACTAAAA	96	VvDIR29	GCATGTGCTTGATGAGCCCT GCCACCACAATGGAACTCCC	135
VvDIR14*	TAGTTGGTGGCAGTGGGCTT GCTACAGTGGGAACACACAACA	199	VvDIR30	TCAGCATTCTCAGAGGGCCA AACCTCACAGTGGAACGGGA	115
VvDIR16	TGGTCGCCGGAAAATCTCAG GACGTGTTTGTCATCCACGC	163	VvDIR31	TCGCCTCGATCCCACTACTC TGCTCAGGCAGGGTACTGTT	189
VvDIR19*	CATGACCAACAAGTCGGCGA TCGGAATAGCCCACTACCGC	271	VvDIR33*	CAAAGCCCCTCACACACACAA GCAAGATCCACTGCTGACACA	118
VvDIR22	GGTGAGGGAGTTGCCGATTG TGTATTCCACGACAGCGTTCC	116	VvDIR34	GGTGTCAGGGAGAAGCGTTC CCCTTTGGAGGCGATGGATG	140
VvDIR24	CCTCAGCGGGAAAAACCCAA TATGCGCCAAAGCATAGCCC	329	VvDIR36	CCATCCTAGGCCTACCCTGG TGGCTGGAGCATTGGGTCTA	273
VvDIR25	GTTGCTGGCCAGTTGACCAA CTGTGATGCCATGGCGTAGA	143	VvDIR37*	CACCTGACATGGCTCCAGTG GGTAGGATTGGACCCGCCTA	149
VvDIR26	CACAGAAGGACCCGACCTGA AATCCACGAGCCATCCGGAA	228	VvDIR42*	CCTCACTAACAACCTCTGTCGC GTTCACATAGATGCCCTGGGCG	281
VvDIR27	CCCCTCCGTGAGATGTCCAT GACAGCTACACCGGCACTAG	108			

* Specific primer set for the corresponding *Vv*DIR chosen as representative for a small group of genes. *Vv*DIR1 (*Vv*DIR2, 3 and 4); *Vv*DIR7 (*Vv*DIR5, 6, 8, 9, 10, 11); *Vv*DIR14 (*Vv*DIR12, 13, 15); *Vv*DIR19 (*Vv*DIR17, 18, 20, 21, 23); *Vv*DIR33 (*Vv*DIR32); *Vv*DIR37 (*Vv*DIR35) ; *Vv*DIR42 (*Vv*DIR38, 39, 40, 41) -not consensus.

According to the previous works published in literature, we knew in advance that *Vv*DIR genes could be differentially expressed during distinct developmental stages as well as in different tissues or organs. The studies performed by Kim and co-workers [9,13,47] are perhaps the most noticeable on the subject: seven *Thuja plicata* DIR genes (DIR-a) were found at significantly different expression levels in parts of the plant such

as flowers, needles, shoots or roots. Also, for the same tissue, variations were observed for the relative abundance of each DIR mRNA [9]; the promoter regions of the same genes were fused to a reporter gene and transformed into *A. thaliana* allowing to evaluate their expression patterns up to several weeks post germination. Remarkably diverse and unique patterns were observed, with some of the promoters evidencing a very localized reporter expression (i.e. one was trichome and root specific whereas other was mainly found in the leaf vasculature of the plant) [47]; a similar strategy was employed to evaluate *A. thaliana* native DIR genes, revealing an equally complex expression pattern [13].

Table 8. *Vv*DIR transcript screening in leaves, trunks and roots.

		Tissue / Organ		
Gene	gDNA	Leaf	Trunk	Root
VvDIR1	✓			
VvDIR7	×			
VvDIR14	✓			
VvDIR16	✓			
VvDIR19	✓			
VvDIR22	✓			
VvDIR24	✓			
VvDIR25	✓			—
VvDIR26	×			
VvDIR27	✓			—
VvDIR28	✓	—	—	—
VvDIR29	✓			
VvDIR30	✓			
VvDIR31	✓			
VvDIR33	✓			
VvDIR34	✓			
VvDIR36	✓	—	—	
VvDIR37	✓	—	—	
VvDIR42	×			

Light grey shade indicates no product amplification in genomic DNA. Dark grey shades indicate transcript detection in the corresponding organ.
— Transcript not detected.

Bearing the previous studies in mind, we decided to perform our transcript screening in a comparable manner, although at an elementary level, detecting the *Vv*DIR transcripts in whole leaves, trunks and roots of grapevines (Table 8). We analyzed 16 transcripts in three grapevine plants. *Vv*DIR expression was considered positive when the corresponding transcript was detected in one or more plants. As seen in the previous table, the majority of the *Vv*DIR genes were found in all the three organs analyzed. Of the five exceptions (*Vv*DIR25, *Vv*DIR27, VvDIR28, *Vv*DIR36 and *Vv*DIR37), only *Vv*DIR28 was never detected. The remaining, evidence the previously mentioned possibility of tissue specific expression: *Vv*DIR36 and *Vv*DIR37 were only expressed in the roots; *Vv*DIR25 and *Vv*DIR27 were found in the aerial parts of the plant (trunk and leaf) but not in the roots.

Since the previous experiments had been performed only for healthy unchallenged plants, there was also a chance that some of the previous genes could be induced by external factors. Addressing this issue, we decided to evaluate that possibility using biotic and abiotic stresses for which corresponding cDNA samples were already available at the laboratory (UV-C irradiation and wounding in leaves; *P. chlamydospora* infection in trunks). Given that, at this stage, we did not intend to perform any type of gene expression quantification, we only accounted for *de novo* expression. Thus, just *Vv*DIR28, *Vv*DIR36 and *Vv*DIR37 were analyzed. No expression induction was detected upon any of the stimulus, which may, in a risky supposition, be a first indicator that these genes may be non-functional in the plant or the particular tissues. On the other hand, they can either be induced or constitutively expressed at extremely low levels falling below the detection limit of our experimental conditions.

_Vv_DIR expression profile during _P. chlamydospora_ infection

Besides elucidating the expression pattern of *Vv*DIR in different parts of the plant, the previous experiments had the primary purpose of identifying DIR genes which could be used in subsequent tasks directed at the investigation of potential connections between DIR proteins and stilbenoid biosynthesis. Provided that not only stilbenoids, but also lignans, are mostly present in the woody tissues of the plants in which they occur, we were particularly interested in *Vv*DIR being expressed in the trunk rather than leaves or roots. Also, given the general association of DIR proteins with plant defence mechanisms, with several DIR genes being reported as upregulated in response to various stresses, it would be appropriate to detect potentially relevant *Vv*DIR expression changes induced by an external stimulus. Therefore, an attempt was made to assess *Vv*DIR expression profile in woody tissues during the early stages of infection with *P. chlamydospora* (Figure 36). Apart from being a biotic stress directly affecting the woody trunk of the plant, the choice of the experimental model was also supported by literature reports describing the accumulation of stilbenes in *V. vinifera* induced by this fungus [48-50].

Although *P. chlamydospora* colonization is a very slow process, where the fungal mycelium can take several months to progress a few centimetres inside the plant, the defence mechanisms are expected to be triggered as soon as the host detects the pathogen [50,51]. In fact, concerning DIR transcripts, rapid expression induction, occurring within minutes or a few hours after treatment (biotic or abiotic), has been reported [11,16,17]. For that reason we chose to conduct the experiments collecting and analyzing samples corresponding to several time points early after fungal inoculation (Figure 36).

Despite our efforts to analyze all 13 genes actively expressed in the wood during the select time points, this task was not successfully accomplished. Unfortunately, accurate expression data was only obtained to four of those

genes, even if two of them were lacking most of the time points. Previous failure to achieve the intended analysis was mainly attributed to the reduced amount of available biological material.

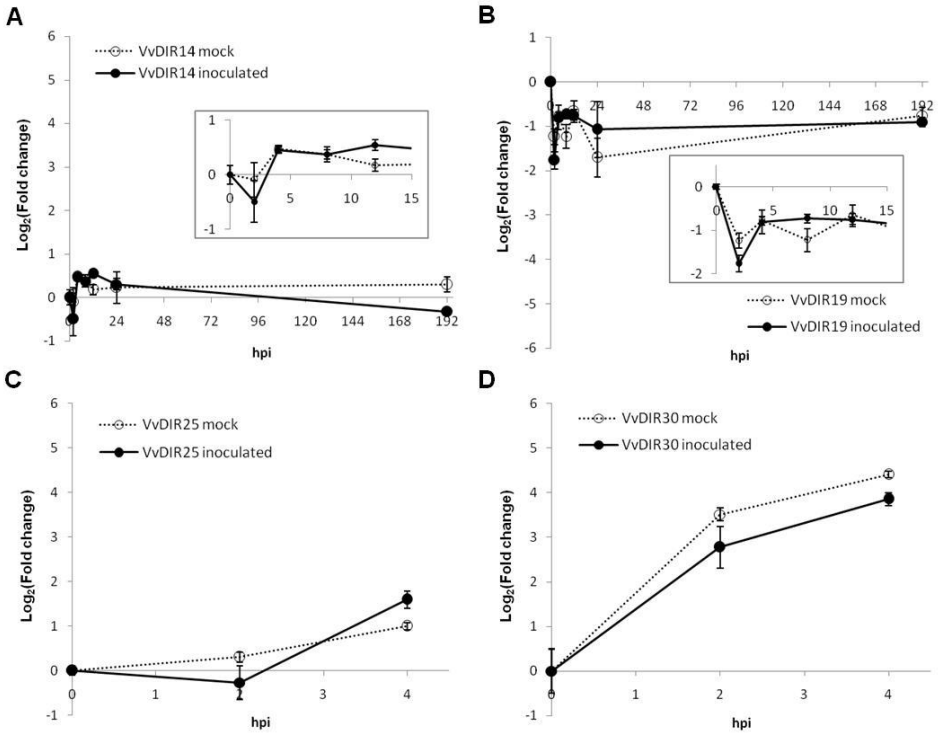

Figure 36. qRT-PCR analysis of *Vv*DIR transcripts (**A**) *Vv*DIR14, (**B**) *Vv*DIR19, (**C**) *Vv*DIR25 and (**D**) *Vv*DIR30 during *P.chlamydospora* infection. Relative gene expression quantification for mock and inoculated plants was calculated based on triplicate PCR reactions from three biological replicates, using *CYP* and *EF1* as normalization genes. Results are expressed as Log_2(mRNA fold change) in mock and infected *V. vinifera* trunks when compared to control plants (0hpi). Inserts show amplified areas of the corresponding graphs for short time periods.

While attempting to ration each individual cDNA sample to afford analysis of all the genes, excessive sample dilution may have been used. As a result, several difficulties were encountered during the expression quantification assays, including amplification of unspecific products, little or no amplification, and lack of consistency among replicates. All together, these problems compromised the relative gene expression quantification for the majority of the samples. In addition, for the four genes where the

quantification was possible, no relevant differences were observed between healthy and diseased plants. Although some transcript level changes are detected during the time lapse of the experiment, none seems to be specifically induced by the fungus. For *Vv*DIR14 and *Vv*DIR19, where the full expression profile was determined, the transcript levels for the mock and the inoculated plants suffer only slight variations when compared to the control plants (0 hpi). Also, both profiles (mock and inoculated) intersect and overlap each other at several time points, translating only in small under or overexpression values. This constancy indicates that these genes may be constitutively expressed in the wood tissues of grapevine. Furthermore, if we attempt to perform a rough estimate of their relative transcript abundance when compared to other *Vv*DIR (comparing *Ct* values obtained during the transcript screening process) we observe that both *Vv*DIR14 and *Vv*DIR19 are already being expressed at considerably higher levels than the remaining (approximately 60 to 250 times higher, inferred from a 6 to 8 *Ct* difference).

As for *Vv*DIR25 and *Vv*DIR30, though only two time points were analyzed, a different behaviour seems to occur, especially concerning *Vv*DIR30. Even if *Vv*DIR30 is actually downregulated in inoculated plants when compared to mock samples (-1.46 fold at 4 hpi), both sets of plants (mock and treatment) are apparently following a similar trend, having their *Vv*DIR30 transcript levels increased over time (21.2 and 14.5 fold at 4 hpi respectively, reporting to control plants). Thus, rather than being fungal-induced, *Vv*DIR30 expression is most likely affected by the mechanical wounding inflicted at the time of inoculation. Previous studies performed by Ralph in *Picea* species, showing a rapid and strong accumulation of DIR transcripts in response to wound and stem-boring insects, corroborate this hypothesis [11].

Heterologous expression of candidate *Vv*DIR proteins

As mentioned before, the main motivation behind the previous studies was the identification of candidate *Vv*DIR genes whose products would potentially be involved in alternative DIR-mediated reactions, namely in the stilbenoid biosynthetic pathway. According to our expectations, ideal candidates would be revealed by the expression profile experiments, where the most relevant fungal-induced changes would constitute the main selection criteria for subsequent recombinant expression and activity evaluation. However, given the several limitations and inability to gather all the intended data, no strong candidates were observed. Nevertheless, considering that our initial strategy was already a "shot in the dark", we still decided to select a group of *Vv*DIR proteins for heterologous expression and activity evaluation towards resveratrol. Thus, the selection of *Vv*DIR genes was performed based only on general considerations, such as gene arquitecture, subfamily, presence/absence of signal peptide sequences and glycosylation sites.

So far, all functionally characterized DIR proteins, either pinoresinol- or gossypol-forming, are composed of a single DIR domain, preceded by a signal peptide sequence and several potential glycosylation sites. Assuming that the hypothetical *Vv*DIR mediating the coupling of resveratrol could have a similar arrangement, we excluded *Vv*DIR genes bearing additional domains (*Vv*DIR31, *Vv*DIR34 and *Vv*DIR35). Also, since we were already dealing with proteins of unknown function, the introduction of other uncharacterized domains was not desirable at this point. Analysis of the remaining sequences, regarding signal peptide sequences and potential glycosylation sites, revealed several other *Vv*DIR proteins that we also excluded from the candidates (*Vv*DIR20, *Vv*DIR22, *Vv*DIR24, *Vv*DIR28, *Vv*DIR29, *Vv*DIR32, *Vv*DIR33, *Vv*DIR36, *Vv*DIR37 and *Vv*DIR39), either because they lacked putative glycosylation sites or due the absence of a signal peptide sequence.

Out of the remaining *Vv*DIR, considering their sub-families, detection in woody tissues and response to external factors, we chose four genes as candidates for recombinant expression in *P. pastoris*: *Vv*DIR14, *Vv*DIR25, *Vv*DIR30 and *Vv*DIR42 (Table 9). Both *Vv*DIR25 and *Vv*DIR30 were chosen due to their apparent response to the mechanical wounding during the expression profile assays. With one belonging to DIR-b/d subfamily and the other to DIR-e, we decided to include also a representative for the DIR-g subfamily (*Vv*DIR42), even if the presence of its transcripts has not been confirmed in grapevine trunks. In addition, given its high level of expression in trunks, we also selected *Vv*DIR14 (DIR-b/d) as a candidate for recombinant expression.

Table 9. Candidate *Vv*DIR genes used for recombinant expression in *P. pastoris*.

	ORF lenght (aa)	Signal Peptide[a]	Glycosylation Sites	Native CAI	Optimized CAI	Predicted MW (kDa)[b]
*Vv*DIR14	193	23-24	Asn64*, 76, 134	0.74	0.9	19.2
*Vv*DIR25	187	23-24	Asn44*, 56, 84, 120, 172	0.61	0.88	16.9
*Vv*DIR30	186	25-26	Asn47, 84	0.68	0.88	17.3
*Vv*DIR42	179	26-27	Asn48, 119, 173	0.63	0.9	17.0

a - cleavage site between indicated amino acids.
b - predicted molecular weight without signal peptide sequence and polyhistidine tag.
* - proline residue occurring just after asparagine - unlikely glycosylation.

In view of our previous experience concerning the recombinant expression of *Vv*DIR1 in *P. pastoris*, we evaluated the selected genes for their codon usage frequency in the host organism and optimized all the sequences prior to transformation. Expression cassettes were constructed in a similar manner (α-factor_*Vv*DIR_His-tag) and transformed into *P. pastoris* (strain KM71H). The selected transformants for each *Vv*DIR were screened for the presence of the recombinant protein during a four day induction period (Figure 37). Again, SDS-PAGE analysis did not allow a straightforward detection of the target proteins. Apart from the low quantities usually produced, the size shift due to potential glycosylation was also unknown. In addition, *P. pastoris* native secretome was shown extremely variable, displaying diverse patterns either for the different strains or even for the

same transformant during separate inductions. For these reasons, most of the times, the correct identification of the recombinant protein band in the gel was only achieved with support of western blot analysis.

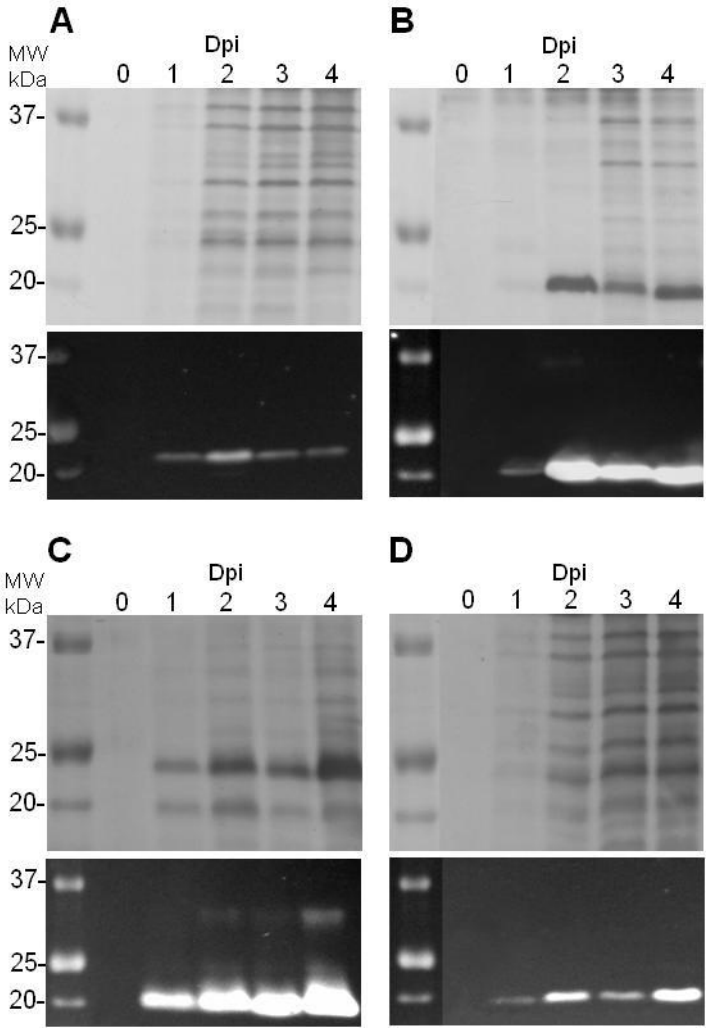

Figure 37. Heterologous expression of (**A**) *Vv*DIR14, (**B**) *Vv*DIR25, (**C**) VvDIR30 and (**D**) *Vv*DIR42 in *P. pastoris* (KM71H strain). SDS-PAGE (silver stained – top) and corresponding immunoblot (anti-His-tag - bottom) analysis of culture supernatants 0 to 4 days post-induction (dpi) using growth conditions for Mut^s phenotype at 28ºC with daily addition of 0.5 % methanol.

As seen in the previous Figure, all four *Vv*DIR proteins were successfully expressed in *P. pastoris,* being detected 24 to 96 h after induction.

However, according to their size in the gel, which corresponds to their predicted molecular weight (accounting for His-tag), they were all mainly produced in their non-glycosylated form. Minimal glycosylation, indicated by the presence of a faint signal between 25 and 37 kDa, was only observed for *Vv*DIR25 at 2 dpi (Fig.37B) and *Vv*DIR30 at 2, 3 and 4 dpi (Fig.37D). According to our initial assumptions, at least for this group of selected proteins, glycosylation would be an essential feature for function. Thus, given the fact that no additional attempts were made to produce *Vv*DIR in the desired form, lack of glycosylation added an inconvenient variable into the study. Nevertheless, an attempt was made to evaluate if the previous recombinant *Vv*DIR would affect *in vitro* oxidative coupling of resveratrol.

Prior to the DIR assays, preliminary resveratrol dimerization reactions, using laccase or peroxidase, were performed based on the ones described in the literature [40,41,43,44]. Reaction parameters, including enzyme and substrate concentrations, as well as reaction times and volumes were adjusted to fit our experimental requirements. Overall, the HPLC profiles of the reaction products (Figure 38) were in accordance with the works reported in literature, with a single major product being observed, presumably a dimer of resveratrol (δ-viniferin). The corresponding peak was isolated and identified as δ-viniferin by NMR analysis and comparison with literature data [52]. As seen in Figure 38, both reactions, peroxidase- and laccase-based, produced comparable HPLC profiles and were used for subsequent experiments involving resveratrol oxidative coupling. Although the peroxidase coupling reactions generated additional products (Figure 38A-square box), they were not identified. According to previous published data on the subject, those could be either trimers or other dimers of resveratrol.

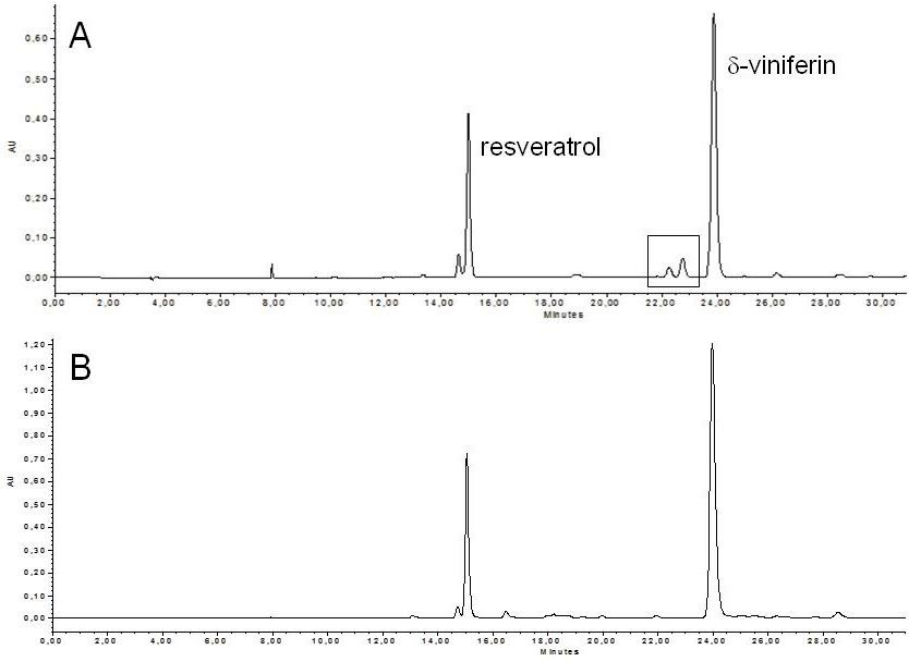

Figure 38. Representative reverse phase HPLC profiles (monitoring at 310 nm) of resveratrol coupling reactions using (**A**) horseradish peroxidase and (**B**) *T. versicolor* laccase. Peaks inside the square box were only observed for the peroxidase assays and were not identified.

The hypothetical effect of the recombinant *Vv*DIR proteins during resveratrol dimerization was evaluated using the laccase-type reactions in the presence of each recombinant protein. The *in vitro* reactions were performed using the total protein from *P. pastoris* culture supernatants. As seen in Figure 39, the HPLC profiles of the reactions show that the recombinant proteins had no effect on the regioselectivity of the oxidative coupling. Invariably, δ-viniferin was the main product being formed, with no other additional compounds being detected (310 nm). The most noticeable effect, and somehow undesirable, was the inhibition of the oxidase activity in the presence of the recombinant protein extracts. Although a quantitative analysis of substrate and product was not performed, a simple visual comparison of the chromatograms evidences the inhibitory effect. This effect was probably caused by insufficient protein

purification prior to the assays. Nevertheless, even in the cases of a low reaction extent, it was clear that an exclusive formation of δ-viniferin occurs.

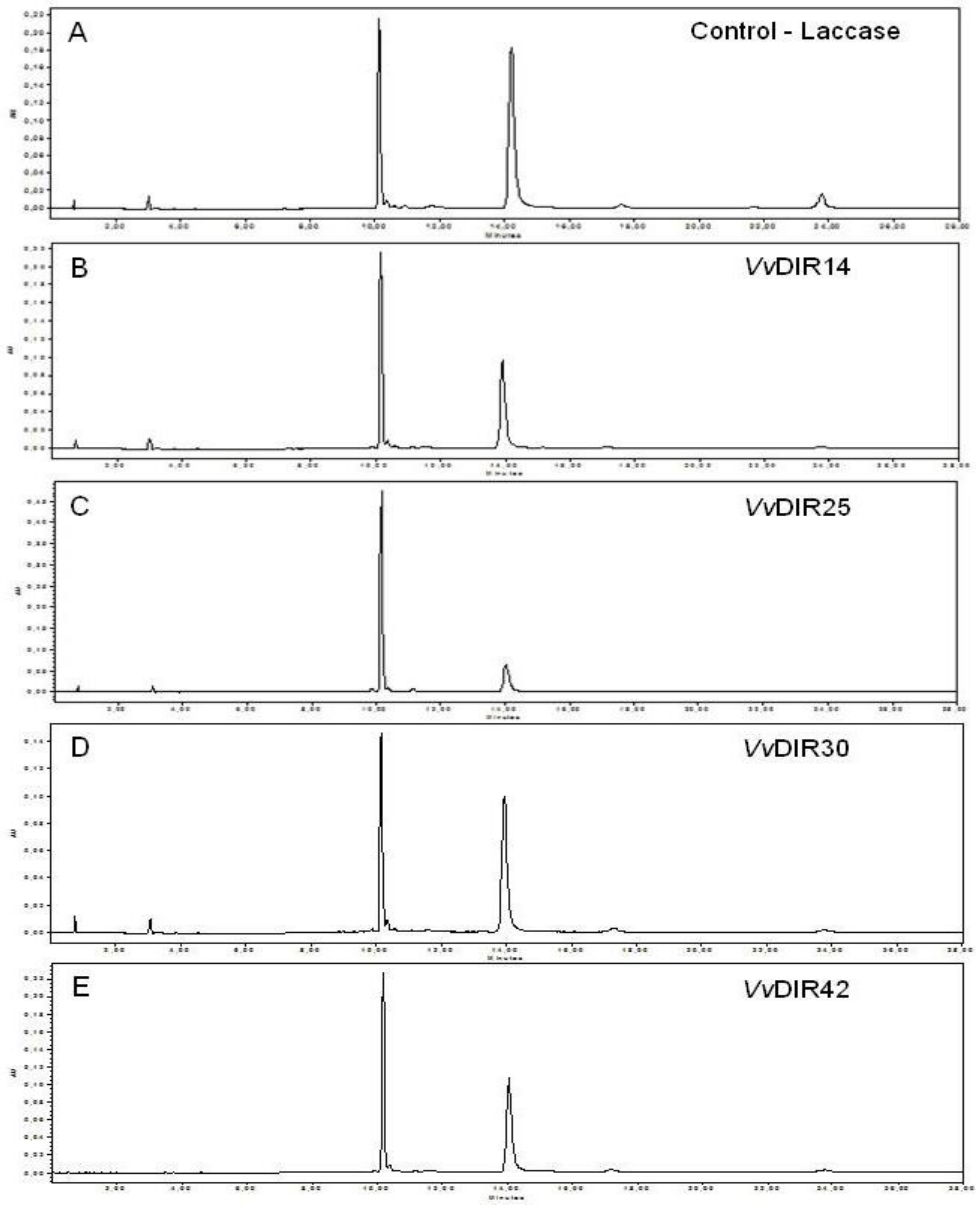

Figure 39. HPLC analysis (monitored at 310 nm) of resveratrol oxidative coupling, using laccase as oxidizing agent, (**A**) in the absence of recombinant protein extracts and in the presence of (**B**) *Vv*DIR14, (**C**) *Vv*DIR25, (**D**) *Vv*DIR30 and (**E**) *Vv*DIR42 recombinant proteins. Reactions were performed using 30 μg of total protein ($V_{reaction}$ = 150 μL) from the *P. pastoris* culture supernatants.

Although δ-viniferin has been reported as a stilbenoid occurring in grapevine (in elicited *callus* or stressed leaves), it is frequently found amongst other resveratrol dimers such as ε-viniferin and pallidol [52-54]. Given that the proposed biosynthetic pathway for those dimers also consists of oxidative dimerization of resveratrol, a coupling control agent must exist in order to determine the preferential formation of one compound over another [41]. Along the hypothesis that DIR proteins may participate in that control, the presence of the "correct" *Vv*DIR during the *in vitro* reactions would result in the formation of additional resveratrol dimers besides δ-viniferin. Unfortunately, this effect was not observed during our present attempt. Excluding possible technical reasons such as low protein concentration or other reaction parameters, additional factors could explain our results: lack of post-translational modifications in the recombinant *Vv*DIR affects their function; *Vv*DIR other than the selected candidates mediate the dimerization of resveratrol; finally, the regioselective control of resveratrol coupling is achieved without the participation of DIR. Further work on this subject will be required in order to confirm or refute our initial hypothesis. In a first step, it would be crucial to optimize the recombinant expression protocol to enhance the production of *Vv*DIR in their glycosylated form.

Despite our strong conviction that the non-glycosylated forms of the recombinant proteins *Vv*DIR14, *Vv*DIR25, *Vv*DIR30 and *Vv*DIR42 were not functional, we performed an additional set of *in vitro* reactions to evaluate the remote possibility of their influence in coniferyl alcohol oxidative coupling. As seen in figure 40, the ratios of the unknown product c and pinoresinol (relative peak areas at 280 nm) were comparable among themselves for all the reactions (control and presence of *Vv*DIR). Although, at first glance, a subtle increase in pinoresinol content seems to occur due to the presence of *Vv*DIR in the reactional mixture, such event was considered negligible. According to our experience, and considering

our rudimentary quantitative analysis procedure, the observed differences lie within the normal variation obtained for control samples.

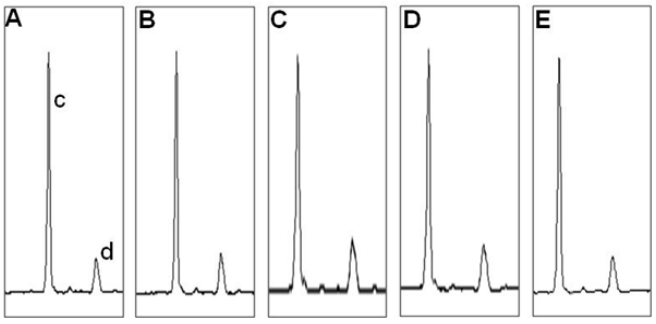

	Ratio (relative peak area at 280 nm)				
product c	81.2 %	78.4 %	76. 2 %	77.6 %	80.4 %
pinoresinol - d	18.8 %	21.6 %	23.8 %	22.4 %	19.6 %

Figure 40. HPLC analysis of coniferyl alcohol *in vitro* coupling products in the (**A**) absence or presence of recombinant protein (**B**) *Vv*DIR14, (**C**) *Vv*DIR25, (**D**) *Vv*DIR30 and (**E**) *Vv*DIR42. Compounds **c** and **d** represent product c and pinoresinol, respectively as in Chapter IV, Figure 26. All reactions were performed using 30 μg of total protein ($V_{reaction}$ = 125 μL) from *P. pastoris* culture supernatants.

Similarly to the previous resveratrol coupling assays, additional work will be required to confirm that the selected *Vv*DIR proteins do not interfere with coniferyl alcohol dimerization. Apart from the above mentioned optimization of yield and glycosylation of the recombinant *Vv*DIR, the development of an accurate quantification method should also be considered. Although the oxidative coupling of coniferyl alcohol is fairly well described in literature, with three main products being formed (dehydrodiconiferyl alcohol, guaiacylglycerol 8-*O*-4'-coniferyl ether and pinoresinol), only two were easily "identified" by HPLC analysis. The correct HPLC peak assignment to each particular product will allow a precise quantification and a better evaluation of product ratio changes hypothetically induced by *Vv*DIR.

*Vv*DIR pursuit in grapevine total protein extracts

Given the numerous adversities encountered in the course of our previous experiments, the following set of experiments was performed using an alternative inverse approach: rather than "guessing" which *Vv*DIR, out of the possible 42, could hypothetically direct resveratrol dimerization, we would look for the presence of the guiding activity in protein extracts.

According to previous reports in the literature, stilbenoids, including viniferins, can be found ubiquitously in most grapevine organs/tissues but are particularly accumulated in woody parts of the plant [55]. ε-Viniferin, for instance, which is not spontaneously formed during a regular phenoxy coupling reaction, can be found as one of the main stilbenoids in grapevine trunks [56,57]. Therefore, wood tissues could be a great starting point for dirigent activity pursuit as they unequivocally present evidence for stereochemical control in resveratrol dimerization. However, protein extraction from tissues highly enriched in phenolic compounds is often a challenging task, as protein oxidation and formation of irreversible linkages with phenolics may interfere with activity and/or cause protein aggregation [58]. For that reason, we first evaluated the possibility of using an alternative tissue as the protein source for the current approach.

According to the works of Douillet-Breuil [59] and Pezet [52], healthy grapevine leaves present only small traces of viniferins which can be significantly induced by UV-C irradiation. Given the easy feasibility of their experimental procedure we reproduced their methodology to confirm and evaluate the suitability of grapevine leaves for the intended experiments. Following UV-C stimulation of grapevine leaves, we performed a simple methanolic extraction of the samples and analyzed the profile of extracted phenolics by HPLC (Figure 41A, B). Simultaneously, for comparison purposes, we also analyzed the phenolic profile of grapevine lignified canes (Figure 41C).

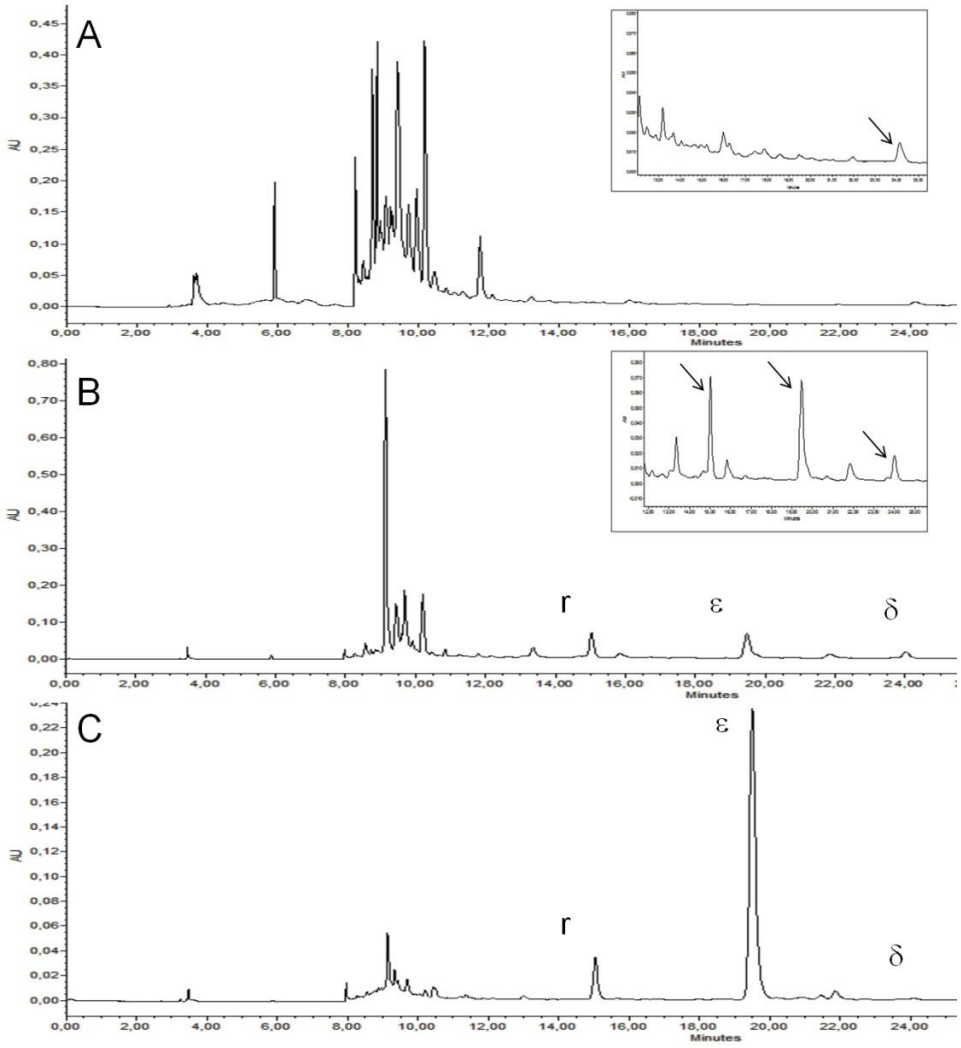

Figure 41. HPLC profile (310 nm) of grapevine methanolic extracts from (**A**) healthy or **(B)** UV-C irradiated leaves and (**C**) lignified canes. Identified metabolites are indicate by r – resveratrol, ε – ε viniferin and δ – δ viniferin with retention times of 15, 19.5 and 24 min, respectively. Inserts: chromatogram magnifications (12 to 26 min) are displayed for A and B with detected products indicated by arrows. Extractions, and HPLC injections for A and B were performed at the same scale.

Despite of our merely comparative analysis, we could confirm the literature reports by observing a UV-C induced production of both resveratrol and viniferins. The presence ε-viniferin was confirmed as the

identified peak in the chromatograms following purification and structure elucidation by NMR analysis.

As seen above, both UV-C induced leaves and canes are able to accumulate ε-viniferin. Although a quantitative analysis was not performed, we can also deduce a higher content of ε-viniferin in the canes when compared to UV-C irradiated leaves (wood methanolic extracts were performed using roughly four times less biological material). However, for the reasons mentioned above, concerning protein extraction issues, our first experiments attempting the detection of a coupling guiding agent were performed using grapevine leaves. Accordingly, total protein extracts from control and UV-C irradiated leaves (using the same experimental conditions as for the methanolic extractions) were obtained and tested for any detectable influence during resveratrol *in vitro* coupling reactions (Figure 42).

Unfortunately, as seen by the presented results, no visible changes were observed in the reaction HPLC profiles caused by the presence of protein extracts from UV-C irradiated leaves. Both control (not shown) and UV-C irradiated samples (20, 100, 500 and 1000 μg) generated profiles comparable to the ones obtained with boiled or no protein extracts. For all the reactions, including controls, a small peak with a retention time similar to the one of ε-viniferin (~19 min) was observed. However, chromophore inspection, as well as the exact retention time, shows that no ε-viniferin was formed during the reaction. Even if it was, its synthesis would not be mediated by the proteins in the extracts.

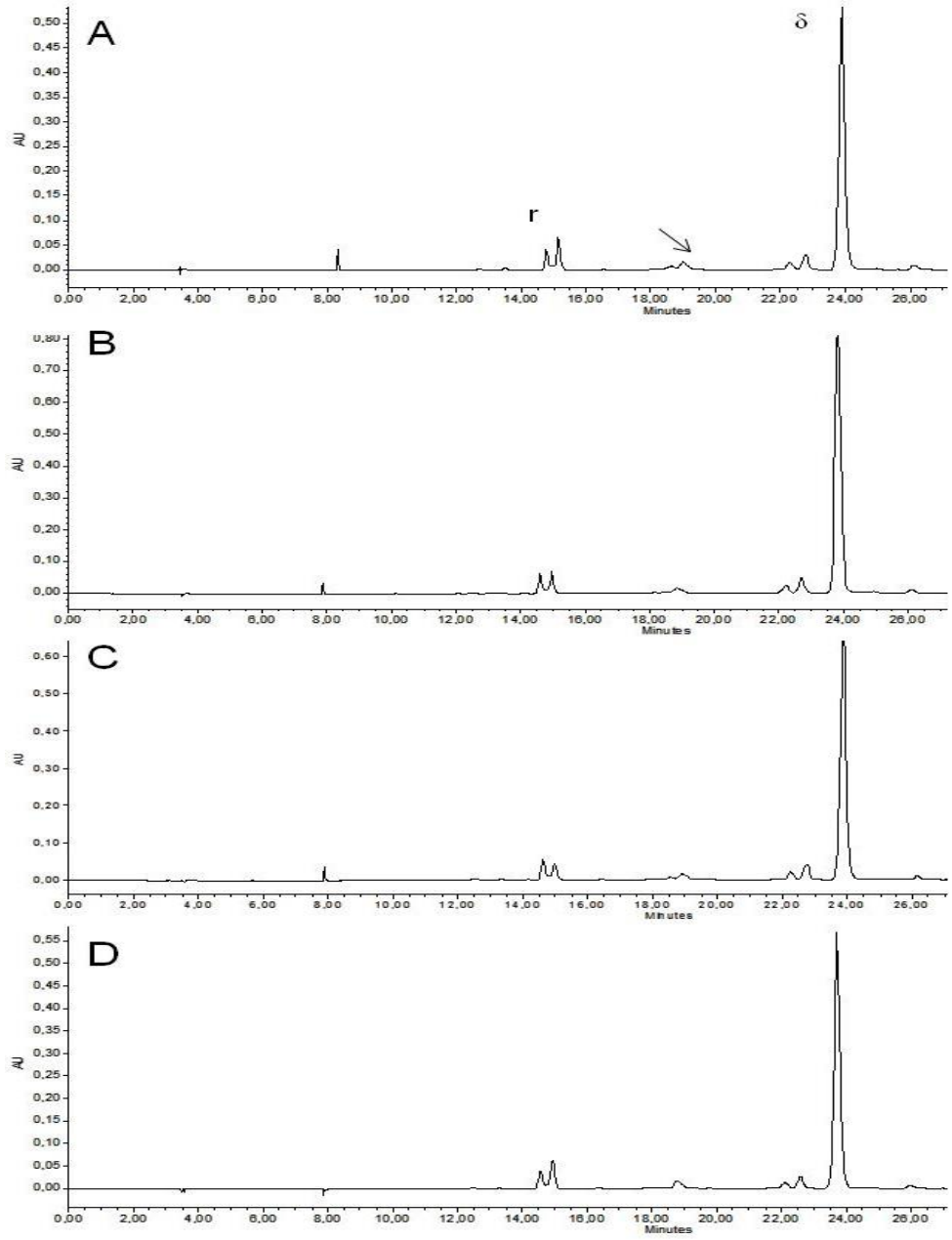

Figure 42. HPLC profile (310 nm) of *in vitro* resveratrol coupling products using peroxidase + H_2O_2 as the oxidizing agent, (**A**) in the absence of grapevine protein extracts; and in the presence of UV-C irradiated leaf extracts (**B**) previously boiled (1 mg), (**C**) 20 μg, (**D**) 1 mg. Chromatograms for 100 and 500 μg of protein extracts are not shown. r- resveratrol, δ – δ-viniferin. Arrow indicates the retention time of ε-viniferin. Reactions were performed in a total volume of 500 μL.

These results were somehow disappointing as we were reasonably confident that the protein extracts (from tissues with previously confirmed guiding ability) would interfere with the regular regiochemistry of the coupling reactions, generating additional products such as ε-viniferin. However, not only was ε-viniferin not detected, as also no additional "encouraging" profile change (even if minor) was observed. Further frustration concerning the previous results arises from the fact that δ-viniferin, though reported as stress inducible by Pezet [52], has not been detected in similar studies performed by Douillet-Breuil [59], Malacarne [60] or Mattivi [53], which suggest that its occurrence under physiological conditions may be unusual.

Given our inability to mimetize the *in vivo* conditions for resveratrol dimerization, at this moment, one can only speculate on the possible factors affecting our experiments: (i) The protein extraction method may not be suitable for the assays either because the target proteins were not extracted or were inactivated (either by manipulation or by the presence of interferents from the extraction buffer); (ii) although a reasonable amount of total protein from leaves was used in the reactions (20 μg to 1 mg per reaction), there is still the possibility that the oxidizing capacity of the external peroxidase can greatly exceed the rate at which a DIR is able to capture resveratrol radicals (assuming *Vv*DIR are involved in the process); (iii) as already mentioned, formation of ε-viniferin may be catalyzed by grapevine proteins other than *Vv*DIR, possibly a specific peroxidase or laccase. In both cases, an alternative extraction protocol must be used as total protein extracts did not display significant oxidase activity.

Additional studies regarding *in vitro* dimerization of resveratrol should account for the previous considerations.

At this point, as a last effort to detect dirigent activity in grapevine protein extracts, we considered our first option and decided to attempt the

analysis of the woody tissues of the plant. Given that our main hypothesis concerned the participation of *Vv*DIR in the oxidative coupling of resveratrol, we adopted a reported protein extraction method previously used to extract the pinoresinol-forming dirigent protein from *Forsythia intermedia* [46]. It comprises three sequential extraction steps in which the last partial extraction yields a fraction (Fc) with the desired *Fi*DIR. Nevertheless, following the extraction protocol, we tested the activity towards resveratrol for all three fractions (Fa, Fb, Fc). While fraction Fc displayed the regular HPLC profile indicating absence of DIR activity, both other fractions, in particular fraction Fa (Figure 43A), showed particularly interesting results, where the coupling reaction seems to be affected to afford additional products (Figure 43B).

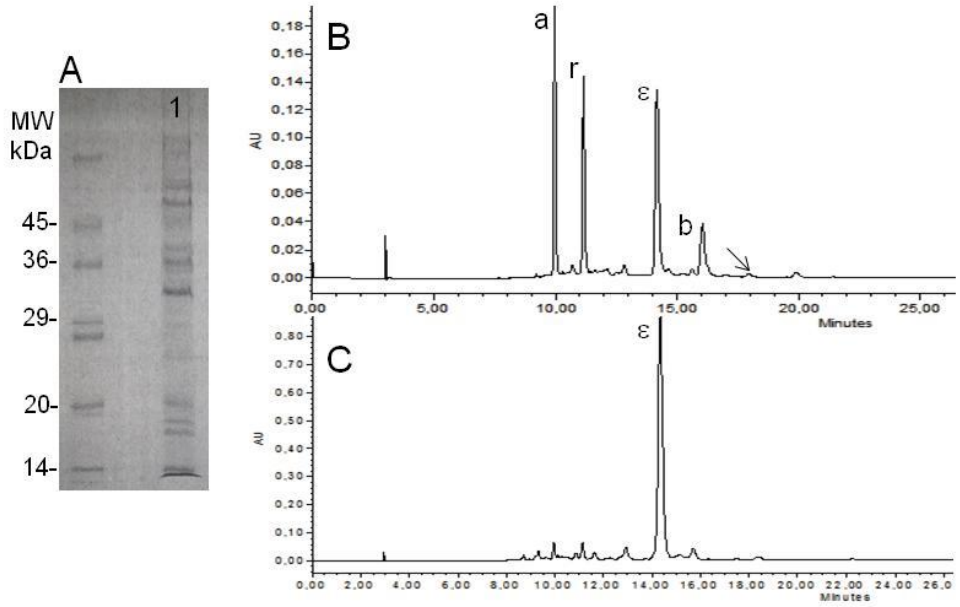

Figure 43. *In vitro* resveratrol coupling reaction in the presence of protein extracts from *V. vinifera* canes. (**A**) Lane 1- SDS-PAGE analysis of the protein extract (Fa) used in the reactional mixtures; (**B**) HPLC profile (310 nm) of resveratrol coupling in the presence of Fa, using laccase as the oxidizing agent: r - resveratrol, ε – ε-viniferin, a – resveratrol dimer, b – uncharacterized product. Arrow indicates the retention time of δ - viniferin. Reaction was performed in a total volume of 300 μL, using 30 μg of protein from fraction Fa; (**C**) HPLC profile (310 nm) of Fa ethyl acetate extraction.

According to our initial observation of the previous results, Fa fraction was apparently able to partially guide the reaction towards the formation of ε-viniferin. In addition, at least two other products (**a** and **b** – Figure 42B) were also be formed. However, during subsequent experiments we could observe that the content of ε-viniferin in the reactional mixtures was not consistent with the extent of the reaction (i.e. remained fairly constant regardless the time of the assay, while product **a** and **b** progressively accumulated). Thus, its presence in the HPLC profiles would likely be an artifact. This was further confirmed by the analysis of the Fa fraction (Figure 43C). As may be seen in the Figure, the HPLC profile of the protein extract alone evidences a reasonably high content of ε-viniferin explaining its detection along with the other resveratrol oxidation products.
Even if these results cannot be easily explained, they provide exciting direct evidence that *in vivo* resveratrol dimerization must be under regioselective control. Although the expected formation of ε-viniferin was not detected, it was interesting to observe that also virtually no δ-viniferin was formed. However, at this point, we cannot attribute the observed "dirigent" activity to the possible presence of a *Vv*DIR in protein extracts. The involvement of a native protein with oxidase activity cannot be excluded. In fact, during additional experiments we have observed that the protein extract itself possessed a reasonably high oxidative capacity and that the addition of the external laccase was irrelevant for the reaction progress and product profile. Thus, the question remains if this event is caused only by a specific oxidase with a regioselective active center or by a combination of both oxidase and *Vv*DIR.
Out of the two unknown products being formed, our first priority went to the identification of product **a** as we initially suspected it could represent an ε-viniferin glucoside. This would explain the high chomophore similarity between the two compounds as well as the retention time shift (increased polarity). Also, assuming extinction coefficients of similar magnitude,

product **a** was apparently being formed in higher amounts. If the presence of an ε-viniferin glucoside was confirmed, in theory, it would also imply the presence of the guiding agent responsible for the formation of the dimer, ε-viniferin.

The unknown compound was isolated by HPLC and its structure was elucidated by one- and two-dimensional NMR experiments, followed by ESI-MS (Figure 44). As observed, according to our experimental data and proposed structure, the unknown product **a** is indeed a dimer of resveratrol, but is neither a glucoside nor structurally similar to ε-viniferin. Instead, it is a symmetric resveratrol dimer, to our knowledge never described before.

	^{1}H (600 MHz)		^{13}C (150 MHz)
H/C	δ(ppm)	*J* (Hz)	δ(ppm)
1/1'	-	-	141.3
2,6/2´,6'	6.45 d	2.1	105.7
3,5/3',5'	-	-	159.6
4			102.8
4''	6.18 t	2.1	102.5
7			127
7'	6.91 d	16.3	126.9
8			129.7
8'	6.77 d	16.1	129.6
9,11/9',11'	-	-	131.1
10			113.8
10'	7	2	113.7
12	-	-	146.5
13			116.5
13'	6.76 d	8.2	116.4
14			120.2
14'	6.85 dd	8.2, 2.0	120.1

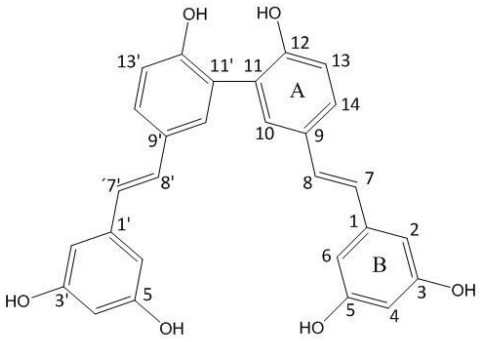

ESI-MS, *m/z*: 455.15 $[M+H]^+$

Figure 44. Structure elucidation of compound **a** (as in Figure 43).NMR data and C-H correlations as inferred from HSQC and HMBC experiments (on the left) and proposed structure supported by ESI-MS data (on the right).

The aromatic proton signals of the new compound resemble those of resveratrol. From the comparative analysis of the ^{1}H-NMR spectra of the two compounds, the aromatic proton signals of the phenyl ring B are present in both (6.45 (d, J=2.1 Hz, 2H); 6.18 (t, J=2.1 Hz)). The same is

verified for the double bond moiety (6.91 (d, J=16.3 Hz); 6.77 (d, J=16.1 Hz)). For the phenyl ring A the patterns are different. The two doublets of the aromatic protons of resveratrol at the correspondent positions C-10, C-11, C-13 and C-14 are absent and instead a trisubstituted phenyl system is present (7.00 (d, J=2.0 Hz); 6.85 (dd, J=8.2 Hz, J=2.0 Hz); 6.76 (d, J=8.2 Hz)). This indicates that the dimer of resveratrol has been formed through the establishment of a C-C bond assigned to C-11 and C-11' of each moiety of the proposed structure. This assignment is based on the correlation found in HMBC spectrum between C-9/H-13, C-12/H-10 and C-14/H-10. The new structure is highly symmetric so that the ^{1}H NMR shows the same chemical shifts for equivalent protons of each monomer. In the ^{13}C NMR this equivalence is not observed for all carbon atoms as described in the spectrum assignment. The presence of a dimer was supported by ESI-MS (*m/z*: 455.15 $[M+H]^+$ (calc. $C_{28}H_{22}O_6$455.14) confirming the molecular formula of the unknown compound. These data allowed elucidating the structure of this new molecule never published before.

Given the much attention resveratrol and other stilbene derivatives have had during the last decade, it is somehow intriguing that this symmetric dimer has never been reported before. A possible explanation for this fact is that this metabolite could serve as a transient precursor for other metabolites, being rapidly depleted upon its formation. In that case, the substrate should undergo significant structural modifications during the enzymatic reaction as similar structures are also not reported. Another possibility is that this compound is not "supposed" to occur *in vivo* and the proteins responsible for the dimerization *in vitro*, under physiological conditions, are well compartmentalized and not allowed to interact with the unspecific substrate, resveratrol. In any case, further investigation is necessary.

Elucidation of this mechanism of synthesis as well as of other by which stilbenoid metabolites are produced *in vivo* might prove of great importance not only for an improved knowledge of plant defence metabolism, but also for other research areas in the field of human health or chemical synthesis.

References

1. Davin LB, Lewis NG (2000) Dirigent proteins and dirigent sites explain the mystery of specificity of radical precursor coupling in lignan and lignin biosynthesis. Plant Physiology 123: 453-462.
2. Leffingwell JC (2003) Chirality & Bioactivity I.: Pharmacology. Leffingwell Reports 3.
3. Mori K (2011) Bioactive natural products and chirality. Chirality 23: 449-462.
4. Dewick PM (2009) Secondary metabolism: The building blocks and construction mechanisms. Medicinal natural products: John Wiley & Sons, Ltd. pp. 7-38.
5. Petersen M, Hans J, Matern U (2010) Biosynthesis of phenylpropanoids and related compounds. Annual Plant Reviews Volume 40: Biochemistry of Plant Secondary Metabolism: Wiley-Blackwell. pp. 182-257.
6. Barceló AR, Ros LVG, Carrasco AE (2007) Looking for syringyl peroxidases. Trends in Plant Science 12: 486-491.
7. Ralph J, Lundquist K, Brunow G, Lu F, Kim H, et al. (2004) Lignins: Natural polymers from oxidative coupling of 4-hydroxyphenyl-propanoids. Phytochemistry Reviews 3: 29-60.
8. Davin LB, Wang HB, Crowell AL, Bedgar DL, Martin DM, et al. (1997) Stereoselective bimolecular phenoxy radical coupling by an auxiliary (dirigent) protein without an active center. Science 275: 362-366.
9. Kim M, Jeon J-H, Fujita M, Davin L, Lewis N (2002) The western red cedar (*Thuja plicata*) 8-8′ DIRIGENT family displays diverse expression patterns and conserved monolignol coupling specificity. Plant Molecular Biology 49: 199-214.

10. Pickel B, Schaller A (2013) Dirigent proteins: molecular characteristics and potential biotechnological applications. Applied Microbiology and Biotechnology 97: 8427-8438.
11. Ralph S, Park J-Y, Bohlmann J, Mansfield S (2006) Dirigent proteins in conifer defense: gene discovery, phylogeny, and differential wound- and insect-induced expression of a family of DIR and DIR-like genes in spruce (*Picea* spp.). Plant Molecular Biology 60: 21-40.
12. Ralph SG, Jancsik S, Bohlmann J (2007) Dirigent proteins in conifer defense II: Extended gene discovery, phylogeny, and constitutive and stress-induced gene expression in spruce (*Picea* spp.). Phytochemistry 68: 1975-1991.
13. Kim K-W, Moinuddin SGA, Atwell KM, Costa MA, Davin LB, et al. (2012) Opposite stereoselectivities of dirigent proteins in *Arabidopsis* and *Schizandra* species. Journal of Biological Chemistry 287: 33957-33972.
14. Liu J, Stipanovic RD, Bell AA, Puckhaber LS, Magill CW (2008) Stereoselective coupling of hemigossypol to form (+)-gossypol in moco cotton is mediated by a dirigent protein. Phytochemistry 69: 3038-3042.
15. Jin-long G, Li-ping X, Jing-ping F, Ya-chun S, Hua-ying F, et al. (2012) A novel dirigent protein gene with highly stem-specific expression from sugarcane, response to drought, salt and oxidative stresses. Plant Cell Reports 31: 1801-1812.
16. Wu R, Wang L, Wang Z, Shang H, Liu X, et al. (2009) Cloning and expression analysis of a dirigent protein gene from the resurrection plant *Boea hygrometrica*. Progress in Natural Science 19: 347-352.
17. Zhu L, Zhang X, Tu L, Zeng F, Nie Y (2007) Isolation and characterization of two novel dirigent-like genes highly induced in cotton (*Gossypium barbadense* and *G. hirsutum*) after infection by *Verticillium dahliae*. Journal of Plant Pathology 89: 41-45.
18. Borges AF, Ferreira RB, Monteiro S (2013) Transcriptomic changes following the compatible interaction *Vitis vinifera-Erysiphe necator*. Paving the way towards an enantioselective role in plant defence modulation. Plant Physiology Biochemistry 68: 71-80.
19. Fung RWM, Gonzalo M, Fekete C, Kovacs LG, He Y, et al. (2008) Powdery mildew induces defense-oriented reprogramming of the transcriptome in a susceptible but not in a resistant grapevine. Plant Physiology 146: 236-249.

20. Konno C, Xue H-Z, Lu Z-Z, Ma B-X, Erdelmeier CAJ, et al. (1989) 1-Aryl tetralin lignans from *Larrea tridentata*. Journal of Natural Products 52: 1113-1117.
21. Moinuddin SGA, Hishiyama S, Cho M-H, Davin LB, Lewis NG (2003) Synthesis and chiral HPLC analysis of the dibenzyltetrahydrofuran lignans, larreatricins, 8'-epi-larreatricins, 3,3'-didemethoxyverrucosins and meso-3,3'-didemethoxynectandrin B in the creosote bush (*Larrea tridentata*): evidence for regiospecific control of coupling. Organic & Biomolecular Chemistry 1: 2307-2313.
22. Lourith N, Katayama T, Ishikawa K, Suzuki T (2005) Biosynthesis of a syringyl 8-O-4′ neolignan in Eucommia ulmoides: formation of syringylglycerol-8-O-4′-(sinapyl alcohol) ether from sinapyl alcohol. Journal of Wood Science 51: 379-386.
23. Lourith N, Katayama T, Suzuki T (2005) Stereochemistry and biosynthesis of 8-O-4′ neolignans in *Eucommia ulmoides*: diastereoselective formation of guaiacylglycerol-8-O-4′-(sinapyl alcohol) ether. Journal of Wood Science 51: 370-378.
24. Katayama T, Ogaki A (2001) Biosynthesis of (+)-syringaresinol in *Liriodendron tulipifera* I: feeding experiments with *L*-[U-^{14}C]phenylalanine and [8-^{14}C]sinapyl alcohol. Journal of Wood Science 47: 41-47.
25. Davin LB, Wang C-Z, Helms GL, Lewis NG (2003) [^{13}C]-Specific labeling of 8–2′ linked (−)-cis-blechnic, (−)-trans-blechnic and (−)-brainic acids in the fern *Blechnum spicant*. Phytochemistry 62: 501-511.
26. Suzuki S, Yamamura M, Shimada M, Umezawa T (2004) A heartwood norlignan, (E)-hinokiresinol, is formed from 4-coumaryl 4-coumarate by a *Cryptomeria japonica* enzyme preparation. Chemical Communications: 2838-2839.
27. Pezet R, Gindro K, Viret O, Spring JL (2004) Glycosylation and oxidative dimerization of resveratrol are respectively associated to sensitivity and resistance of grapevine cultivars to downy mildew. Physiological and Molecular Plant Pathology 65: 297-303.
28. Packter NM (1995) Biochemistry of stilbenoids: By J Gorham (with contributions by M Tori and Y Asakawa). pp 262. Chapman & Hall, London. 1995. Biochemical Education 23: 179-179.
29. Chong J, Poutaraud A, Hugueney P (2009) Metabolism and roles of stilbenes in plants. Plant Science 177: 143-155.

30. Schöppner A, Kindl H (1984) Purification and properties of a stilbene synthase from induced cell suspension cultures of peanut. Journal of Biological Chemistry 259: 6806-6811.
31. Fliegmann J, Schröder G, Schanz S, Britsch L, Schröder J (1992) Molecular analysis of chalcone and dihydropinosylvin synthase from Scots pine (*Pinus sylvestris*), and differential regulation of these and related enzyme activities in stressed plants. Plant Molecular Biology 18: 489-503.
32. Raiber S, Schröder G, Schröder J (1995) Molecular and enzymatic characterization of two stilbene synthases from Eastern white pine (*Pinus strobus*). A single Arg/His difference determines the activity and the pH dependence of the enzymes. FEBS Letters 361: 299-302.
33. Riviere C, Pawlus AD, Merillon J-M (2012) Natural stilbenoids: distribution in the plant kingdom and chemotaxonomic interest in *Vitaceae*. Natural Product Reports 29: 1317-1333.
34. Xiao K, Zhang H-J, Xuan L-J, Zhang J, Xu Y-M, et al. (2008) Stilbenoids: Chemistry and bioactivities. In: Atta ur R, editor. Studies in natural products chemistry: Elsevier. pp. 453-646.
35. Shen T, Wang X-N, Lou H-X (2009) Natural stilbenes: an overview. Natural Product Reports 26: 916-935.
36. Ito T, Abe N, Oyama M, Iinuma M (2009) Absolute structures of C-glucosides of resveratrol oligomers from *Shorea uliginosa*. Tetrahedron Letters 50: 2516-2520.
37. Kurihara H, Kawabata J, Ichikawa S, Mizutani J (1990) (−)-ε-Viniferin and related oligostilbenes from *Carex pumita* Thunb. (*Gyperaceae*). Agricultural and Biological Chemistry 54: 1097-1099.
38. Langcake P, Pryce RJ (1977) Oxidative dimerisation of 4-hydroxystilbenes in vitro: production of a grapevine phytoalexin mimic. Journal of the Chemical Society, Chemical Communications: 208-210.
39. Pezet R, Pont V, Hoang-Van K (1991) Evidence of oxidative detoxication of pterostilbene and resveratrol by a laccase-like stilbene oxidase produced by *Botrytis cinerea*. Physiological and Molecular Plant Pathology 39: 441-450.
40. Nicotra S, Cramarossa MR, Mucci A, Pagnoni UM, Riva S, et al. (2004) Biotransformation of resveratrol: synthesis of trans-dehydrodimers catalyzed by laccases from Myceliophtora

thermophyla and from *Trametes pubescens*. Tetrahedron 60: 595-600.

41. Takaya Y, Terashima K, Ito J, He Y-H, Tateoka M, et al. (2005) Biomimic transformation of resveratrol. Tetrahedron 61: 10285-10290.
42. Ponzoni C, Beneventi E, Cramarossa MR, Raimondi S, Trevisi G, et al. (2007) Laccase-catalyzed dimerization of hydroxystilbenes. Advanced Synthesis & Catalysis 349: 1497-1506.
43. Wilkens A, Paulsen J, Wray V, Winterhalter P (2010) Structures of two novel trimeric stilbenes obtained by horseradish peroxidase catalyzed biotransformation of trans-resveratrol and (−)-ε-viniferin. Journal Agricultural and Food Chemistry 58: 6754-6761.
44. Yu B-B, Han X-Z, Lou H-X (2007) Oligomers of resveratrol and ferulic acid prepared by peroxidase-catalyzed oxidation and their protective effects on cardiac injury. Journal of Agricultural and Food Chemistry 55: 7753-7757.
45. Pawlus AD, Waffo-Téguo P, Shaver J, Mérillon J (2012) Stilbenoid chemistry from wine and the genus *Vitis*, a review. Journal International des Sciences de la Vigne et du Vin 46.
46. Halls SC, Lewis NG (2002) Secondary and quaternary structures of the (+)-pinoresinol-forming dirigent protein. Biochemistry 41: 9455-9461.
47. Kim MK, Jeon J-H, Davin LB, Lewis NG (2002) Monolignol radical–radical coupling networks in western red cedar and *Arabidopsis* and their evolutionary implications. Phytochemistry 61: 311-322.
48. Lima MM, Ferreres F, Dias AP (2012) Response of *Vitis vinifera* cell cultures to *Phaeomoniella chlamydospora*: changes in phenolic production, oxidative state and expression of defence-related genes. European Journal of Plant Pathology 132: 133-146.
49. Amalfitano C, Agrelli D, Arrigo A, Mugnai L, Surico G, et al. (2011) Stilbene polyphenols in the brown red wood of *Vitis vinifera* cv. Sangiovese affected by "esca proper". Phytopathologia Mediterranea [S.I.]: 224-235
50. Martin N, Vesentini D, Rego C, Monteiro S, Oliveira H, et al. (2009) *Phaeomoniella chlamydospora* infection induces changes in phenolic compounds content in *Vitis vinifera*. Phytopathologia Mediterranea 48: 101-116.
51. Landi L, Murolo S, Romanazzi G (2012) Colonization of *Vitis* spp. wood by sGFP-transformed *Phaeomoniella chlamydospora*, a

tracheomycotic fungus involved in esca disease. Phytopathology 102: 290-297.
52. Pezet R, Perret C, Jean-Denis JB, Tabacchi R, Gindro K, et al. (2003) Delta-viniferin, a resveratrol dehydrodimer: one of the major stilbenes synthesized by stressed grapevine leaves. Journal of Agricultural and Food Chemistry 51: 5488-5492.
53. Mattivi F, Vrhovsek U, Malacarne G, Masuero D, Zulini L, et al. (2011) Profiling of resveratrol oligomers, important stress metabolites, accumulating in the leaves of hybrid *Vitis vinifera* (Merzling × Teroldego) genotypes infected with *Plasmopara viticola*. Journal of Agricultural and Food Chemistry 59: 5364-5375.
54. Santamaria AR, Mulinacci N, Valletta A, Innocenti M, Pasqua G (2011) Effects of elicitors on the production of resveratrol and viniferins in cell cultures of *Vitis vinifera* L. cv Italia. Journal of Agricultural and Food Chemistry 59: 9094-9101.
55. Vergara C, von Baer D, Mardones C, Wilkens A, Wernekinck K, et al. (2011) Stilbene levels in grape cane of different cultivars in southern Chile: Determination by HPLC-DAD-MS/MS method. Journal of Agricultural and Food Chemistry 60: 929-933.
56. Rayne S, Karacabey E, Mazza G (2008) Grape cane waste as a source of trans-resveratrol and trans-viniferin: High-value phytochemicals with medicinal and anti-phytopathogenic applications. Industrial Crops and Products 27: 335-340.
57. Lambert C, Richard T, Renouf E, Bisson J, Waffo-Téguo P, et al. (2013) Comparative analyses of stilbenoids in canes of major *Vitis vinifera* L. cultivars. Journal of Agricultural and Food Chemistry 61: 11392-11399.
58. Pierpoint W (2004) The extraction of enzymes from plant tissues rich in phenolic compounds. In: Cutler P, editor. Protein purification protocols: Humana Press. pp. 65-74.
59. Douillet-Breuil A-C, Jeandet P, Adrian M, Bessis R (1999) Changes in the phytoalexin content of various *Vitis* Spp. in response to ultraviolet C elicitation. Journal of Agricultural and Food Chemistry 47: 4456-4461.
60. Malacarne G, Vrhovsek U, Zulini L, Cestaro A, Stefanini M, et al. (2011) Resistance to *Plasmopara viticola* in a grapevine segregating population is associated with stilbenoid accumulation and with specific host transcriptional responses. BMC Plant Biology 11: 114-114.

Chapter VI: Antimicrobial Activity of *V. vinifera* Methanolic Extracts and Individual Phenolic compounds

This chapter presents unpublished data

Author contribution:

AFB performed all the experimental work.

Abstract

Plants and their extracts have long been used for medicinal purposes due to their wide range of bioactivities. Among the species of interest, *Vitis vinifera* has deserved particular attention especially due to its high content in phenolic compounds. Among others, those compounds can display a significant antimicrobial activity. In this study, we evaluated the antimicrobial activity of methanolic extracts from grapevine canes against two grapevine wood colonizing fungal pathogens (*P. chlamydospora* and *P. aleophillum*). No growth inhibition was observed for either fungus at the tested concentration. Those extracts were also tested for antibacterial activity against human pathogenic bacteria (*P. aeruginosa*, *E. coli*, *S. enteritidis*, *K. pneumonia*, *P. mirabilis*, *L. monocytogenes*, *S. aureus*, *B. subtilis* and *E. faecalis*). In addition, twelve isolated phenolic compounds, hydroxycinnamic and stilbene derivatives, either naturally occurring in plants or chemically synthesised, were studied. Only gram-positive bacteria were susceptible to methanolic extracts and to 4 isolated stilbenoids (resveratrol, δ-viniferin, ε-viniferin and a synthetic resveratrol *O*-methylated dimer). A MIC value of 780 μg/mL was obtained for the methanolic extract against all the gram-positive bacteria. Out of the four active stilbenoids, δ-viniferin displays the highest toxicity against the tested microorganisms with a MIC of 2.9 μg/mL for all the tested bacteria while resveratrol is the least potent compound (MIC values ranging 94 and 375 μg/mL), indicating that dimerisation enhances its antimicrobial properties. The high toxicity displayed by both δ-viniferin and ε-viniferin evidences a great potential for their use as alternatives to the current antibiotics.

Introduction

The plant kingdom is well known for its superior production of chemical compounds, synthesizing a vast array of natural products with potential bioactive properties. Medicinal properties of plants have long been explored, dating from the existence of ancient civilizations to the present days [1,2]. Most of the bioactive compounds in plants are secondary metabolites which are produced by the host organism to cope with a number of external aggressions [3]. Belonging to several distinct classes such as phenolics, flavonoids, alkaloids, terpenoids and others, many thousands of secondary metabolites have been isolated so far. However, current estimates suggest that those may only represent a small fraction of nature's diversity, with potential hundreds of thousands of unknown compounds remaining to be discovered [4-6]. Thus, plant secondary metabolism still remains as large reservoir of chemical structures with promising applications in the areas of drug development [7]. Moreover, given the defence-oriented synthesis of these compounds, they can also represent viable alternatives to the use of chemical pesticides in agriculture [8,9].

Among the species of interest, *Vitis vinifera* has deserved particular attention especially due to its high content in phenolic compounds which are often associated to health benefits. These include, among others, anti-inflammatory, antioxidant, anticancer and antimicrobial activities [10]. Although a few studies exist on the bioactivity of grapevine extracts or isolated compounds, most were performed in fruits, including skins or seeds, wine and leaves [10,11]. Even if some active compounds are shared between the several parts of the plant, whole extracts of the woody tissues have not been studied in much detail. Recently, Schnee and colleagues have reported the antifungal activity of methanolic and ethanolic extracts from grapevine canes against three important pathogens in viticulture (*Erysiphe necator*, *Plasmopara viticola* and

Botrytis cinerea) [12]. In the present study, we evaluated the potential bioactivity of methanolic extracts from grapevine canes against two additional grapevine pathogens, *Phaeomoniella chlamydospora* and *Phaeoacremonium aleophilum*. The same extracts were also evaluated for antibacterial activity against human pathogenic bacteria. In addition, pure and structurally related phenolic compounds were tested. Some of those are naturally occurring metabolites, whereas others were chemically synthesized.

Materials and Methods

Microbial strains and growth conditions

Plant pathogenic fungi *P. chlamydospora* and *P. aleophilum* were obtained from *Laboratório de Patologia Vegetal Veríssimo de Almeida* (LPVVA-ISA) and maintained in Potato Dextrose Agar (PDA) media at 25ºC.

Human pathogenic bacteria were obtained from *Consumo Em Verde*, S.A. (CEV) collection. The species used in this study were *Pseudomonas aeruginosa*, *Escherichia coli* O157, *Salmonella enteritidis*, *Klebsiella pneumonia*, *Proteus mirabilis*, *Listeria monocytogenes*, *Staphylococcus aureus*, *Bacillus subtilis* and *Enterococcus faecalis*. All bacteria were maintained in Mueller-Hinton Agar media (MHA) at 35ºC.

Inoculum preparation

A cell/spore suspension was prepared in saline solution (0,9% NaCl-containing 0.5% Tween-20 for spores) with approximately 1 x 10^8 cells/mL (OD_{550nm} = 0,15) or 0,4 to 5 x 10^6 spores/mL. The suspension was diluted 50 fold and 100 fold in double strength appropriate culture media for bacteria and fungal spores, respectively.

Agar well diffusion assays

Petri dishes containing 1% agar media (selected according to the organism under study) were evenly inoculated with the previously prepared inocula using a cotton swab. A cork-borer (7 mm diameter) was used to make the agar wells in which the extracts/compounds were placed (50 μL). Cultures were incubated at 25 ºC during 2 to 4 days for fungal spores and at 37 ºC during 24 h for bacteria. After the incubation period the inhibition zones were measured. MICs (minimum inhibitory concentration) were determined as the zero intercept of a linear regression of the squared size of the inhibition zone plotted against the logarithm of concentration. Assays were performed in triplicate using three different concentrations.

Microdilution assays

A two-fold serial dilution was performed for each compound in 96-well microplates. The compounds were diluted up to 12 times in water. An equal volume of the previously prepared double strength inoculated media was added to each well. Plates were incubated at 35 ºC for 24 h and analysed for microbial growth. MICs were determined as the lowest concentration at which no visible growth was observed. Assays were performed in triplicate.

Methanolic extracts and phenolic compounds

Grapevine cane methanolic extracts were performed as previously described in chapter V. Following extraction, samples were evaporated to dryness and resuspended in dimethyl sulfoxide (DMSO). Initial activity screening was performed at a concentration of 25 mg/mL.

Individual phenolic compounds were screened at 1 mg/mL. Resveratrol was purchased from Extrasynthese. ε-Viniferin and F4peak1 (unidentified

flavonoid glycoside) were isolated from cane methanolic extracts. δ-Viniferin was produced from enzymatic dimerization of resveratrol. All the remaining compounds were obtained as synthetic compounds from the Organic Chemistry Group at FCT/UNL.

Results and discussion

Antimicrobial activity of *V. vinifera* cane extracts

Methanolic extracts from *V. vinifera* canes were tested for antimicrobial activity against two wood colonizing fungi (*P. chlamydospora* and *P. aleophilum*) and two human pathogenic bacteria (*S. aureus* and *P. aeruginosa*) using agar well diffusion assays (Figure 45).

As seen in the Figure, for both fungi no growth inhibition was observed (Figure 45A, B). In a sense, with grapevine wood being their natural habitat, we would anticipate that both fungi displayed a certain tolerance to the extracts. However, total lack of extract activity, especially at such high concentrations, was not expected. Although unpredicted by us, such tolerance can somehow be supported by the results obtained by Lambert and colleagues [13], who tested the bioactivity of several phenolic compounds encountered in wood against a group of wood colonizing fungi. None of the molecules inhibited *P. aleophilum* and only trans-pterostilbene significantly affected the growth of *P. chlamydospora.* At the same time, *p*-coumaric acid and epicatechin-gallate induced the growth of *P. aleophilum* and *P. chlamydospora*, respectively. A complete characterization of our extract would be required for a comprehensive comparison. Nevertheless, neither resveratrol nor ε-viniferin, whose presence was confirmed in the extracts, had any effect on both fungi.

For the human pathogenic bacteria, preliminary experiments were performed using only *S. aureus* and *P. aeruginosa* as representative species of gram-positive and -negative bacteria, respectively (Figure 45 C,

D). Only *S. aureus* was susceptible to the methanolic extract. *P. aeruginosa* small inhibition zone was comparable to the control (DMSO). This differential susceptibility is in line with the well-known fact that gram-negative bacteria are generally more resistant to antimicrobial agents. Higher tolerance of gram-negative bacteria is mainly attributed to the presence of the outer membrane, which constitutes an active barrier against antibiotic compounds [14]. A similar trend can also be observed in other works in the literature, where grapevine extracts from seeds, wine and leaves were evaluated [15-17].

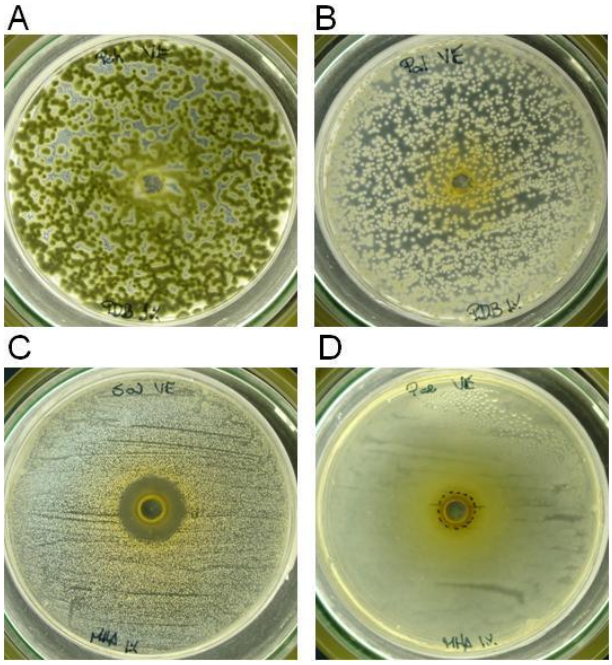

Figure 45. Antimicrobial effect of *V. vinifera* methanolic extracts from canes at 25 mg/mL in DMSO using agar well diffusion method. (**A**) *P. chlamydospora*, (**B**) *P. aleophilum*, (**C**) *S. aureus*, (**D**) *P. aeruginosa*.

As a first attempt to quantify the inhibitory effect of the previous extract, we used the agar well diffusion method to determine MIC values in solid media against different microorganisms. Given the reduced sensitivity of *P. aeruginosa*, only gram-positive bacteria were assayed (*B. subtilis*, *L. monocytogenes E. faecalis* and *S.aureus*). In addition to the extract, we

also determined the MIC values for resveratrol (as positive control and an active constituent of the extract). Determined MIC values are shown in Table 10.

Table 10. MIC values for *V. vinifera* cane methanolic extracts and resveratrol.

MIC (mg/mL)	*B. subtilis*	*L. monocytogenes*	*E. faecalis*	*S. aureus*
Methanol extract	4.31	13.04	10.1	6.26
Resveratrol	1.27	nd	nd	0.7

nd – not determined

According to our results, *B. subtilis* and *S. aureus* were the most susceptible organisms to both methanolic extracts and resveratrol. Resveratrol MIC values could not be determined for *L. monocytogenes* and *E. faecalis* due to the reduced concentration range chosen for the test. As for the methanolic extracts, these organisms exhibited a higher tolerance to resveratrol than *B. subtilis* and *S. aureus*. Though we were able to quantify the inhibitory effect of methanolic extracts (and resveratrol), subsequent assays have demonstrated the lack of reproducibility of this method. Additional well diffusion experiments for both “compounds” have generated fairly different results. This may be explained by solubility and diffusion problems encountered during the assay. Taking this into consideration, for the following tests, the well diffusion assay was only used as an initial screening tool.

Antimicrobial activity of isolated phenolic compounds

Following assays focused on individual phenolic compounds (Figure 46). The majority of the studied compounds were chemically synthesised but commonly occur in plants and could possibly integrate the previously studied methanolic extracts. Most of them are structurally related, being hydroxycinnamic or stilbene derivatives, either in their monomeric or dimeric form. A pentamer of coniferyl alcohol was also studied [18].

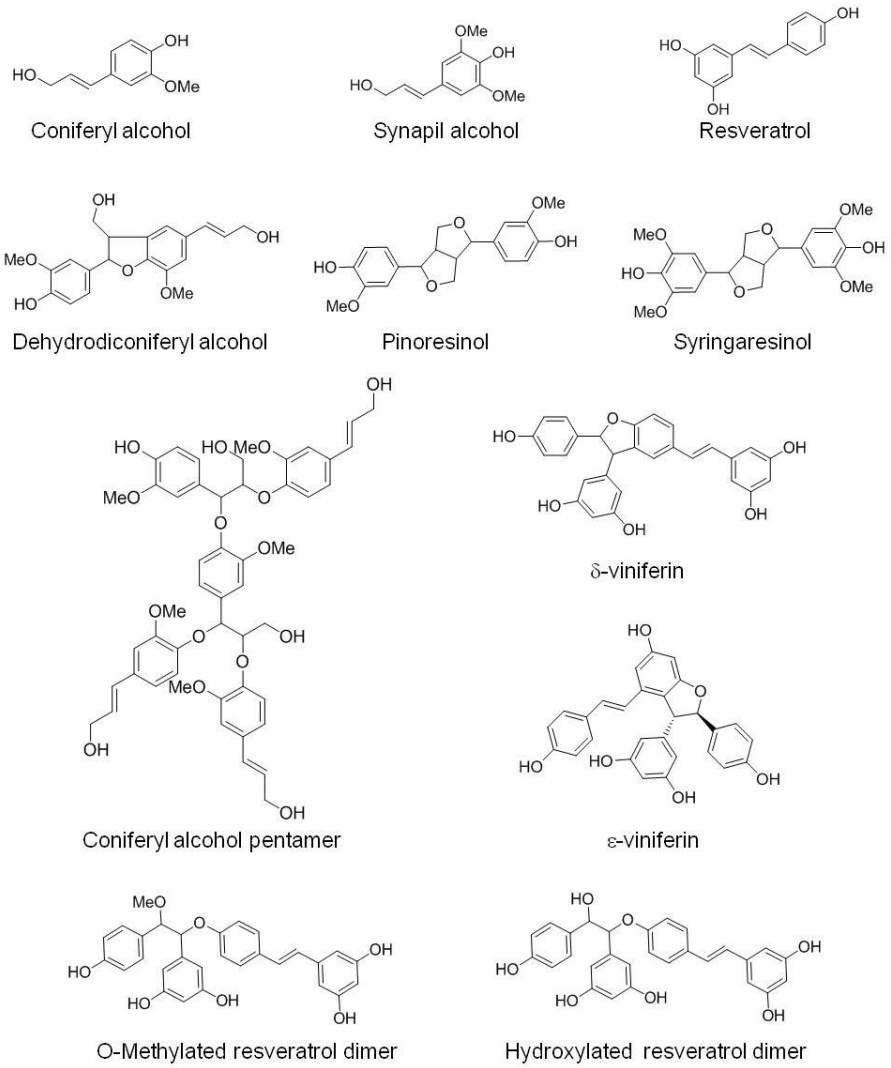

Figure 46. Phenolic compounds screened for antimicrobial activity in this study. Most are coniferyl alcohol and resveratrol derivatives and occur naturally in plants. Coniferyl alcohol pentamer, *O*-methylated and hydroxylated resveratrol dimers were chemically synthesised and were never reported in plants. An additional flavonoid glycoside, whose structure was not fully determined was also used (F4peak1).

All compounds, including resveratrol, were tested (1 mg/mL) for antibacterial activity against a group of gram-positive and –negative bacteria using the agar well diffusion method (Table 11).

Table 11. Antibacterial activity of isolated phenolic compounds using agar well diffusion method at 1 mg/mL. – indicates that no inhibition was observed. + indicates susceptibility to the corresponding compound.

	Pae	Eco	Sen	Kpn	Pmi	Lmo	Sau	Bsu	Efa
Coniferyl alcohol	-	-	-	-	-	-	-	-	-
Sinapyl alcohol	-	-	-	-	-	-	-	-	-
Resveratrol	-	-	-	-	-	+	+	+	+
Dehydrodiconiferyl alcohol	-	-	-	-	-	-	-	-	-
Pinoresinol	-	-	-	-	-	-	-	-	-
Syringaresinol	-	-	-	-	-	-	-	-	-
Pentamer	-	-	-	-	-	-	-	-	-
δ-viniferin	-	-	-	-	-	+	+	+	+
ε-viniferin	-	-	-	-	-	+	+	+	+
O-Me resveratrol dimer	-	-	-	-	-	+	+	+	+
OH resveratrol dimer	-	-	-	-	-	-	-	-	-
F4peak1 (unidentified)	-	-	-	-	-	-	-	-	-

Pae: *P. aeruginosa*, Eco: *E. coli*, Sen: *S. enteritidis,* Kpn: *K. pneumoniae,* Pmi: *P. mirabilis*
Lmo: *L. monocytogenes*, Sau: *S. aureus*, Bsu: B. subtilis, Efa: *E. faecalis.*

At the selected concentration, none of the gram-negative bacteria were affected by the tested compounds. On the other side, for the gram-positive bacteria most of the stilbene derivatives (resveratrol, δ-viniferin, ε-viniferin and *O*-methylated resveratrol dimer) displayed antimicrobial activity. The exception was the hydroxylated resveratrol dimer, which differs from the other dimer only by a methyl group. The fact that the substituent group dramatically affects the bioactivity of the molecule provides only a small example of how semisynthesis can prove important in the drug discovery field.

As for the remaining compounds, although some of them are known to display antibacterial activity, we could not observe any bacterial growth inhibition, possibly due to the tested low concentration of the compounds. For instance, the lignans pinoresinol and syringaresinol were both reported as bioactive against *S. aureus* and *B. subtillis* [19,20]. Nevertheless, according to our results, their antimicrobial activity must be significantly lower when compared to the active stilbenes. For that reason, and given the limited amount for some of the compounds, MIC values

were only determined for the four phenolics displaying activity in the previous assay. An attempt was also made to quantify the inhibitory effect of the total methanolic extracts. MICs were determined by the broth microdilution method against the gram-positive bacteria (Table 12).

Table 12. MIC values of resveratrol, resveratrol dimers and methanolic extracts against gram-positive bacteria.

	MIC (μg/mL)			
	Lmo	Sau	Bsu	Efa
Resveratrol	375	94	375	188
δ-Viniferin	2.9	2.9	2.9	2.9
ε-Viniferin	23.4	5.9	11.7	11.7
O-Me resveratrol dimer	23.4	23.4	23.4	11.7
Methanol extract	780	780	780	780

Lmo: *L. monocytogenes*, Sau: *S. aureus*, Bsu: *B. subtilis*, Efa: *E. faecalis*.

According to the previous results, δ-viniferin displays the highest toxicity against the tested microorganisms with a MIC of 2.9 μg/mL for all the bacteria while resveratrol is the least potent compound, indicating that dimerisation greatly enhances its antimicrobial properties. For the methanolic extract of grapevine canes, also the same MIC value was obtained for all the bacteria (780 μg/mL). This result disagrees with our previous agar well diffusion assays, where a differential susceptibility to the extract was observed for each microorganism. A possible explanation may rely on the concentration values used for the assay. Given the substantial difference between two consecutive concentrations (e.g. 780 and 1560 μg/mL), the MIC values for each microorganism can lay anywhere within that concentration range. Additional assays using a reduced concentration range would be required to evaluate the different microorganism susceptibilities to the extract.

Concerning the individual phenolic compounds used in this study, an attempt was made to correlate our results with the ones existing in the

literature. However, for the most part, such comparison has proven laborious and inconclusive; either due to the absence of reports for some of the compounds or, in the case of resveratrol, due to the several different methods employed for MIC determination or the different microorganisms evaluated in each study. For ε-viniferin, only one study was found in which the antibacterial activity of the compound was evaluated against *S. aureus* [21]. The experimental procedure employed by the authors was similar to ours. However, the reported MIC value (400 μg/mL) is largely discrepant from the one determined in this study (5.9 μg/mL). In our opinion, a possible explanation for the accentuated MIC difference in both studies may be related with the type of solvent used for the phenolic compound. As for resveratrol, concerning also *S. aureus* inhibition, our results are consistent with other similar works in the literature, where MIC values of 170, 125 and 100 μg/mL were obtained [22-24].

Overall, our results suggest that antibacterial activity observed for the grapevine extracts may be attributed, though not exclusively, to their stilbenoid content, in particular to ε-viniferin which is a major phenolic constituent of the extract. In addition, the MIC values for *S. aureus* obtained for both viniferins are in the range of those obtained with the currently used antibiotics [25]. This evidences their great potential to be used in the drug development area.

References

1. Jones SFA (1996) Herbs - useful plants. Their role in history and today. European Journal of Gastroenterology & Hepatology 8: 1227-1231.
2. Ríos JL, Recio MC (2005) Medicinal plants and antimicrobial activity. Journal of Ethnopharmacology 100: 80-84.
3. Bennett RN, Wallsgrove RM (1994) Secondary metabolites in plant defence mechanisms. New Phytologist 127: 617-633.

4. Cowan MM (1999) Plant products as antimicrobial agents. Clinical Microbiology Reviews 12: 564-582.
5. Hadacek F (2002) Secondary metabolites as plant traits: Current assessment and future perspectives. Critical Reviews in Plant Sciences 21: 273-322.
6. Kennedy DO, Wightman EL (2011) Herbal extracts and phytochemicals: Plant secondary metabolites and the enhancement of human brain function. advances in nutrition: An International Review Journal 2: 32-50.
7. Salim AA, Chin Y-W, Kinghorn AD (2008) Drug discovery from plants. In: Ramawat KG, Merillon JM, editors. Bioactive molecules and medicinal plants: Springer Berlin Heidelberg. pp. 1-24.
8. Wedge D, Smith B (2006) Discovery and evaluation of natural product-based fungicides for disease control of small fruits. In: Inderjit, Mukerji KG, editors. Allelochemicals: Biological control of plant pathogens and diseases: Springer Netherlands. pp. 1-14.
9. Al-Samarrai G, Singh H, Syarhabil M (2012) Evaluating eco-friendly botanicals (natural plant extracts) as alternatives to synthetic fungicides. Annals of Agricultural and Environmental Medicine 19: 673-676.
10. Xia E-Q, Deng G-F, Guo Y-J, Li H-B (2010) Biological activities of polyphenols from grapes. International Journal of Molecular Sciences 11: 622-646.
11. Yadav M, Jain S, Bhardwaj A, Nagpal R, Puniya M, et al. (2009) Biological and medicinal properties of grapes and their bioactive constituents: An update. Journal of Medicinal Food 12: 473-484.
12. Schnee S, Queiroz EF, Voinesco F, Marcourt L, Dubuis P-H, et al. (2013) *Vitis vinifera* canes, a new source of antifungal compounds against *Plasmopara viticola*, *Erysiphe necator*, and *Botrytis cinerea*. Journal of Agricultural and Food Chemistry 61: 5459-5467.
13. Lambert C, Bisson J, Waffo-Téguo P, Papastamoulis Y, Richard T, et al. (2012) Phenolics and their antifungal role in grapevine wood decay: Focus on the *Botryosphaeriaceae* family. Journal of Agricultural and Food Chemistry 60: 11859-11868.
14. Nikaido H (1989) Outer membrane barrier as a mechanism of antimicrobial resistance. Antimicrobial Agents and Chemotherapy 33: 1831-1836.

15. Jayaprakasha GK, Selvi T, Sakariah KK (2003) Antibacterial and antioxidant activities of grape (*Vitis vinifera*) seed extracts. Food Research International 36: 117-122.
16. Papadopoulou C, Kalliopi KS, Roussis IG (2005) Potential antimicrobial activity of red and white wine phenolic extracts against strains of *Staphylococcus aureus, Escherichia coli* and *Candida albicans*. Food Technology and Biotechnology 43: 41-46.
17. Ceyhan N, Keskin D, Zorlu Z, Ugur A (2012) In-vitro Antimicrobial activities of different extracts of grapevine leaves (*Vitis vinifera* L.) from west Anatolia against some pathogenic microorganisms. Journal of Pure and Applied Microbiology 6: 1303-1308.
18. Reale S, Attanasio F, Spreti N, De Angelis F (2010) Lignin chemistry: Biosynthetic study and structural characterisation of coniferyl alcohol oligomers formed *in vitro* in a micellar environment. Chemistry – A European Journal 16: 6077-6087.
19. Cespedes CL, Avila JG, Garcia AM, Becerra J, Flores C, et al. (2006) Antifungal and antibacterial activities of *Araucaria araucana* (Mol.) K. Koch heartwood lignans. Zeitschrift für Naturforschung C. 61: 35-43.
20. Yang B, Chen G, Song X, Chen Z, Wang J (2010) Chemical constituents and antimicrobial activities of *Canthium horridum*. Natural Product Communications 5: 913-914.
21. Basri DF, Luoi CK, Azmi AM, Latip J (2012) Evaluation of the combined effects of stilbenoid from *Shorea gibbosa* and vancomycin against methicillin-resistant *Staphylococcus aureus* (MRSA). Pharmaceuticals 5: 1032-1043.
22. Chan MM-Y (2002) Antimicrobial effect of resveratrol on dermatophytes and bacterial pathogens of the skin. Biochemical Pharmacology 63: 99-104.
23. Tegos G, Stermitz FR, Lomovskaya O, Lewis K (2002) Multidrug pump inhibitors uncover remarkable activity of plant antimicrobials. Antimicrobial Agents Chemotherapy 46: 3133-3141.
24. Paulo L, Ferreira S, Gallardo E, Queiroz J, Domingues F (2010) Antimicrobial activity and effects of resveratrol on human pathogenic bacteria. World Journal of Microbiology and Biotechnology 26: 1533-1538.
25. Dhand A, Sakoulas G (2012) Reduced vancomycin susceptibility among clinical *Staphylococcus aureus* isolates ('the MIC Creep'): implications for therapy. F1000 Medicine Reports 4: 4.

Chapter VII: General Discussion

Discussion

Grapevine is the most economically important fruit crop worldwide. As in other cultures, the yield and quality of the crops are often affected by external factors in which fungal pathogens play a major part [1]. Thus, in a broad sense, a great deal of grapevine research is directed towards a better understanding of the plant defence mechanisms and characterization of the particular plant-pathogen interactions affecting the species. In this general context, the aim of the current work was to increase our knowledge on grapevine, providing small pieces for the big puzzle of secondary metabolism and defence strategies of the species.

As a preliminary side task, which would be valuable for the present and future works, we evaluated the expression stability of reference genes to be used in grapevine qRT-PCR studies (Chapter II). Sample normalization, achieved by the use of internal reference genes, is a crucial factor for accurate gene expression quantification. Nevertheless, the selected reference genes must remain stably expressed across all samples under study [2].

In the literature, several studies exist, including for grapevine, where reference gene selection/validation had not been properly carried [3]. We also found there were already published reports evaluating qRT-PCR reference genes for grapevine samples [3-7]. However, although comprising a wide variety of conditions including developmental stages in berries, biotic and abiotic stresses, other relevant stresses had not been addressed. Therefore, we conducted a study to evaluate the most suitable reference genes, among a set of candidates, to be used in grapevine samples during specific biotic and abiotic stresses which were considered relevant for the species. Although the obtained stability ranks varied reasonably depending on the analysis method used, we were able to

observe that the relative expression stability of the candidate genes is, as expected, affected by the selected treatment. Moreover, bigger stability changes occur when comparing different tissues (leaves and canes). Therefore, a careful selection of reference genes should be performed prior to any gene expression study.

Even though our analysis can be useful for the appropriate selection of references in forthcoming gene expression studies, it does not eliminate the need for further investigation. In theory, for every experimental condition, an evaluation of the most suitable reference genes should be performed. However, since that is not always possible, either due to experimental or economical constraints, whenever treatments and conditions are similar to ours, a reasoned choice of suitable reference genes can be made.

Regarding the experimental design of this study (Chapter II), a criticism can be made concerning the selection method of the candidate genes to be analyzed. Apart from the initial requisite to avoid co-regulation (i.e. participation in distinct metabolic pathways), the selection was made solely based on their frequent use as reference genes in other plant gene expression studies [8-10]. Although certain expression stability is expected (i.e. some of them were reported as the most stable among a group of candidates), better candidates may exist. In the present era of high-throughput analysis, there is increasing availability of grapevine microarrays and RNA-Seq data. Therefore, a preliminary database analysis, choosing data sets involving similar or related stimuli to the ones in our study, would have brought additional value to the work. This has been done for *A. thaliana* in the past, allowing the identification of novel reference genes which outperformed the traditional ones [11]. Similar, though less extensive, approaches have been adopted for grapevine samples, where specific microarray data was analysed (identifying stably expressed candidates) prior to qRT-PCR validation [3,5]. Considering the

previous observations, despite the unquestionable importance of our study, superior reference genes may exist for each of the particular stimulus addressed.

In a second task (Chapter III), we devised a transcriptomic approach aiming at a better characterization of the plant-pathogen interaction, *V. vinifera* - *E. necator*. Regardless of its economical impact, added knowledge on this interaction is of great significance, not only for viticulture, but also for a further understanding of the biotrophic lifestyle.
Among all plant pathogens, obligate biotrophs are perhaps the most complex, developing highly sophisticated interactions with their hosts [12]. The infection process goes beyond the simple invasion and feeding on the host, as the pathogen is entirely dependent on living tissues [13]. Thus, besides manipulating the host's metabolism to its own benefice without causing cell death, it must also be able to avoid or disable the defences of the plant (e.g. programmed cell death) [13]. Nevertheless, the initial stages of infection do not differ much from other pathogens with different nutritional needs [14]. Hence our choice for studying the later stages of infection, as results might reflect the specific consequences of the compatible interaction. In addition, the fact that we compared symptomatic and asymptomatic leaves (both from diseased plants), rather than healthy and infected plants, accounts for genes potentially involved in systemic acquired resistance.
An overview of the genes identified as differentially expressed, backed up by the corresponding up or downregulation, illustrates the chemical warfare undergoing between both organisms of the pathosystem. Although highly speculative, one can perceive either the plant attempts to fight the invading pathogen, upregulating signalling genes and the synthesis of toxic metabolites (e.g. glycerol-3-phosphate dehydrogenase, triterpene synthase, resveratrol *O*-methyltransferase and *DIR*), or the

manipulation of the host metabolism by the fungus, hijacking potentially important defence signalling pathways (e.g. inositol transporter, MAPK, gibberellic acid receptor). The latter might deserve greater attention in the future, as it may conceal the answer for pathogen resistance while maintaining the original weaponry of the plant. The fact that asymptomatic leaves remained uninfected during several lifecycles of the pathogen evidences the innate ability of the host to prevent fungal colonization. Considering a long term scenario, where the genetic engineering of grapevines would be reasonably accepted, exploring the native resistance potential of the host would be preferred to a transgene approach.

Out of the differentially expressed genes identified in this work, a DIR gene (*Vv*DIR1) stood out from the remaining due to its magnitude of overexpression in symptomatic leaves. Considering a potentially important role of this gene in plant defence, most of the following work was focused on several aspects of *Vv*DIR1 and other DIR/DIR-like genes encoded by *V. vinifera*. Interesting results were obtained when analysing the differential expression of genes whose products would be closely related to *Vv*DIR1 (Chapter III). The observation that, under the same experimental conditions, *Vv*DIR1 was highly upregulated while PRR, coding for the following enzyme in the pathway, was significantly repressed, was not in accordance to our expectations. Reasonably, although a high homology existed between *Vv*DIR1 and other functionally characterized pinoresinol-forming DIRs, we were led to one of two hypotheses to tentatively explain the magnitude of overtranscription of *Vv*DIR1: either an unknown alternative lignan biosynthetic pathway existed (directing the pools of pinoresinol to the formation of other lignans instead of lariciresinol), or *Vv*DIR1 could mediate the formation of compounds other than pinoresinol. Even if we have later demonstrated the involvement of *Vv*DIR1 in the preferential formation of pinoresinol (Chapter IV), both hypotheses cannot be ruled out. Nevertheless, if one of

them is to be true, we would risk saying the second as the most likely one: despite existing reports of pinoresinol, lariciresinol and other lignans in wine samples [15], those lignans must be of reduced abundance in *V. vinifera* as they are not usually detected [16,17] (neither was pinoresinol detected in this study – leaves or canes). However, considering this hypothesis, the resulting product would still be originated from same precursor (coniferyl alcohol) due to the described DIR substrate specificity [18]. This would point, for instance, towards a possible involvement of *Vv*DIR1 in lignin formation which was not properly evaluated in this work (Chapter IV): the increase in lignin content upon *E. necator* infection is not, alone, indicative of *Vv*DIR1 participation in the process. On the contrary, had the intended reverse genetic strategy been successful, we would now be confirming/refuting that hypothesis. Instead, additional questions were raised, such as why a homozygous *At*DIR5 T-DNA mutant could not be obtained. Though we advanced with a possibility of a lethal phenotype, such supposition should be carefully evaluated.

Following work (Chapter V) was dedicated to the possible involvement of DIR proteins in the biosynthesis of stilbenoids, namely ε-viniferin. According to several aspects reported or suggested by the literature, and also assessed by us, the biosynthesis of this metabolite can be under the influence of a DIR/DIR-like protein: (i) resveratrol may be its direct precursor through oxidative dimerization, resembling the lignan biosynthesis [19]. Oxidative coupling is a prominent reaction type in the biosynthesis of many natural products, especially for phenolic compounds [20]; (ii) *in vitro* oxidative coupling reactions, using resveratrol as substrate, result in the thermodynamically spontaneous formation of δ-viniferin [19,21]; (iii) under physiological conditions, particularly in woody tissues, ε-viniferin is one of the major occurring phenolics [22,23]; (iv) ε-

viniferin has been isolated as its (+)- or (-)-antipode, depending on the source organism [24].

To evaluate the possibility of DIR participation in the stilbenoid biosynthetic pathway, two different strategies were adopted: a “forward” gene-to-function approach (recombinant production of *Vv*DIR), and “reverse” function-to-protein approach (protein extracts from *V. vinifera*). Though neither produced the expected results, both added useful information to our current knowledge on this matter.

While we attempted to find potential candidates for recombinant expression, we unveiled the *Vv*DIR family, a group of 42 putative DIR proteins encoded by *V. vinifera* genome. According to what is currently known, *Vv*DIR is the second biggest DIR family described, only smaller after *O. sativa* family (54 genes) [25]. As observed for other species, *Vv*DIR family is also very heterogeneous among its members. With only four members of the subfamily DIR-a, which most likely would have redundant functions either in different tissues or distinct developmental stages, the existence of the remaining 38 reinforces the possibility of additional DIR-mediated reactions yet to be discovered.

In our opinion, considering all the existing facts, it would be surprising if the synthesis of ε-viniferin did not involve the participation of a DIR/DIR-like protein. Yet, using our “forward” approach, no clear *Vv*DIR candidates were observed. Putting it into perspective, given the number of variables and the level of uncertainty involved, we should not have considered this approach as a first option. In our defence, such strategy was devised planning for an ideal scenario where, (i) a smaller *Vv*DIR family would be encoded in grapevine genome, (ii) fewer transcripts would be specific to the woody parts of the plant and (iii) a portion of those would respond to the biotic stress in study. None of the previous has happened. Thus, our narrowing process was mostly conditioned by experimental constrains and/or unfounded assumptions rather than reasoned choices. As for, we

were not surprised none of the selected proteins displayed activity towards resveratrol.

On the other hand, concerning the "reverse" approach, the obtained results were as exciting as they were intriguing. For the first time, we had observed direct evidence of regioselective control over resveratrol dimerization. The protein extracts from *V. vinifera* woody tissues had the ability to block the spontaneous formation of δ-viniferin and afford alternative products. Interestingly, the formation of the expected metabolite, ε-viniferin, was not observed. Instead, a new symmetric resveratrol dimer was formed. Having previously confirmed its presence in grapevine canes, we were quite confident that, if any guiding activity was to happen, it would lead to the formation of ε-viniferin. However, it is worth to mention that the presence of ε-viniferin in the woody tissues, even if in high amounts, does not necessarily mean it was actively being produced at that time. In this sense, it is also curious that, being actively produced by the protein extracts, the presence of the symmetric dimer has not been detected in the tissues. Whether it is a transient metabolite or an unnatural product, we cannot tell.

Finally, as a complementary task (Chapter VI) we decided to evaluate the possible antimicrobial activity of both methanolic extracts from grapevine canes and individual phenolic compounds (stilbene and hydroxycinnamic acid derivatives). The primary objective of the study was to assess whether the phenolic content of grapevine canes had itself the potential to be used against fungal pathogens colonizing the same tissues (*P. chlamydospora* and *P. aleophilum*). As observed by our results, and somehow corroborated by the work of Lambert and colleagues [26], the two pathogens may be highly adapted to prosper under the potentially aggressive physiological environment of grapevine wood. Stilbenes are known for their antifungal activity. Yet, against wood colonizing fungi their

efficacy seems reduced [27]. This may be explained by years of co-evolution and adaptation between host and the pathogens. Moreover, the outcome of this long battle seems now obvious, as demonstrated by the worldwide increased incidence and severity of esca, a disease complex comprising both *P. chlamydospora* and *P. aleophilum* [28,29].

Alternatively, we tested both the extracts and individual phenolic compounds against human pathogenic bacteria. Although the methanolic extracts from grapevine canes had demonstrated antibacterial activity against gram-positive bacteria, the most interesting results were obtained for the individual phenolic compounds, where some of the stilbene derivatives evidenced a high toxicity against some of the bacteria. In particular, viniferins (δ- and ε-viniferin) displayed promising activity against *S. aureus*. MIC values for both compounds were significantly close to the ones obtained with currently used antibiotics [30,31]. Given increased capacity of *S. aureus* to acquire antibiotic resistance and the constant quest for new active drugs against this pathogen [32], viniferins could possibly be on the list of available and viable options to be considered.

Considering the results obtained in this thesis, we were particularly fascinated by the formation of the new resveratrol symmetric dimer and also by the very likely possibility of ε-viniferin biosynthesis being guided by DIR proteins. Therefore, immediate future work will focus on these two subjects. In theory, the same strategy will reveal both guiding agents, whether DIR proteins or not. Total protein extracts will be fractionated consecutively using different strategies while following the desired guiding activity. It will also be important to assess the bioactivity of the new resveratrol dimer, testing it for a wide range of activities including antiproliferative, antioxidant and antimicrobial activity. At last, we would also like to complete our analysis on *Vv*DIR1, which is dependent on the optimization of the recombinant expression. Higher protein yields will allow

us to determine the enantioselective character of this protein ((+)- or (-)-pinoresinol-forming), adding it to the group of functionally characterized DIR proteins.

References

1. Ferreira RB, Monteiro SS, Piçarra-Pereira MA, Teixeira AR (2004) Engineering grapevine for increased resistance to fungal pathogens without compromising wine stability. Trends in Biotechnology 22: 168-173.
2. Vandesompele J, De Preter K, Pattyn F, Poppe B, Van Roy N, et al. (2002) Accurate normalization of real-time quantitative RT-PCR data by geometric averaging of multiple internal control genes. Genome Biology 3: 0034.
3. Gamm M, Héloir M-C, Kelloniemi J, Poinssot B, Wendehenne D, et al. (2011) Identification of reference genes suitable for qRT-PCR in grapevine and application for the study of the expression of genes involved in pterostilbene synthesis. Molecular Genetics and Genomics 285: 273-285.
4. Reid K, Olsson N, Schlosser J, Peng F, Lund S (2006) An optimized grapevine RNA isolation procedure and statistical determination of reference genes for real-time RT-PCR during berry development. BMC Plant Biology 6: 27.
5. Coito J, Rocheta M, Carvalho L, Amancio S (2012) Microarray-based uncovering reference genes for quantitative real time PCR in grapevine under abiotic stress. BMC Research Notes 5: 220.
6. Monteiro F, Sebastiana M, Pais MS, Figueiredo A (2013) Reference gene selection and validation for the early responses to downy mildew infection in susceptible and resistant *Vitis vinifera* Cultivars. PLoS ONE 8: e72998.
7. Selim M, Legay S, Berkelmann-Löhnertz B, Langen G, Kogel KH, et al. (2012) Identification of suitable reference genes for real-time RT-PCR normalization in the grapevine-downy mildew pathosystem. Plant Cell Reports 31: 205-216.
8. Mallona I, Lischewski S, Weiss J, Hause B, Egea-Cortines M (2010) Validation of reference genes for quantitative real-time PCR during leaf and flower development in *Petunia hybrida*. BMC Plant Biology 10: 4-4.

9. Nicot N, Hausman J-F, Hoffmann L, Evers D (2005) Housekeeping gene selection for real-time RT-PCR normalization in potato during biotic and abiotic stress. Journal of Experimental Botany 56: 2907-2914.
10. Jain M, Nijhawan A, Tyagi AK, Khurana JP (2006) Validation of housekeeping genes as internal control for studying gene expression in rice by quantitative real-time PCR. Biochemical and Biophysical Research Communications 345: 646-651.
11. Czechowski T, Stitt M, Altmann T, Udvardi MK, Scheible W-R (2005) Genome-wide identification and testing of superior reference genes for transcript normalization in *Arabidopsis*. Plant Physiology 139: 5-17.
12. O'Connell RJ, Panstruga R (2006) Tête à tête inside a plant cell: establishing compatibility between plants and biotrophic fungi and oomycetes. New Phytologist 171: 699-718.
13. Panstruga R (2003) Establishing compatibility between plants and obligate biotrophic pathogens. Current Opinion in Plant Biology 6: 320-326.
14. Mendgen K, Hahn M (2002) Plant infection and the establishment of fungal biotrophy. Trends in Plant Science 7: 352-356.
15. Nurmi T, Heinonen S, Mazur W, Deyama T, Nishibe S, et al. (2003) Lignans in selected wines. Food Chemistry 83: 303-309.
16. Teixeira A, Eiras-Dias J, Castellarin S, Gerós H (2013) Berry phenolics of grapevine under challenging environments. International Journal of Molecular Sciences 14: 18711-18739.
17. Perestrelo R, Lu Y, Santos SAO, Silvestre AJD, Neto CP, et al. (2012) Phenolic profile of Sercial and Tinta Negra *Vitis vinifera* L. grape skins by HPLC–DAD–ESI-MSn: Novel phenolic compounds in *Vitis vinifera* L. grape. Food Chemistry 135: 94-104.
18. Davin LB, Lewis NG (2000) Dirigent proteins and dirigent sites explain the mystery of specificity of radical precursor coupling in lignan and lignin biosynthesis. Plant Physiology 123: 453-462.
19. Takaya Y, Terashima K, Ito J, He Y-H, Tateoka M, et al. (2005) Biomimic transformation of resveratrol. Tetrahedron 61: 10285-10290.
20. Dewick PM (2001) Secondary metabolism: The building blocks and construction mechanisms. Medicinal Natural Products: John Wiley & Sons, Ltd. pp. 7-34.

21. Wilkens A, Paulsen J, Wray V, Winterhalter P (2010) Structures of two novel trimeric stilbenes obtained by horseradish peroxidase catalyzed biotransformation of *trans*-resveratrol and (−)-ε-viniferin. Journal of Agricultural and Food Chemistry 58: 6754-6761.
22. Vergara C, von Baer D, Mardones C, Wilkens A, Wernekinck K, et al. (2011) Stilbene levels in grape cane of different cultivars in southern Chile: Determination by HPLC-DAD-MS/MS method. Journal of Agricultural and Food Chemistry 60: 929-933.
23. Lambert C, Richard T, Renouf E, Bisson J, Waffo-Téguo P, et al. (2013) Comparative analyses of stilbenoids in canes of major *Vitis vinifera* L. cultivars. Journal of Agricultural and Food Chemistry 61: 11392-11399.
24. Riviere C, Pawlus AD, Merillon J-M (2012) Natural stilbenoids: distribution in the plant kingdom and chemotaxonomic interest in *Vitaceae*. Natural Product Reports 29: 1317-1333.
25. Ralph SG, Jancsik S, Bohlmann J (2007) Dirigent proteins in conifer defense II: Extended gene discovery, phylogeny, and constitutive and stress-induced gene expression in spruce (*Picea* spp.). Phytochemistry 68: 1975-1991.
26. Lambert C, Bisson J, Waffo-Téguo P, Papastamoulis Y, Richard T, et al. (2012) Phenolics and their antifungal role in grapevine wood decay: Focus on the *Botryosphaeriaceae* family. Journal of Agricultural and Food Chemistry 60: 11859-11868.
27. Bavaresco L, Fregoni C, de Macedo Basto Gonçalves MIv, Vezzulli S (2009) Physiology & molecular biology of grapevine stilbenes: An update. In: Roubelakis-Angelakis K, editor. Grapevine molecular physiology & biotechnology: Springer Netherlands. pp. 341-364.
28. Edwards J, Pascoe IG (2004) Occurrence of *Phaeomoniella chlamydospora* and *Phaeoacremonium aleophilum* associated with Petri disease and esca in Australian grapevines. Australasian Plant Pathology 33: 273-279.
29. Martín MT, Cobos R, Martín L, López-Enríquez L (2012) Real-time PCR detection of *Phaeomoniella chlamydospora* and *Phaeoacremonium aleophilum*. Applied and Environmental Microbiology 78: 3985-3991.
30. Dhand A, Sakoulas G (2012) Reduced vancomycin susceptibility among clinical *Staphylococcus aureus* isolates ('the MIC Creep'): implications for therapy. F1000 Medicine Reports 4: 4.

31. Hu J, Ma XX, Tian Y, Pang L, Cui LZ, et al. (2013) Reduced vancomycin susceptibility found in methicillin-resistant and methicillin-sensitive *Staphylococcus aureus* clinical isolates in northeast China. PLoS ONE 8: e73300.
32. Chambers HF, DeLeo FR (2009) Waves of resistance: *Staphylococcus aureus* in the antibiotic era. Nature reviews Microbiology 7: 629-641.